Degradation in presence of different types of maintenance : modelling, inference and decision making

Margaux Leroy

THÈSE

Pour obtenir le grade de

DOCTEUR DE L'UNIVERSITÉ GRENOBLE ALPES

École doctorale : MSTII - Mathématiques, Sciences et technologies de l'information, Informatique
Spécialité : Mathématiques Appliquées
Unité de recherche : Laboratoire Jean Kuntzmann

Dégradation en présence de différents types de maintenance : modélisation, inférence et prise de décision

Degradation in presence of different types of maintenance: modelling, inference and decision making

Présentée par :

Margaux LEROY

Direction de thèse :

Laurent DOYEN MAITRE DE CONFERENCES HDR, UNIVERSITE GRENOBLE ALPES	Directeur de thèse
Christophe BERENGUER PROFESSEUR DES UNIVERSITES, GRENOBLE INP - UGA	Co-directeur de thèse

Rapporteurs :

MARIA INMACULADA TORRES CASTRO
FULL PROFESSOR, UNIVERSIDAD DE EXTREMADURA
CHRISTIAN PAROISSIN
MAITRE DE CONFERENCES HDR, UNIVERSITE DE PAU ET PAYS DE L'ADOUR

Thèse soutenue publiquement le **12 juin 2024**, devant le jury composé de :

ADELINE LECLERCQ-SAMSON, PROFESSEURE DES UNIVERSITES, UNIVERSITE GRENOBLE ALPES	Présidente
LAURENT DOYEN, MAITRE DE CONFERENCES HDR, UNIVERSITE GRENOBLE ALPES	Directeur de thèse
CHRISTOPHE BERENGUER, PROFESSEUR DES UNIVERSITES, GRENOBLE INP	Co-directeur de thèse
MARIA INMACULADA TORRES CASTRO, FULL PROFESSOR, UNIVERSIDAD DE EXTREMADURA	Rapporteure
CHRISTIAN PAROISSIN, MAITRE DE CONFERENCES HDR, UNIVERSITE DE PAU ET PAYS DE L'ADOUR	Rapporteur
MITRA FOULADIRAD, PROFESSEURE, ECOLE CENTRALE MARSEILLE	Examinatrice
VINCENT COUALLIER, MAITRE DE CONFERENCES, UNIVERSITE DE BORDEAUX	Examinateur

Invités :

EMMANUEL REMY
INGENIEUR DE RECHERCHE, EDF R&D

Degradation in presence of different types of maintenance: Modeling, Inference and Decision-making

Margaux Leroy

Université Grenoble Alpes
Laboratoire Jean Kuntzmann
GIPSA-Lab

Under the supervision of:
Laurent Doyen
Christophe Bérenguer

Remerciements

Merci tout d'abord à mes directeurs de thèse, Laurent et Christophe, d'avoir été très présents tout au long de cette thèse, d'avoir pris le temps de me conseiller, me relire et répondre à mes questions. Évidemment merci à Olivier, avec qui j'ai beaucoup interagi les deux premières années. Réellement investi dans ce projet, merci pour la pédagogie dont tu fais constamment preuve, merci pour tous les bons conseils et les encouragements si précieux lors des présentations. Durant ces trois dernières années, j'ai énormément appris à vos côtés, tant scientifiquement qu'humainement. Et en fin de compte, je suis contente d'être arrivée au bout.

Merci aux membres du jury, qui, fait rare, étaient tous présents à cette soutenance, je vous en remercie beaucoup ! A Inma et Christian rapporteurs de cette thèse, pour leur lecture attentionnée de ce manuscrit et tous leurs retours très intéressants. A Mitra, Vincent et Emmanuel d'avoir également accepté de faire partie de ce jury. J'ai eu la chance d'avoir pu tous vous rencontrer avant la soutenance et d'avoir pu discuter avec chacun d'entre vous lors de conférences ou autres. J'étais vraiment ravie d'apprendre que vous feriez partie de ce jury. Merci pour votre bienveillance, pour tous vos bons conseils et votre soutien. J'espère qu'on gardera contact !

Bien-sûr, merci à Adeline, d'avoir accepté de présider ce jury, et de m'avoir permis de donner les cours/TDs et TPs de statistique pendant quatre ans. J'ai eu beaucoup de plaisir à enseigner ce cours, et c'est la raison principale pour laquelle j'ai accepté de finir cette dernière année de thèse par un ATER. Merci d'avoir toujours été disponible pour discuter, pour ta bienveillance, tes encouragements, et tes conseils réconfortants.

J'en profite pour remercier tous les autres enseignants avec qui j'ai eu la chance de donner des cours de statistique et mathématique. Merci à Christelle, François, Jeff, Yvonne, Julien, Elise, Frédérique et Carole.

J'aimerais aussi remercier les administratifs que j'ai pu côtoyer au labo, à savoir : Laurence, Aurore, Suzanne, Aristide et Cathy. Merci pour l'aide au quotidien, pour votre disponibilité et votre bonne humeur contagieuse.

Merci à Laurence Wazné et Emmanuelle Crépeau d'organiser des rendez-vous annuels de discussions libres et informelles avec les doctorants. C'est tellement important ! Merci pour votre précieuse écoute.

Merci à la QVT de nous avoir permis d'organiser toutes les activités du labo et à Ginette pour les accès aux terrains de beach.

Merci à Franck Pérignon et Frederic Audra pour leur aide et formation sur l'accès aux clusters de calculs. Merci aussi d'avoir participé aux matchs de volley cet hiver, et d'avoir bien relevé le niveau !

Merci à Vincent Brault, mon responsable de stage de fin d'étude, et véritable rayon de soleil. Merci pour le temps passé à animer la vie du labo, pour toujours s'assurer que tout va bien, pour les conseils, notamment sur l'après-thèse, pour le soutien en général et la bienveillance. J'aurais beaucoup aimé que l'on continue à travailler ensemble, mais mon éternelle indécision, mes doutes permanents et le temps qui presse m'ont fait changer de route. J'espère que tu ne m'en veux pas trop et qu'on continuera de se donner des nouvelles ! Merci aux autres permanents du LJK que j'ai eu la chance de croiser, et avec qui j'ai toujours apprécié discuter. Merci à Julien, Jean-Charles, Kévin, Manel, Brigitte.

Merci Rémy pour ta sympathie, ta confiance et ton temps. Merci pour ces heures de discussion et d'écoute. Et bien-sûr merci d'avoir pris le temps, encore aujourd'hui, de m'initier à RRRulia !

Merci à Boris pour toutes nos conversations, les précieux conseils pour préparer les entretiens, pour le soutien en général et pour tous ces matchs intenses de beach volley, qui vont, je l'espère, continuer encore longtemps ! Puisqu'on est sur le beach volley, je remercie bien-sûr Sergei, qui insista il y a trois ans pour jouer tous ensemble au basket et au volley. S'en suivit un nombre incalculable de matchs, d'entorses, luxations et autres tendinites (coucou le CHU sud). Mais ça marqua surtout le début d'une super ambiance au labo, de beaucoup de rencontres et d'amitiés. J'espère que ça va continuer !

A présent, j'aimerais m'étendre un peu sur les remerciements des non-permanents du LJK sans qui ces quatre dernières années n'auraient pas eu la même saveur. A tous ces déjeuners partagés, ces pauses cafés, ces TDs enseignés, à toutes les activités et sports pratiqués, à toutes nos conversations animées et nos bières sirotées (je m'arrête là je suis à cours de rimes en « é »). Ces rencontres ont contribué à la si bonne ambiance au LJK, ont effacé le blues du dimanche soir et égayé toutes mes journées. Gratitude infinie donc à (attention la liste est longue) : Dima, Sélim, Flora, Gabrielle, Manon, Lucia, Théo, Sasila et Yannis mes buddies de fin de thèse, Alexis P., Manu, Julien, JB, Yunjiao, Alexandre D., Alexis A., Kajal (Chetori ?), Laura, Chi, Hubert, Nils, Yu-Guan, Waïss, Victor Victor (un grand merci pour cette virée à Chamrousse en moto, c'était un aprèm vraiment mémorable !), Florian, Carlos, Hélène, Angélique, Tâm, Ieva , Alexandre W., Rishabh, Manolis, Qiao, Valentin, Gianluca, Kliment, Benji, Claudia, Wu Jiahao, Gabriel, Rémi, Alexis G., Maya, Cambyse, Alice, Yassine, Thibault, Anatole, Gilles, Hippolyte, Eloua, Tom, Zineb et tous

les autres.

Parmi eux, je remercie particulièrement mes co-bureaux. Dima, merci pour ta grande gentillesse, ton flegme implacable dans les situations de rush, toutes tes petites attentions et ton humour ! Dima est un véritable standuper, vous le saviez ?

Flora, pour tout le temps que tu as passé à animer la vie des non-permas. Si l'ambiance était si dingue, c'est aussi grâce à toi ! Tu as laissé un grand vide en partant. Merci de m'avoir si bien accueillie à mon arrivée alors que je ne connaissais presque personne. Merci pour tous nos échanges, ta douceur, ta bienveillance et ton écoute. Merci pour tes excellents cookies et sneakers vegans que je n'ai jamais réussis à reproduire et qui m'ont tant manqué cette année ! Et merci d'avoir fait du bureau 135 un espace ultra cosy que beaucoup nous enviait.

Sélim, merci pour ta grande générosité, des biscuits à l'IPad en passant par quantité de chargeurs et Serflex. Merci infiniment pour toutes nos conversations et le soutien, surtout cette dernière année, le bureau paraissait bien vide lorsque tu télétravaillais. Surtout ne perds jamais ton âme d'artiste et courage pour cette dernière ligne droite !

Un merci aussi tout particulier aux non-permas des bureaux d'à côté, devenus également de véritables amis. Merci JB (prononcez Jaybee), pour toute l'aide que tu m'as apportée, de l'informatique à la réparation de vélo. Pour toutes les activités qu'on a organisées ensemble. Merci pour les petits cadeaux que je retrouvais sur mon bureau, je les garde tous précieusement (sauf les crèmes de marrons, déjà finies) !

Merci Carlos, pour ta bonne humeur quotidienne, pour l'énorme soutien cette année, merci pour la danse, les airs de guitare, les séances ciné, et merci d'être très très laxiste quant à mon espagnol, voy a mejorar, ¡ lo prometo ! Hâte que l'on aille danser à Paris !

Merci Manon, d'avoir su trouver les mots justes et de m'avoir réconfortée tellement de fois. Quelle chance d'avoir pu vivre cette fin de thèse ensemble. Merci d'avoir animé la vie du labo l'année dernière, c'était intense et on a quitté le labo la tête chargée de souvenirs. Merci aussi pour tous les moments qu'on a partagés au sein du LJK ou ailleurs, pour tous ces cafés et soirées, j'espère que ça ne fait que commencer !

Enfin, merci à mes proches, aux amis grenoblois et parisiens, qui ont été très présents et qui m'ont apporté un soutien sans faille ces dernières années. Tout d'abord, merci aux grenoblois et particulièrement aux amis de Rémi, les anciens du Lycée Marie Curie d'Echirolles, les premiers que j'ai eu la chance de rencontrer en arrivant à Grenoble et que j'ai toujours plaisir à retrouver : Merci donc à Robin, Mathilde, Vass, Vince, Gaëtan, Yann, François, Tintin et tout le reste de la troupe. Merci à la famille de Rémi et leurs amis, à

toutes nos randos, aux vacances en Corse et aux tournois de coinche sur la plage. Merci Corinne, Hervé, Manon, Mathieu (qui connaît tout Grenoble et grâce à qui j'ai pu faire un super pot de thèse), David, Clem, Céline, Delphine, Pablo.

Merci à mon équipe de volley, et aux filles géniales qui en font partie. Merci pour votre compréhension sur mes absences cette dernière année qui fût ô combien stressante. J'ai hâte d'entamer une nouvelle saison avec vous !

Merci aux amis de master avec qui j'ai gardé contact, j'espère qu'on ne se perdra pas de vue ! Côté parisien, merci à Nathan, Kerian et Stéphane, puis côté grenoblois merci à Ipek, Stefania, Azat, Javi, François, Théo et Maxime.

Merci aux amis d'enfance. Pour nos longues discussions, pour tous les coups de boost et l'énergie que vous me transmettez. Merci Marie, Meg, Vivi et Claire, ça fait un bien fou de vous voir à chaque fois. Merci aux potes parisiens avec qui on arpente les arrondissements de Paris depuis douze ans maintenant : à ma chica d'amour Marine, et à Chris avec qui on peut parler de tout (et surtout de ciné), merci d'avoir fait le déplacement pour la soutenance, ça m'a fait tellement plaisir !

Merci à ma famille. A ma mère, mon père mon oncle et ma sœur. Merci de nous avoir fait confiance et de nous avoir toujours laissé une grande liberté, à Alice et moi, dans nos études et nos choix, même si parfois je pense que vous étiez sûrement autant dans le flou que nous. On a fait fausse route quelque fois, expérimenté des domaines très différents, changé de parcours plusieurs fois, mais finalement est ce que ce n'est pas mieux comme ça ? Merci pour votre grande ouverture d'esprit et nous avoir toujours transmis des valeurs d'altruisme, d'empathie et de bienveillance (et une solide culture ciné !). Merci aussi à Maguy et son sourire permanent d'avoir fait le déplacement pour la soutenance, c'était super de te revoir !

Merci bien-sûr à Alice, ma sœur d'amour et partner in crime depuis plus de trente ans maintenant. Véritable source d'inspiration, tu es tout simplement la personne la plus géniale sur Terre à tout point de vue (oui je peux l'affirmer et oui je connais les huit milliards d'humains de cette planète). Je serai toujours là pour toi Al ♡.

Enfin, merci à Rémi, mon freerider du quotidien avec qui je ne m'ennuie pas une seule seconde (même peut être pas assez parfois :)). Merci de constamment m'épauler et d'être présent quoiqu'il arrive. Merci de m'avoir appris à skier, à coincher, à conduire et j'en passe. Je t'aime très fort et pas qu'à Treffort (no joke).

Accroche toi, surtout ne cède rien de ta joie.
Nicolas Mathieu

Abstract

This thesis focuses on degradation models with imperfect maintenance actions. First, a literature review presents the existing research on degradation modeling, in particular the different processes used, and the impact of maintenance on degradation over time. It also discusses various statistical inference methods, particularly for estimating model parameters, and different approaches to assessing maintenance costs over time, and determining optimal maintenance policies to aid in the decision making process. The initial research of this manuscript focuses on statistical inference in a degradation model with imperfect maintenance. The underlying degradation process is a Wiener process with drift. Maintenance effects are assumed to be imperfect, described by an Arithmetic Reduction of Degradation (ARD1) model. The system is regularly inspected and degradation levels are measured. Four different observation schemes are considered so that degradation levels can be observed between maintenance actions as well as just before or immediately after maintenance. In this first study, the estimation of the model parameters under the four observation schemes are examined. Maximum likelihood estimators are derived for each scheme. The quality of the estimations is assessed and the observation schemes are compared through an extensive simulation and performance study. Following that, a more realistic way of modeling imperfect maintenance in degradation models is proposed, assuming that maintenance affects only a part of the degradation process. More precisely, the global degradation process is the sum of two dependent Wiener processes with drift. Maintenance has an ARD1-type effect on only one of these processes. Two particular cases of the model are considered: perturbed ARD1 and partial replacement models. The usual ARD1 model is also a specific case of this new degradation model. The system is regularly inspected in order to measure the global degradation level. A general observation scheme is considered, including various possible observation schemes, where degradation levels are only measured between maintenance actions but can be measured as close as possible from maintenance times. As previously, the maximum likelihood estimation of the model parameters is studied in both particular models. The quality of the estimators is assessed through a simulation study. Finally, based on this last degradation model, decision making is considered in the last chapter of this manuscript. Two inspection schemes are explored, whether degradation is inspected before maintenance or after repairs. In the pre-maintenance inspection scheme, the asymptotic maintenance cost per time unit is assessed using two different methods. A purely simulation-based method that evaluates maintenance costs across multiple life cycles

of the system, and a hybrid method, based on semi-regenerative Markov properties, that evaluates maintenance costs between two inspections. The inter-inspection period and the preventive replacement threshold are the decision variables considered to derive an optimal maintenance policy. Numerical outcomes of the optimal policies are presented and compared under both inspection schemes, according to model parameters and cost coefficients.

Résumé

Cette thèse se concentre sur des modèles de dégradation en présence de maintenances imparfaites. Tout d'abord, une revue de la littérature présente les travaux existants concernant les modèles de dégradation, notamment les différents processus et approches étudiés pour la modélisation de la dégradation et des effets de la maintenance. Elle présente également diverses méthodes d'inférence statistique, en particulier pour estimer les paramètres du modèle, ainsi que différentes approches pour évaluer les coûts de maintenance sur un intervalle de temps donné et établir des politiques de maintenances optimales, aidant à la prise de décision. Le premier travail de ce manuscrit se concentre sur l'inférence statistique d'un modèle de dégradation avec maintenances imparfaites. Le processus de dégradation sous-jacent est un processus de Wiener avec drift. Les effets de la maintenance sont supposés imparfaits et décrits par une réduction arithmétique de la dégradation d'ordre 1 (modèle ARD1). Le système est régulièrement inspecté et les niveaux de dégradation sont mesurés. Quatre différents schémas d'observation sont considérés de telle sorte que les niveaux de dégradation peuvent être aussi bien observés entre les maintenances, comme aux instants de maintenance, juste avant ou juste après celle-ci. Dans cette étude, les paramètres du modèle sont estimés suivant les quatre schémas d'observation. Les estimateurs du maximum de vraisemblance sont obtenus pour chacun de ces schémas. La qualité des estimations est évaluée et les schémas d'observation sont comparés à travers une étude de simulation et performance. Dans un second temps, un nouveau modèle de dégradation est proposé, plus adapté aux situations pratiques. L'effet de la maintenance n'affecte cette fois-ci qu'une partie du processus de dégradation. Plus précisément, le processus global de dégradation est la somme de deux processus de Wiener dépendants avec drift. La maintenance a un effet de type ARD1 seulement sur un de ces deux processus. Deux cas particuliers de ce modèle émergent : le modèle ARD1 perturbé et le modèle de remplacement partiel. Le modèle ARD1 usuel, tel que décrit dans le second chapitre, est aussi un cas particulier de ce nouveau modèle plus général. Le système est régulièrement inspecté pour mesurer le niveau de

dégradation global. Un schéma d'observation général est pris en compte pour l'inférence statistique, englobant plusieurs politiques d'observation possibles. Notamment, les niveaux de dégradation ne sont pas mesurés aux instants de maintenance mais peuvent être mesurés à tout autre moment, aussi proches possibles de ces instants là. A l'instar du premier modèle étudié dans le second chapitre, les paramètres des deux cas particuliers de ce nouveau modèle sont estimés par maximum de vraisemblance. La qualité des estimations est évaluée à travers une étude de simulation. En dernier lieu, la prise de décision est étudiée dans le dernier chapitre de ce manuscrit. Deux schémas d'inspection sont considérés, selon si l'inspection est réalisée juste avant maintenance ou juste après réparation. Pour le schéma d'inspection "pré-maintenance", le coût asymptotique par unité de temps est évalué suivant deux méthodes. Une méthode purement simulatoire qui évalue les coûts de maintenance sur un cycle de vie du système, et une méthode dite hybride, basée sur les propriétés de semi-régénération d'un processus de Markov qui évalue les coûts de maintenance entre deux inspections. La période entre deux inspections et le seuil de renouvellement préventif sont les variables de décision prises en compte dans l'optimisation de la politique de maintenance. Les résultats numériques des politiques de maintenance optimales obtenues sont présentés et comparés suivant les deux schémas d'inspection et en fonction de divers paramètres du modèle et coefficients de coût considérés.

Acknowledgement

This work is supported by the French National Research Agency in the framework of the « France 2030 » program (ANR-15-IDEX-0002) and by the LabEx PERSYVAL-Lab (ANR-11-LABX-0025-01).

Contents

List of Figures

List of Tables

Notations

f_X probability density function of X.

$f_{X|Y}$ conditional density of X given Y.

τ last potential observation time. Page. , 48

k number of maintenance actions. Page. , 48, 55, 59, 62, 66, 84, 93

τ_j maintenance times, $\forall\, j \in \{1, ..., k+1\}$. $\tau_0 = 0$, $\tau_{k+1} = \tau$. Page. , 35, 49, 50, 66, 78, 85, 86, 87, 91, 104, 105, 109, 134

n_j number of observations on $]\tau_{j-1}, \tau_j[$. Page. , 50, 53, 56, 62, 66, 67, 70, 71, 72, 84, 93

$t_{j,i}$ times where a degradation level can be observed, $\forall\, j \in \{1, ..., k+1\}$, $\forall\, i \in \{0, ..., n_j+1\}$. Page. , 50, 84

n total number of observations on $[0, \tau]$. Page. , 66, 69, 93

$N = \sum_{j=1}^{k+1} n_j$. Page. , 50

$\Delta t_{j,i} = t_{j,i} - t_{j,i-1}$, time interval between the $i-1^{th}$ and i^{th} observations over $[\tau_{j-1}, \tau_j]$. Page. , 50, 84

$\Delta\tau_j = \tau_j - \tau_{j-1}$, elapsed time between the $j-1^{th}$ and the j^{th} maintenance action. Page. , 79, 91

Δt_j^g elapsed time between the first and last observation on $]\tau_{j-1}, \tau_j[$ under the general observation scheme. For $j \geq 2$, $\Delta t_j^g = t_{j,n_j} - t_{j,1}$. For $j = 1$, $\Delta t_1^g = t_{1,n_1}$. Page. , 89

$X = \{X(t)\}_{t\geq 0}$: underlying degradation process, without maintenance actions. Page. , 48, 49

$X^U = \{X^U(t)\}_{t\geq 0}$, part of the underlying degradation process not affected by maintenance actions (U stands for Unmaintained). Page. , 77, 78, 79, 104, 128, 132, 136, 139

$X^M = \{X^M(t)\}_{t\geq 0}$, part of the underlying degradation process affected by maintenance actions (M stands for Maintained). Page. , 77, 78, 79, 81, 82, 83, 84, 86, 104, 109, 128, 132, 139

$X^S = \{X^S(t)\}_{t\geq 0}$ global underlying degradation process of the unmaintained system, $X^S = X^U + X^M$. Page. , 79, 81, 82, 83, 84, 86, 104, 136

$\Delta X_j^\ell = X^\ell(\tau_j) - X^\ell(\tau_{j-1})$, increment of the degradation process ℓ ($\ell \in \{S, M\}$) between the $j-1^{th}$ and the j^{th} maintenance action. Page.

$Y = \{Y(t)\}_{t\geq 0}$, degradation process of the maintained system. Page. , 48, 49, 78, 79, 81, 82, 112

$Y(\tau_j^-) = Y(t_{j,n_j+1})$, degradation level just before the j^{th} maintenance action. Page. , 35, 50, 55, 59, 62, 78, 86, 104, 109

$Y(\tau_j^+) = Y(t_{j+1,0})$, degradation level just after the j^{th} maintenance action. Page. , 35, 50, 62, 78, 86, 109, 135

$\Delta Y_{j,i} = Y(t_{j,i}) - Y(t_{j,i-1})$, increments of degradation, $\forall\, j \in \{1, ..., k+1\}$, $\forall\, i \in \{1, ..., n_j + 1\}$. Page. , 53, 54

$\rightarrow$ The random quantities are denoted by uppercase letters and their realizations by lowercase letters. For instance, $\Delta y_{j,i}$ is the observed value of $\Delta Y_{j,i}$.

$\Delta Y_{j,i}^c = Y(t_{j,i}) - Y(t_{j,i-1})$: i^{th} degradation increment in $[\tau_{j-1}, \tau_j]$. Page. , 85, 87

$\Delta Y_j^c = Y(\tau_j^-) - Y(\tau_{j-1}^+) = \Delta X_j^{(1)}$: observed degradation increment on $[\tau_{j-1}, \tau_j]$ under the complete observation scheme. Page. , 91

$\Delta Y_j^g = Y(t_{j,n_j}) - Y(t_{j,\mathbb{1}_{j>1}})$: observed degradation increment on $]\tau_{j-1}, \tau_j[$ under the general observation scheme. As the first degradation increment $\Delta y_{1,1}^c$ is always observed, $\Delta Y_1^g = Y(t_{1,n_1})$ and $\forall\, j \in \{2, ..., k+1\}$, $\Delta Y_j^g = Y(t_{j,n_j}) - Y(t_{j,1})$. Page. , 89

Z_j^s observed degradation jump around the j^{th} maintenance for observation scheme s. Page. , 52, 53, 54

$Z_j^c = Y(\tau_j^+) - Y(\tau_j^-)$: observed degradation jump at the j^{th} maintenance time for the complete observation scheme. Page. , 49, 52, 54, 79, 86, 99

$Z_j^g = \Delta Y_{j+1,1}^c + Z_j^c + \Delta Y_{j,n_j+1}^c$: observed degradation jump around the j^{th} maintenance time for the general observation scheme. Page. , 63, 64

μ_U drift parameter of the underlying degradation process X^U. Page. , 77, 104, 128

μ_M drift parameter of the underlying degradation process X^M. Page. , 77, 80, 95, 96, 104, 128, 132, 139, 141

μ_S drift parameter of the underlying degradation process X^S. Page. , 80, 95, 96

σ_U^2 variance parameter of the underlying degradation process X^U. Page. , 77, 104, 128

σ_M^2 variance parameter of the underlying degradation process X^M. Page. , 77, 80, 93, 95, 96, 97, 104, 128

σ_S^2 variance parameter of the underlying degradation process X^S. Page. , 80, 93, 95, 96, 97, 99

c_{UM} covariance parameter of the underlying degradation processes X^U and X^M. Page. , 77, 104

c_{SM} covariance parameter of the underlying degradation processes X^S and X^M. Page. , 80

r_{UM} coefficient of correlation parameter of the underlying degradation processes X^U and X^M. Page. , 104, 128, 132

r_{SM} coefficient of correlation parameter of the underlying degradation processes X^S and X^M. Page. , 80, 93, 95, 96, 97, 99

ρ maintenance efficiency parameter. Page. , 35, 52, 56, 59, 66, 67, 68, 69, 72, 73, 78, 93, 95, 97, 104, 128, 133, 141

Θ set of all parameters in the second parametrization, $\Theta = (\mu_S, \mu_M, \sigma_S^2, \sigma_M^2, \rho, r_{SM})$. Page. , 84

$\Theta_1 = (\mu, \sigma_S^2, \sigma_M^2, \rho, r_{SM})$, set of parameters for the perturbed ARD_1 model. Page. , 92

$\Theta_2 = (\mu_S, \mu_M, \sigma_S^2, \sigma_M^2, r_{SM})$, set of parameters for the partial replacement model. Page. , 92

$\mathcal{O}_t^h$ set of observed data before time t for scheme h. $h \in \{c, g\}$ where c stands for "complete" and g stands for "general"..

$\mathcal{O}_t^s$ set of observed data before time t for scheme s. $s \in \{1, 2, 3, 4\}$ where 1 is equivalent to the "complete" observation scheme and 4 is equivalent to the "general" observation scheme..

$\widetilde{\tau}$ inter-inspection time, $\forall\ j \geq 1,\ j\widetilde{\tau} = \tau_j$. Page. , 104, 105, 112, 113, 119, 122, 124, 126, 127, 129, 130, 131, 133, 136, 137, 138, 139, 141

T duration of a life cycle of a system. Page. , 108

M preventive replacement threshold. Page. , 105, 116, 119, 122, 124, 126, 127, 129, 130, 131, 132, 134, 136, 137, 138, 139, 141

L corrective replacement threshold. Page. , 105, 113, 116, 118, 119, 129, 130, 134

$c(t)$ global maintenance cost at time t. Page. , 107

c_I cost of inspection. Page. , 106

c_R cost of repair. Page. , 106

c_P cost of preventive replacement. Page. , 106

c_C cost of corrective replacement. Page. , 106

c_D cost rate of unavailability after failure. Page. , 107

$d(t)$ time during which the system is not available over $[0, t]$. Page.

$\widetilde{\tau}^*$ optimal inter-inspection time (the inter-inspection time that minimizes the average cost). Page. , 131, 132, 133, 138, 139

M^* optimal preventive threshold. Page. , 127, 130, 131, 132, 133, 137, 138, 139, 141

Q_ℓ index of the inspection time referring to the ℓ^{th} replacement. Page. , 108

R_j random variable describing the type of the j^{th} maintenance action, such that $R_j = \mathbb{1}_{\{R_j^p=1\}} + \mathbb{1}_{\{R_j^c=1\}}$ and $R_0 = 0$, where R_j^p, resp. R_j^c, equals 1 when the j^{th} maintenance action is a preventive replacement, resp. corrective replacement. Page. , 108

N_{cyc} Number of life cycles specified for the simulation of degradation trajectories. Page. , 111, 136

Acronyms

ABAO As Bad As Old. , 35

AGAN As Good As New. , 35, 103, 108

ARA Arithmetic Reduction of Age.

ARA$_\infty$ Arithmetic Reduction of Age of order infinity. , 34, 35

ARA$_1$ Arithmetic Reduction of Age of order 1. , 35, 48

ARD Arithmetic Reduction of Degradation.

ARD$_\infty$ Arithmetic Reduction of Degradation of order infinity. , 36, 37

ARD$_1$ Arithmetic Reduction of Degradation of order 1. , 35, 36, 37, 47, 48, 49, 52, 56, 73, 76, 77, 78, 82, 83, 84, 85, 86, 92, 93, 95, 97, 99, 100, 104

EM Expectation Maximization. , 37

MLE Maximum likelihood Estimation. , 37

PDF Probability Density Function. , 20, 21, 37, 56, 63, 85, 100, 101, 116, 117, 144

RUL Remaining Useful Life. , 29, 41, 43

Introduction

Technological or industrial equipment and engineering assets (or systems) such as dikes, dams, wind turbines or power plants undergo degradation due to intrinsic wear, usage imposed by operating conditions or exposure to environmental factors. For such repairable industrial equipment and assets, a critical concern is to maintain their operation within specific conditions that ensure safety and availability. In order to reduce deterioration and mitigating risks, maintenance actions are performed on these industrial systems, altering their degrading behavior over time.

Degrading systems in historical contexts

Throughout history, many examples have shown the critical importance of understanding the reliability of reparable systems over time to prevent failures (when degradation exceeds a critical threshold) and accidents. To name a few, on April 27, 1895, the Bouzey dam, built a few years earlier in Eastern of France, failed, releasing a massive flood wave that caused extensive damage to the nearby villages and infrastructures, Figure 1. A few years before the failure, several cracks and leaks had been reported, but ineffectively repaired, leading to the accident [88]. On June 3, 1998, an ICE 1 train operating on the Hannover-Hamburg railway derailed near Eschede in Lower Saxony, Germany, claiming 101 lives and causing many injuries. This accident was attributed to a fatigue crack in the wheel, leading to wheel failure. A part of the wheel got caught in a railroad switch, changing its direction as the train passed over it. Consequently, the carriages of the train followed two distinct tracks, resulting in the derailment [32]. On 14 August 2018, a section of the Morandi bridge collapsed in Genoa, Italy, sweeping away around 30 vehicles and resulting in the loss of 43 people, Figure 2. This accident was attributed to a general fatigue problem

and corrosion in the tendons (high-strength cables or strands) [13].

As illustrated in these tragic events, in many different fields, effectively modeling the degradation of industrial systems in order to anticipate failures and implement better maintenance policies presents a key challenge to ensure safety and reliability of the system.

Figure 1: Repair of the post-failure Bouzey dam, 1895

Figure 2: A photography of Morandi bridge post-collapse [23]

Degradation modeling

In order to represent the degradation behavior, better anticipate eventual failures, and efficiently plan maintenance activities, one of the main issue consists in developing a practical degradation model that considers real-world scenarios and takes maintenance effects into account.

First of all, let us briefly remind some fundamental probability concepts [2], which are widely used throughout this manuscript.

- In probability theory and statistics, a random variable is a variable whose value depends on the outcome of a random experiment.
- A probability distribution is a mathematical model that describes the behavior of a random experiment. More precisely, this distribution quantifies the probabilities associated with each possible outcome of the random experiment.
- A probability density function (PDF) is a function describing the probability distribution of a continuous random variable.
- A stochastic process is a model used to describe the evolution of a random variable over time [26].

In this manuscript, degradation is considered random and continuous over time. Consequently, continuous-time stochastic processes prove to be well-suited for modeling the evolution of the system deterioration with time. Specifically, Levy processes [67], with their independent and stationary increments (these properties are further detailed in Chapters 1 and 2), are particularly convenient for degradation modeling over continuous time. These increments follow a specific probability distribution, chosen based on the degradation indicator of the considered system, or, more generally, chosen to align with various practical case studies. For instance, in practice, system degradation may occasionally decrease during short time intervals, indicating an improvement in the system condition. To model that specific situation, the selected probability distribution must allow the simulated degradation to be non-monotonous. As an example, when modeling degradation increments, the Gaussian distribution (or normal distribution) is a commonly used model, characterized by two parameters: its mean and its variance (see [97] for a review on common probability distributions). The values of the Gaussian-distributed increments are defined over $\mathbb{R}$ and are symmetrically distributed around the mean parameter, with a higher probability of values being close to this parameter. The variance parameter represents the dispersion of all these increments values from the mean. Alternatively, when degradation is monotonically increasing over time, it is more accurate to describe it using a positively defined distribution. For example, positive degradation increments can be modeled by a Gamma distribution, whose PDF is positively defined. Besides, the Poisson distribution, frequently used to model the number of occasional events within a limited time, can be included in the degradation process to describe occasional shocks that accelerate the degradation of a system.

Furthermore, within a single system, several components can undergo degradation. This degradation can be modeled by multivariate processes, more or less correlated, within the same degradation model. For example, considering the track geometry of a railway in Figure 3, the track alignment tends to undergo deformation over time, both longitudinally and transversely. Then, two distinct yet correlated processes can be proposed to model this type of deterioration.

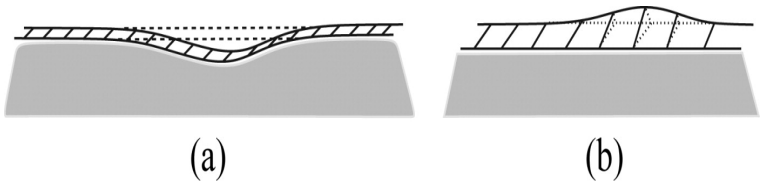

Figure 3: Examples of longitudinal and transversal track levelling [74]

However, the behavior of system degradation experiences punctual changes when maintenance actions are performed. Within its life cycle, the system can undergo various maintenance actions. Maintenance can be referred to "imperfect" when its impact fails to reduce degradation to its initial state. On the opposite, "perfect" maintenance resets degradation to the initial system condition, initiating a new life cycle for the system. Typically, this last type of maintenance can consist in a replacement of the system or the component. In addition, maintenance can be preventive or corrective. On the one hand, preventive maintenance is regularly performed to prevent potential failures, either periodically or by optimizing its frequency based on inspected degradation levels over time. Corrective maintenance, on the other hand, is carried out after the failure of the system. Its frequency depends on the system's condition. Corrective maintenance is generally more costly than preventive maintenance and may involve an unavailaibilty period of the system. Hence, the challenge is to identify an appropriate model capable of precisely depicting both the evolution of degradation and multiple maintenance effects on the system.

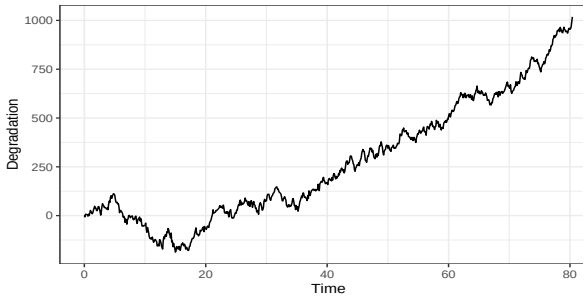

Figure 4: Example of a degradation trajectory over time, simulated through multiple degradation increments modeled by a Wiener process with positive drift

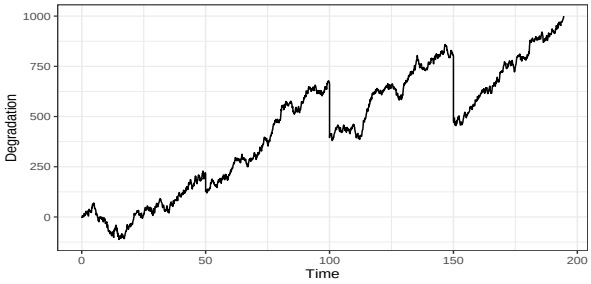

Figure 5: Example of a degradation trajectory with periodic imperfect maintenance actions (every 50 time units)

An example of a simulated degradation trajectory is presented in Figure 4 over the time

interval $[0, 80]$. In this figure, the degradation increments of the process follow a Gaussian distribution with a positive mean. Since the support for a Gaussian distribution is $\mathbb{R}$, even if the general trend of degradation increases over $[0, 80]$, degradation can still decrease over some time intervals. In Figure 5, degradation undergoes three periodic imperfect maintenance actions carried out at times $\{50, 100, 150\}$, illustrated by the vertical segments. In this example, the maintenance effect is considered instantaneous and is proportional to the accumulation of degradation since the last maintenance action. This explains why the depicted maintenance effects differ from each other. Specifically, the first imperfect maintenance shows a minimal impact on degradation, as degradation does not significantly increase over the first time interval $[0, 50]$.

Additionally, the system can undergo partial maintenance effects, wherein maintenance interventions are carried out only on specific components rather than the entire system. In that scenario, while a part of the system is regularly maintained, the remainder is left unchanged, keeping degrading over time. As an illustration, considering a vehicle's braking system, it is often necessary to evaluate degradation and conduct repairs on the brake pads but not on the whole disc, Figure 6. Therefore, when multiple processes are involved in the degradation model, partial maintenance effects can consist in affecting only a limited number of these processes.

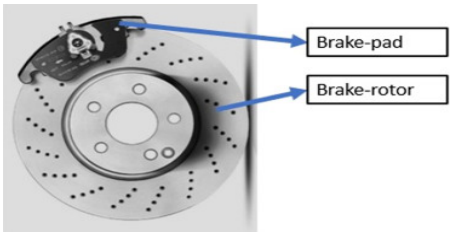

Figure 6: Disk-brake assembly [77]

Another practical illustration regarding degradation modeling is depicted in Figures 7 and 8. EDF (Électricité de France) presents a case study that consists in modeling support tube plates degradation in a steam generator, as shown in Figure 7. Within a steam generator, the tubes undergo significant vibrations, and the support plates play a crucial role in preventing this shaking. Over time, these plates accumulate dirt, reducing their efficiency. The thickness of dirt can serve as an indicator of degradation. In Figure 8, degradation levels are observed using three different monitoring techniques. These three methods describe the same degradation phenomenon within the steam generator. The first graph (located at the top of the figure) is a visual indicator, regularly capturing degradation on the support plates via a camera positioned within the system. This procedure requires a temporary system shutdown. In the second graph, degradation is punctually monitored using Eddy current testing [17], also requiring a system shutdown. In the third graph, fluid pressure measurements inside the tubes are collected through frequent monitoring. No

shutdown are needed for this last technique. Degradation levels are observed at different locations inside the steam generator, either in the hot leg pipe or in the cold leg pipe (refer to Figure 7), denoted by crosses and points. Notably, in this figure, the maintenance effect is clearly visible. The observed degradation levels are increasing over time (the x-axis), then instantaneously reduced right after the maintenance action (denoted by the blue dashed line). In this example, time scale is censored to ensure confidentiality.

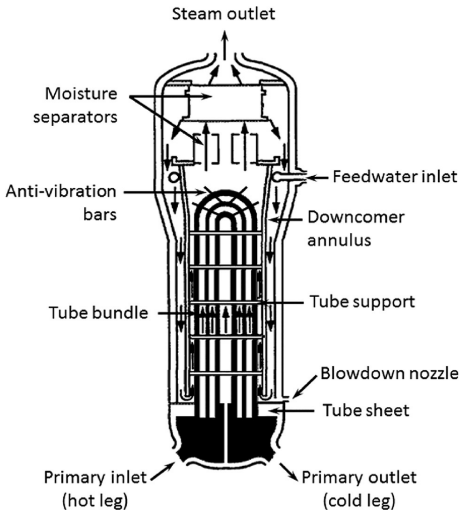

Figure 7: Support plates inside a steam generator [84]

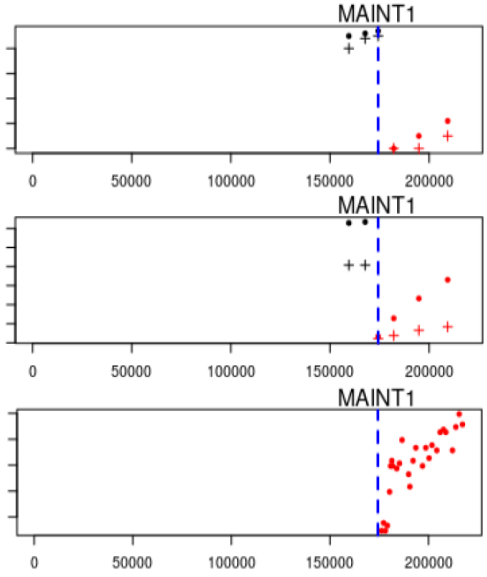

Figure 8: Inspected degradation levels as a function of time, collected on support plates inside a steam generator

Statistical inference

The selected degradation model includes multiple parameters. These parameters can be associated with the underlying degradation process, describing for example its drift, its variance, its shape, its scale etc. and can also be related to the maintenance effect, outlining its efficiency. For instance, in Figure 9, three degradation trajectories are displayed, modeled by independent underlying degradation processes based on three Gaussian distributions with different values of drift (μ) and variance (σ^2), respectively $\mathcal{N}(5, 200)$ (this notation stands for the normal distribution with drift parameter equals 5 and variance parameter

equals 200) in purple, $\mathcal{N}(15, 1000)$ in pink and $\mathcal{N}(30, 30)$ in orange. As shown in this figure, the model parameters define the behavior of the degradation evolution. Thus, assessing the theoretical value of these parameters is a major task to precisely describe the degradation.

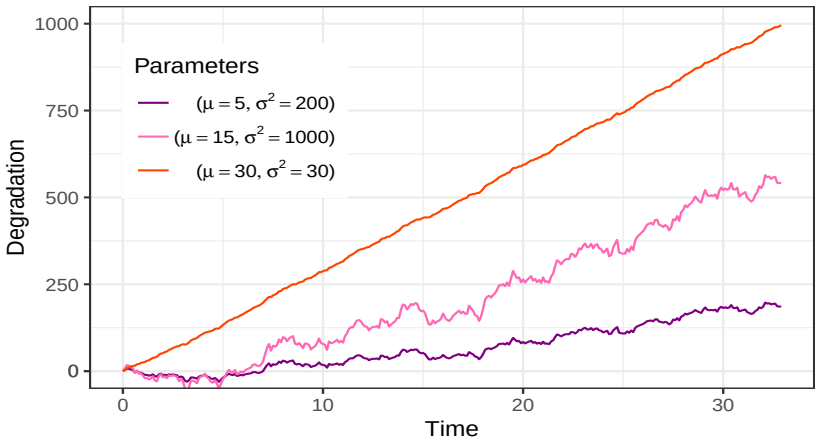

Figure 9: Examples of three simulated degradation trajectories based on different values of the model parameters

The complexity and the precision of their estimation in the degradation process is mainly influenced by the number of considered parameters, their interdependence, their theoretical values, the number of available observed degradation levels, and the location of these observations along the degradation trajectory. Particularly, in practical situations, providing limited data samples and keeping data confidentiality, such as censoring maintenance times, adds complexity to modeling degradation and maintenance effects as well as assessing the parameters. This procedure of evaluating model parameters based on a limited sample of observations is referred to as statistical inference [82].

Moreover, based on the characteristics of the system, degradation levels can be observed at different times: At the exact maintenance times (immediately before and/or after the intervention), only between maintenance times, or even both between and during maintenance times. In this manuscript, the chosen scheme describing the instants and locations of the observations along the degradation trajectory is called the observation scheme. In addition, in practice, the observation scheme can differ from one maintenance to another within a single system. Besides, in some specific scenarios, degradation levels can also be observed continuously on the system. As the choice of the location of the observations around the maintenance action provides different insights into degradation and maintenance effect, the

chosen observation scheme may impact the quality of parameter estimations. Therefore, it is necessary to opt for a relevant and realistic observation scheme that ensures high-quality parameter estimations.

Decision making

Another issue regarding degrading systems consists in optimizing the maintenance scheduling. Indeed, each type of maintenance action incurs its own specific cost. In practice, preventive maintenances are frequently scheduled periodically, without considering the current state of the system or the global maintenance cost, which includes the cost of all the considered maintenance actions carried out on the system within a specific time period. In addition, conducting maintenance actions or just inspections can be very expensive as it may require the shutdown of system components or complicate operational procedures. Furthermore, performing a maintenance action can sometimes partially damage the system, accelerating its degradation. Therefore, in order to avoid premature or unnecessary interventions, anticipate costly failures and make better decisions regarding future maintenance actions, it is crucial to implement a suitable maintenance strategy. To achieve this, factors such as degradation thresholds, above which a specific maintenance action must be triggered, as well as imperfect maintenance or inspection frequencies are considered in the assessment of the global maintenance cost. These decision variables can be optimized by minimizing the maintenance cost over a specific time period. Thus, proper methods need to be proposed to precisely evaluate the maintenance cost over time, and, thereafter, determine optimized maintenance policies based on specific decision variables.

Hence, based on the observation of various industrial degrading assets, the main difficulty in apprehending deterioration, entails identifying an appropriate degradation model that can precisely describe the unique deterioration of the system. In this manuscript, stochastic processes over continuous time are chosen to model degradation. Therefore, determining a proper model involves exploring one or multiple degradation processes, more or less dependent, to describe degradation impacted by specific maintenance effects over the system's lifespan. This model should be able to adjust to various observation schemes, enabling properly chosen methods to precisely estimate model parameters. Based on this

model, maintenance assumptions can be suggested, specifying the effect of different possible interventions performed on the system according to the current degradation level. Thereafter, suitable methods should be proposed to assess the cost of each considered maintenance over a specific period. The derived costs, considering various values of the studied decision variables, should enable the recommendation of enhanced maintenance policies.

Chapter 1

Degradation models with imperfect maintenance actions

This chapter provides an overview of degradation models in the literature. To analyze the system deterioration process, gain deeper insights into the failure behavior, and enable better maintenance decisions, various degradation models are studied in many different fields. These models should be able of capturing the underlying random degradation phenomena. Nowadays the representation of maintenance effects regarding degradation models is increasingly prevalent in the literature. In Section 1.1, a review on multiple stochastic processes is presented for modeling degradation with possible maintenance effects. Modeling such processes may introduce additional challenges, such as identifying analytic distributions associated with these degradation models (for example the Remaining Useful Life (RUL), the first hitting time, etc.), ensuring the model's identifiability for statistical inference studies, and evaluating maintenance costs, among other considerations. As outlined in Section 1.2, statistical inference is mainly mentioned in the literature regarding degradation models and various techniques are used to assess model parameters. After choosing a proper degradation model, multiple maintenance policies are suggested and described in Section 1.3, based on specific decision variables, such as the inter-inspection period, the inter-repairs period, the preventive replacement threshold or the corrective replacement threshold. Maintenance policies can be optimized by evaluating and minimizing the maintenance cost.

1.1 Degradation modeling

Multiple models are available to represent the reliability of a system. To characterize the lifespan of components, anticipate potential failures and the remaining life of a system, and plan preventive maintenances, survival analysis models are frequently considered in the literature. A classic challenge regarding these types of analyses consists in modeling the failure rate, i.e. the probability for a component to fail in the next instant, given that it has survived up to a certain point in time. To choose the proper model, commonly distributions are proposed in the literature, such as exponential, normal, lognormal, Weibull, Gamma, among others [8, 76]. These distributions can be chosen based on a specific case study and take into account the unique characteristics of the system. However, these survival analyses will not be further explored, as it is out of the scope of this manuscript. Another approach to assess system reliability involves the use of degradation models, where the degradation behavior of the system is modeled over time. This degradation as a function of time can be either discrete or continuous, as well as characterized over discrete or continuous times. A typical way to describe such models is the use of stochastic processes, where degradation is random and evolves with time. Extensive research in the literature has focused on these processes, using a variety of specifically selected distributions. More recently, maintenance effects have been added to this degradation process to better apprehend the system's deterioration over its life cycle.

1.1.1 Overview of different stochastic processes

Since a system's degradation randomly evolves with time, stochastic processes are well suited for modeling system's deterioration, as described in [26]. For example, Levy processes are widely used to model degradation over continuous time. A Levy process [67], $\{X_t\}_{t\geq 0}$, is defined by:

- $X(0) = 0$ almost surely
- The independence of its increments: For any $s, t;\ 0 \leq s < t$, all its increments $X_t - X_s$ are independent over disjoints time intervals
- Its stationary increments : For any $s, t;\ 0 \leq s < t$, $X_t - X_s$ is similarly distributed as X_{t-s}
- $t \to X_t$ is almost surely right-continuous with left limits

Specific distributions are commonly employed to characterize the degradation increments over time intervals. Among the well known Levy processes are the Gamma process, with increments following a Gamma distribution defined by a shape and a scale parameter, the Wiener process, with increments following a normal distribution defined by its drift and variance parameters and the Poisson process, where increments follow a Poisson distribution with an intensity parameter. First of all, Gamma processes are very popular in modeling system degradation [1, 59, 93, 37]. In [71], the leveling of railway track is altering with time. Based on expert judgments, this type of deterioration is modeled by a gamma process. In the same application field, and already mentioned in the introduction, Mercier et al. [74] model both longitudinal and transversal leveling of a railway track using a trivariate reduction: Three independent Gamma processes are initially considered to construct a bivariate Gamma process that describes the two leveling indicators.

Wiener processes are also widely used in degradation models. A Wiener process $\{X_t\}_{t\geq 0}$ with drift is described as follows.

$$X(t) = \mu\ t + \sigma\ B(t)\ ; \qquad X(0) = 0$$

Here, $X(t)$ represents the degradation level at time t, μ is the drift parameter, σ is the standard deviation parameter and $B(t)$ is a Brownian motion. Specifically, for any $s, t;\ 0 \leq s < t$, the increment $B(t) - B(s)$ follows a normal distribution with zero drift and a variance equal to $t-s$. The degradation increments of a Wiener process, as a Levy process, are notably characterized by their independence over disjoints time intervals and by their associated normal distribution, such that $X(t)-X(s) \sim \mathcal{N}\big(\mu(t-s), \sigma^2(t-s)\big)$. Thus, unlike gamma processes, the evolution of degradation modeled by a Wiener process can be non-monotonous, and decrease over some time intervals. In [25], a Wiener process with drift is used as a health indicator to represent the biomarker decrease for HIV infected individuals. Whitemore [98] also uses a Wiener process to model the wear of components and materials. Different variants of the Wiener-based degradation model are also described in literature: Ye et al. [102] propose to add random effects on a Wiener-based degradation model. The accuracy of this model is demonstrated on real datasets, such as a fatigue crack growth and head wear of hard disk drives. In Zhang et al. [104], a nonstationary Wiener process (i.e. a Wiener process with a non-linear drift) is considered and applied to gyroscopic drifts in inertial navigation systems. In [107], multiple variants of Wiener-based degradation models are considered, involving nonlinearity, multisource variability, covariates and multivariate

aspects in the model. Yet, degradation might as well presents a non-continuous pattern. In [94], a homogeneous Poisson process, i.e. a Poisson process with constant rate parameter, is used to model fatal and nonfatal shocks, each one occurring with a specific probability. Markov processes are also commonly used in the literature regarding degradation models. A Markov process is a stochastic process in which the future state of the system depends only on the current state [31]. Therefore, the system has no memory of its past states. The different levels of a system state can be defined on a continuous state space or on a discrete space state and occur over continuous time or discrete time. For instance, Kallen et al. [53], employs a Markov process over continuous time and discrete condition states using bridge condition data in the Netherlands. Le et al. [60] also uses a continuous-time Markov process to model multi-state systems. Moreover, a discrete state-space Markov process over discrete time, and initially based on a gamma process, is proposed in [81] to study pitting corrosion. Finally, Zhang et al. [105] use a discrete-time semi-Markov degradation model to describe the deterioration of the roads. In this article, the degradation level of the road is categorized into discrete performance states, and the duration for which the process remains in the current state, referred to as the holding time, follows a discrete Weibull distribution. The term "semi" Markov process comes from the non-exponential distribution of the holding time (in a standard Markov process, the holding time follows an exponential distribution) [44]. Let us also highlight that, as previously mentioned in some specific case studies, system degradation is often caused either by the deterioration of multiple dependent components, each may which exhibit a unique degradation behavior within the same considered system, or by various environmental factors. To model such complex degradation scenarios, multivariate stochastic processes can be used, taking into account multiple degrading as well as non-degrading components [4, 74, 64, 107, 95, 6].

Deterioration can also be modeled by less common stochastic processes. Hsieh et al. [45] propose to model the leakage current of thin gate oxides by a discrete degradation model based on a non homogeneous Weibull-compound Poisson process. The variance-gamma process is used in [85] to model the continuous leakage rate of a centrifugal pump, the inverse-gamma process, first introduced in [43] as a wear model to describe an increasing degradation, has been reused ever since [39]. Wang and Xu, Ye and Chen [96, 101] propose the inverse Gaussian process where increments are also independent on disjoint time intervals and follow an inverse Gaussian distribution. In [35], the transformed-beta process is introduced but this time, degradation increments are positively correlated over disjoint time intervals. Degradation can also be characterized by continuous processes over discrete

times. For instance, [38] introduces a generalization of the non-stationary Gamma process, which can be seen as the extended Gamma process based on a time discretization. Another approach consists in including differential equations into stochastic processes, which are well-suited for describing physical models. In [29], a degradation model relies on differential equations to depict the degradation process of wind turbines. In [66], the studied degradation model is based on a stochastic partial differential equation, connecting statistics and physics and including space-time covariances to provide a more relevant model to practical situations.

However, alternative approaches, not necessarily relying on stochastic processes, can be used to model systems degradation. For example, certain industrial units are better suited to be characterized by physics-based models. Starters in auxiliary power units, which generate energy in aircraft, undergo degradation over their lifespan, potentially leading to failure. Hanachi et al. [42] explore the degradation of gas turbine engines, employed in both aircraft propulsion and industrial power generation. Their approach involves a thermodynamic model using the heat loss and power deficit as degradation indicators. Additionally, Zhang et al. [106] employ exhaust gas temperature as a degradation indicator and propose two distinct models. One physics-based model involves measures of the peak exhaust gas temperature, the shaft speed at peak, the ambient temperature and the ambient pressure. Another generic model is proposed based on neural networks.

Let us also point out that, for a more realistic approach and based on a specific degrading system, degradation models sometimes incorporate human errors. In Zhai et al.'s study [103], an underlying Wiener process is used to model degradation in burn-in models (burn-in refers to the initial period of operation for a system, during which it undergoes multiple tests to identify potential issues or failures [5]). Human errors in the degradation measurements are taken into account in these burn-in degradation models and are characterized by a Gaussian distribution added to the degradation process. Moreover, Che et al.'s research [16], show the interdependence between degrading systems and human errors induced by system manipulation. In their article, degradation is modeled by a semi-Markov process and human errors follow a non homogeneous Poisson process. However, human errors are not considered in this manuscript, as the explored degradation models are more general and not applied to a specific system whose degradation could be influenced by these types of errors.

1.1.2 Maintenance effect in degradation models

In order to contain degradation or avoid failures, systems undergo preventive or corrective maintenances. Nowadays, an increasing number of degradation models consider maintenance effects. Various types of maintenance actions can be performed on a degrading system.

For instance, replacement of components can be carried out on the system when the inspected degradation level exceeds a given threshold, or to prevent or respond to a failure. These replacements can be partially performed. For example, only one or few components of the system can be replaced while the other part of the system keeps deteriorating with time. In [65], in the context of traffic light systems of the Norwegian railway network, processes approximated by virtual age models (such as ARA_∞ and copula models, based on multivariate distribution functions) are studied and compared to each other to model independent industrial components in series configuration. A failed component is automatically replaced whereas the other components are minimally maintained.

In practice, repairs, excluding replacements, are often imperfect as the system does not return to a brand-new state after the intervention. Various techniques are used to model such effects. In [104], a degradation-rate function and a degradation-rate reduction factor are considered to describe the maintenance effect. In [110], a time-scale transformation function is included in the Wiener-based model to capture non-linearity in degradation and an improvement factor characterizes the maintenance effect. Ma et al. [69] consider that all the degradation model's parameters are random variables, and a residual damage coefficient is added to the degradation level after each maintenance. Furthermore, the degradation level can also be directly reduced when maintenance is performed: In [63], degradation is modeled by a Wiener process and the degradation level just after maintenance is a random variable described by a beta distribution (which is a special case of the Dirichlet distribution, [22]). Similarly, Kamranfar et al. [54] consider a Gamma process as a degradation model, and the maintenance effect reduces degradation by a random quantity that follows a doubly truncated gamma distribution (both left and right tails of the distribution are cut). In [18], degradation levels right after imperfect maintenance follow an exponential distribution. Using an exponential distribution for degradation value just after maintenance can be better suited for practical situations and can simplify analysis and calculations [40].

Maintenance effects can also be presented as a reduction in the system's age. The concept of virtual age, initially introduced by Kijima [56] in the context of survival analyses

and reused in [28], when applied to degradation models, consists in reducing degradation such that the system rejuvenates after repair. Based on this idea, Mercier et al. [73, 72] propose the ARA_1 model on a gamma process. In these last articles, each repair removes a certain percentage of age accumulated since the last maintenance. Kahle et al. [50] consider Kijima's approach to model the maintenance effect on a Wiener-based degradation model describing both the reduction of degradation level and the reduction of virtual age. Wang et al. [95] also use the ARA_1 and ARA_∞ model on a time scale adjustment model using a multivariate Wiener process.

Mercier et al. [73] first introduced the ARD_1 model (Arithmetic Reduction of Deterioration of order 1) which involves reducing degradation at maintenance times by a certain quantity, proportional to the degradation accumulated since the last maintenance action. Based on this approach, Salles et al. [87] also use the ARD_1 model on a non homogeneous gamma process where $\rho \in [0, 1]$ is the maintenance efficiency parameter, i.e. the proportion of the accumulated degradation since the last maintenance that is removed every time a repair is performed. When $\rho = 0$, maintenance effect is minimal and degradation keeps increasing as if no maintenance had been performed on the system. This specific situation is called ABAO (As Bad As Old). On the opposite, when $\rho = 1$, the maintenance is optimal and the system is like a new one after the maintenance. This situation is called AGAN (As Good As New). More specifically, the ARD_1-type maintenance effect on a given univariate process $\{X(t)\}_{t\geq 0}$ can be described as follows:

Let $\tau_1, \tau_2, ..., \tau_k$ be the maintenance times, i.e. times at which a maintenance is performed. Let $X(t)$ be the degradation level of a non-maintained system at time t. Let $Y(t)$ be the degradation level of a maintained system at time t and $\rho \in [0, 1]$ the maintenance efficiency parameter, which equals zero when the maintenance effect is minimal. If maintenance actions are assumed to be instantaneous, let $\forall\ j \in \{1, ..., k\}$, $Y(\tau_j^-)$ and $Y(\tau_j^+)$ respectively be the degradation level right before and right after the j^{th} maintenance at time τ_j. If maintenance effects are ARD_1-type, the degradation level just after the j^{th} maintenance is:

$$Y(\tau_j^+) = (1 - \rho)\ X(\tau_j)$$

The value of degradation jumps $Y(\tau_j^+) - Y(\tau_j^-)$ for all $j \in \{1, ..., k\}$ at maintenance times is proportional to the degradation accumulated since the last maintenance:

$$Y(\tau_j^+) - Y(\tau_j^-) = -\rho \ (X(\tau_j) - X(\tau_{j-1}))$$

The arithmetic reduction of degradation is often used as a maintenance effect in the literature: Corset et al. [21] model degradation using a gamma process, and maintenance effect is ARD_∞. Based on this model, the degradation level just after maintenance depends on all the degradation accumulated since the very beginning of the system's deterioration process. In [86], both ARD_1 and ARD_∞ are explored in the context of a gamma-based degradation model. Lastly, in [85], a variance gamma process is used to model the leakage rate of a centrifugal pump, and maintenance effects decrease degradation by varying percentages.

Hence, the literature on degradation models offers multiple stochastic processes to effectively model degradation over time. Specifically, these processes can be univariate or multivariate, exhibiting varying degrees of dependency. They may be compound processes based on different distributions and can include various sets of parameters, which are not necessarily homogeneous (i.e. constant over time). Covariates can also be taken into account in the degradation process. Additionally, maintenance effects are more and more considered in this process. Many different approaches have been proposed to capture this notable shift in the evolution of system degradation. This diversity of degradation models enables a precise description of the unique evolution of deterioration for each asset and its response to maintenance interventions.

1.2 Statistical inference

After establishing an appropriate deterioration model, statistical inference can be conducted to estimate the parameters of the model. For instance, in a Wiener-based degradation model with imperfect maintenances, the theoretical values of both drift and variance of the Wiener process along with the maintenance efficiency parameter should be considered for statistical inference. The chosen methods to estimate parameters rely on the selected model, the number of involved parameters, their correlation and the available data. Deriving an analytic writing of the estimators can be a complex task. Thus, numerical approaches can be preferred in the parameters estimation process.

1.2.1 Methods for inference

Statistical inference is often explored in the context of degradation models, where different techniques are employed to estimate the model parameters. As a reminder, in statistics, the likelihood function represents the joint probability density function (PDF) of the observed data as a function of the model parameters [48]. Maximum Likelihood Estimation (MLE), further detailed in [48], is frequently used to estimate parameters of degradation processes. The key concept is to determine optimal parameters that maximize the log-likelihood function given the observed data [51, 54, 109, 35, 21, 45]. In the article by Chuang et al. [18], degradation levels after maintenance follow an exponential distribution that incorporates a rectification effort parameter estimated using the MLE method [24]. Additionally, there are many alternative methods for parameter estimation. For instance, in [108], the Expectation-Maximization (EM) algorithm is employed when degradation levels are not observable after maintenances. Zhang et al. [104] use a quasi Monte-Carlo method, introduced in [83], to evaluate fixed parameters of the model and a specific filtering technique to assess the maintenance effect. As mentioned earlier, [74] employ a bivariate gamma process based on a trivariate reduction to model the leveling of a railway track. Given that the likelihood's expression is more complex to optimize in this case compared to the likelihood of a univariate process, both EM algorithm and MLE are employed to estimate all five model parameters. Salles et al. article [87] estimates the maintenance efficiency parameter from an ARD_1 model using a semiparametric method, as the estimation of this parameter relies only on the data and not on the other parameters of the underlying Gamma process. In [54], two different maintenance effects are proposed for inference depending on the available data: If the sample of degradation levels just before corrective maintenance is available, then a reduction of the degradation is taken into account. Alternatively, if only time durations of a maintenance cycle are available, a reduction in the system's age is studied. In both scenarios, two specific likelihoods are derived and globally maximized, even though this process can be time-consuming. Furthermore, the method of moments is also quite popular for inference [9, 3, 86]. Grounded in the law of large numbers, this intuitive method expresses the expectations of power of random variables as functions of parameters. In [86], the method of moments and MLE are used to estimate the model's parameters and are successively applied to the ARD_1 and ARD_∞ models. In addition, various algorithms and numerical tools are employed to estimate parameter values. In [85], in order to maximize the likelihood function, developed numerical functions are used, in-

cluding numerical optimization algorithms such as the Nelder-Mead [78], the BFGS method [12] and a Newton-type algorithm [34].

1.2.2 Observation schemes

Statistical inference relies on the observation scheme of the degradation levels. The likelihood, being a function of the observed data, is directly influenced by the observed degradation values, thereby affecting parameter estimations. Hence, the amount of available data as well as the chosen observation scheme can significantly impact the quality of estimations.

The best scenario for modeling degradation occurs when degradation is under continuous monitoring. This is particularly recommended for highly critical system that require constant inspection of their condition. For instance, in practice, electrical car batteries or the braking system of skyscraper elevators can undergo continuous monitoring. Although this situation is rarely encountered due to its complexity and high cost, more engineering devices are proposed to facilitate ongoing checks [61]. In the literature, the deterioration of continuously monitored system can be taken into account in various degradation models [10, 60, 72]. In that situation, any alterations are promptly identified in the system, allowing interventions to be scheduled as soon as possible.

However, in many practical examples, systems are punctually monitored. As mentioned earlier, inspection times are mainly discussed and optimized regarding degradation models. In the literature, different inspection time scheduling are considered to align models with practical scenarios. For instance, degradation levels can be observed just before and after maintenance actions, providing an optimal knowledge of the maintenance impact on degradation [109]. However, this observation scheme is relatively uncommon in practice due to its potential cost complexity. In cases such as [108], inference is conducted whether degradation levels just after maintenance are observable or not. Real data from the electric industry, like an electrical distribution device, are provided and degradation's value right after each inspection need to be determined by the company's engineers. Additionally, degradation levels can be inspected between maintenances and potentially right before a preventive or corrective maintenance when observed degradation surpasses a certain threshold. In Zhang et al. [104], the system is periodically monitored but fails when the degradation level exceeds a critical threshold. In other cases, like [74, 35, 85], the system is monitored at specific time intervals. If the inspected degradation level exceeds a certain threshold, a preventive maintenance is triggered. Consequently, inspections take place both between and before preventive maintenances. More frequently degradation levels can also only be observed just

before maintenances [87, 54, 21].

Therefore, statistical inference offers a better understanding of the degradation model based on the available observations. Various methods are employed for estimating model parameters, and many distinct observation schemes are considered. Yet, besides the specific case of continuous monitoring, none of these mentioned examples consider simultaneously multiple observation schemes for one unique degradation model with imperfect maintenance. Nevertheless, in practice, inspection schemes can easily differ from one maintenance to another within the same asset. Moreover, considering another observation scheme can have a significant impact on parameter estimation, as it provides different insights into degradation and maintenance effects. Consequently, considering only one observation scheme results in a limited analysis of statistical inference and does not align with many real-world scenarios. That is why a novel approach to statistical inference, considering diverse observation schemes, should be undertaken based on a proposed degradation model in presence of imperfect maintenance.

1.3 Maintenance policy and decision making

In the industrial field, a significant challenge is establishing an efficient maintenance policy that contains degradation while minimizing financial costs. To achieve this goal, it is necessary to conduct maintenance actions at the appropriate times, according to predefined degradation thresholds. Many different maintenance policies are explored and optimized in the literature, based on various degradation models [49].

1.3.1 Maintenance strategies

Inspections and different types of maintenance, such as preventive maintenances, preventive or corrective replacements, can be considered in a maintenance policy, each associated to a specific cost.

Usually, the type of maintenance action to trigger is initially determined by inspecting the system state. Indeed, inspections are carried out to evaluate its condition and eventually determining the appropriate timing for triggering repairs or replacements. In practice, inspections are often performed periodically [30, 53, 104, 55, 11], regardless of the system's current condition, making its implementation easier. Yet, to avoid costly and premature inspections, it is sometimes more relevant to adjust their frequency. This

involves determining the optimal inspection period or the optimal time for the next inspection that minimizes the inspection costs [37, 14, 4, 79, 15]. Specifically, various inspection time functions, such as linear, convex or concave, whether deterministic [4] or random [79], are proposed and optimized to determinate the next inspection time. In some practical situations, inspections may require partial or total system shutdowns, incurring significant costs and time. For instance, in Hameed et al's article [41], inspections and other maintenance activities are performed during the shutdown of systems, such as in process plants. Thereafter, the optimization of this shutdown period involves minimizing the financial costs associated with production loss, asset loss, and safety concerns. Additionally, inspections can also cause damage to the system. In their article, Zhao et al [109] provide a relevant example from Schneider Electric company where some electrical distribution devices are subject to corrosion. Inspections can impact the surface treatments, leaving the system more vulnerable to future corrosion and contributing to its degradation over time. Hence, due to their cost, time constraints and potential adverse effects, inspections are not always conducted frequently in real-world situations and their scheduling needs to be improved. One the one hand, this lack of frequent inspection data entails a significant challenge in properly modeling degradation and anticipating eventual failures. On the other hand, poor decision-making in inspection scheduling may result in an excessive number of scheduled inspections, leading to an increased global inspection cost over a specific period and potentially causing damage to the system. Hence, determining the inter-inspection frequency or the timing of the next scheduled inspection are critical decisions that should be considered when formulating the maintenance policy.

Moreover, in order to establish a maintenance strategy, one or several degradation thresholds are given. By evaluating the degradation levels against these predefined thresholds, one can determine the most suitable type of action to undertake. In [92, 47, 21, 99, 40, 80], similar maintenance policies are proposed. In these articles, degradation is modeled by various processes such as Gamma processes, Wiener process or Markov process, and a preventive or a corrective threshold are given. If degradation value is lower than the preventive threshold, then the system is left unchanged. If the inspected degradation value is between the preventive and the corrective threshold, then a preventive maintenance is carried out. If the inspected degradation level is beyond the corrective threshold, the system fails and a corrective replacement of the system is triggered with an eventual downtime. In the article [37], the maintenance policy is slightly different. This time, if the inspected degradation value is located between the preventive and corrective threshold then a pre-

ventive replacement is carried out. In [111], one threshold is presented and two types of maintenances are described: the preventive replacement when the inspected degradation levels remains below the unique threshold and corrective replacement when the inspection's value exceeds this threshold. Likewise, in the study by Xuping et al. [100], only preventive and corrective replacements are considered, such that each maintenance initiates a new life cycle for wind turbine equipment. In [46], the RUL, i.e. the distribution of the remaining lifetime of a system before failure, is studied and helps to determine the maintenance policy. In this article, a single threshold is defined. If inspected degradation is below this threshold, then two options are considered: either the RUL estimated standard deviation is less than a predefined value, the system's RUL is predicted to schedule the next maintenance. Conversely, if the estimated RUL standard deviation exceeds the predefined value, more inspections are required for a better RUL prediction. Furthermore, when inspired by practical scenarios, maintenance policies must take into account the unique characteristics of the case study. For instance, in [11] an Italian Railway track-line is considered and the vertical and horizontal alignment of the tracks are studied. Then, two alignment quality thresholds are given. If the tracks alignment is still considered in good condition, then no maintenance need to be performed. If the length of alignment gap exceeds the first threshold, a maintenance is strongly recommended. If the alignment quality is really deteriorated or exceeds the second threshold, then a maintenance needs to be performed in a limited time frame. In [60], the degradation of a multi-state system is represented through a continuous-time Markov process. Two observation schemes are considered, one discrete and the other continuous. Under the sequential observation scheme, either a failure is observed and a corrective maintenance is performed, or the system is still working and is left unchanged. In the continuous observation scheme, inspections are perfect, i.e. every change in the system state is detected. Depending on the observed degradation state, the system can undergo either minimal repair or preventive replacement.

After evaluating various maintenance approaches, the maintenance cost is computed and its asymptotic form per time unit minimized, helping in the decision-making process for selecting an appropriate maintenance policy.

1.3.2 Cost optimization and optimal decision variables

Every type of intervention carried out on the system to maintain or just observe degradation, such as inspections, preventive maintenances or replacements entails a specific cost. Over the system's entire lifespan, one can properly choose the decision variables in order to

minimize the overall cost of these operations. For instance, periods between inspections, values of degradation thresholds or parameters associated with the degradation process can be evaluated to align with cost optimization goals.

First of all, a global maintenance cost $c(t)$, which encompasses costs related to all the maintenance actions performed on a system over a specific period of time $[0, t]$, needs to be assessed to properly evaluate optimal maintenance policies thereafter. To achieve this purpose, various approaches are proposed in the literature. Specifically, regenerative properties, initially detailed in [89], and semi-regenerative properties of stochastic processes [70] are widely employed. Regenerative properties specify that the stochastic process has regeneration states, where it resets to its initial state or to a state similarly distributed as the initial one. Moreover, a semi-regenerative process does not fully reset to its initial state as it shares some regenerative properties but considers a dependency between the regeneration states. Based on the regenerative properties and the renewal theory, introduced in [33, 27], and applied to Markov processes in [19], it follows that the asymptotic cost per time unit $\lim_{t\to+\infty} \frac{c(t)}{t}$ equals the expectation of the cost over the regenerative period T divided by the expectation of this period, expressed as $\lim_{t\to+\infty} \frac{c(t)}{t} = \frac{\mathbb{E}[c(T)]}{\mathbb{E}[T]}$. These properties help assessing precisely this cost rate. For instance, numerical methods, as the popular Monte Carlo simulations [75], when used to simulate degradation trajectories over multiple regenerative periods, enable the evaluation of this cost rate. Furthermore, in Cocozza's work [20], the asymptotic cost per time unit can also be computed between two inspections, considering this time semi-regenerative properties.

In the literature, various maintenance policies are suggested and optimized by minimizing the asymptotic maintenance cost per time unit, often based on different decision variables such as inter-inspection intervals and preventive thresholds. For instance, in the already mentioned work by Huynh et al. [47], they aim to minimize costs by adjusting the timing of inspections and preventive replacements of the system. Van's study [92] introduces the (M, Q) policy, where M defines the preventive threshold, and inspections are scheduled so that the probability of failure before the next inspection falls below a defined limit Q. In Grall et al. [37], the $(m(X), M)$ policy is optimized where, this time, $m(X)$ is the inter-inspection time function, gradually decreasing until a preventive replacement is performed. As the system's condition worsens, more frequent monitoring becomes essential. In Zhu's work [111], the frequency of the inspections is also taken into account in the policy (Θ, b, L_p). Θ denotes the initial inspection time, b controls the change in inspection frequency and L_p is the preventive threshold. In [46] more parameters are included in

the studied policies. In this paper, one of the examined maintenance policy is denoted as $(\gamma, \sigma, \alpha, \tau)$, with γ representing the inspection period, σ as the empirical standard deviation threshold of the RUL, α as the probability of the RUL not to exceed a certain value and τ a time threshold beyond which a repair should be conducted. In [99], the life cycle cost is optimized according to the inter-inspection time and the predefined degradation level right after repair. This paper highlights that extending the inter-inspection time interval raises the risk of potential system failure. It is observed that the degradation level after an preventive repair can be lowered when increasing the cost of condition monitoring. In Grall et al.'s paper [36] a multi-threshold policy structure is considered. In this article, the threshold determines the time of the next inspection. Specifically, as the system deteriorates more, the time until the next inspection shortens. If the inspected degradation falls within the predefined "inspection zone" thresholds, the system remains as it is, and another inspection is scheduled based on these thresholds. However, if the degradation level exceeds the preventive threshold, a preventive replacement is carried out, and if it exceeds the corrective threshold, a corrective replacement is performed. In this article, various maintenance policies are studied, aiming to minimize the cost by considering the number of thresholds and the speed of the system deterioration. It appears that for slowly deteriorating systems, a high number of thresholds is favored, but their values must be carefully chosen for decision making. In cases of accelerated deterioration, the earlier the next inspection are scheduled and the weaker the thresholds values must be chosen. This multi-threshold policy is also explored in Castanier et al.'s work [14]. This time, preventive repairs involving a restarting threshold are considered and each type of maintenance (inspections, repairs and replacements) takes a non-negligible time. Consequently, an unavailability cost must be taken into account into the life cycle cost analysis, which is optimized based on both the preventive and restarting thresholds. In [29], wind turbines data coming from German wind farms are analyzed. The study employs stochastic differential equations to describe the degradation model of these turbines. When the system experiences failures before its scheduled maintenance, corrective maintenance actions are undertaken. As an alternative, if the system remains operational until its planned maintenance, preventive maintenance procedures are executed. Then, various costs coefficients are considered, such as the repair cost after failure, the preventive maintenance cost, the eventual downtime cost and financial losses resulting from the interruption of power generation during a wind turbine maintenance. In another field, crest-level of Dutch dikes tend to sink away into the sea due to various environmental factors, needing regular heightening. To model these

crest-level declines, Speijker et al. [90] propose models, including both linear and non-linear ones represented by mixtures of exponential densities. Two costs are considered: a fixed cost for mobilization and road reconstruction and a variable cost estimated per cubic meter of dike volume. This study focuses on computing the optimal dike heightening based on crest-level decline and evaluating the financial requirements for upcoming maintenance. In [68], a multi-component model is introduced including update parameters. Multiple repairable components are taken into account. Each component undergoes different maintenance actions based on its degradation level after inspection. Components can either be subject to preventive maintenance, replacement or can be left unchanged. Opportunistic maintenances entail the system shutdown. Then, the system's downtime is determined by the longest unavailability time among all components. A cost value is associated to each of these maintenances. The study shows that using this proposed model with updated parameters leads to smaller expected maintenance costs compared to other models such as a one-component Wiener-based degradation model.

Hence, maintenance costs assessment and the optimization of maintenance policies are widely explored in the literature on degradation modeling. Various methodologies are proposed to evaluate maintenance costs over specific periods and subsequently optimize maintenance strategies based on selected decision variables. The complexity of cost assessment and the methods proposed for it depend on the chosen degradation model and the predefined inspection scheme. Therefore, the derived optimized policies will be influenced by these factors. To my knowledge, the effect of the location of the inspections (whether degradation is inspected before or after imperfect maintenance) on cost assessment and the derived optimal policies has not yet been studied. This impact, as well as adapted methodologies, should be further explored in the context of degradation modeling.

1.3.3 Conclusion on modeling, inference and decision-making for degradation with imperfect maintenance

A significant challenge consists in constructing a degradation model, relevant to practical need. This model should apprehend deterioration of possible dependent components within a single system. In literature, degradation models typically assume that maintenance affects the entire system, whereas in practice, it often only impacts certain parts of the system. Furthermore, from my understanding of literature on degradation models, statistical inference on degradation models with imperfect maintenance is consistently studied under one specific observation scheme, which describes the location of the inspection along the degradation trajectory. However, in practice, many different inspection schemes can be employed within a single system from one maintenance action to another . Thus, the considered model should take into account realistic maintenance and inspection scenarios and handle statistical inference under different observation schemes using appropriate methods. Furthermore, maintenance policies can be suggested and specific methods should be proposed to enable the evaluation of the asymptotic cost per time unit. The impact of model parameters, chosen cost coefficients and the inspection scheme on the derived optimal policies should be considered.

This manuscript presents an initial degradation model involving maintenance effects, relying on an univariate stochastic process. In practical situations, degradation levels are mostly identified through inspections conducted at different times on the system. One issue consists in finding a model adaptable to any of these scenarios. Chapter 2 details a univariate Wiener-based degradation model that considers all these observation configurations, studying statistical inference corresponding to these different schemes.

As previously mentioned, different components, more or less interdependent, can undergo degradation within a single system. Maintenance actions frequently affect specific components rather than the entire system. In Chapter 3, a realistic degradation model with partial maintenance effects is introduced. This new model is based on a bivariate Wiener process and inference is studied according to a general observation scheme that includes all possible inspection policies.

Based on that new model, an inspection/replacement policy is established in Chapter 4. The asymptotic cost per time unit is assessed thanks to a new method that combines analytic and numerical results. Eventually, numerical studies are carried out to optimize the suggested maintenance strategy, analyzing the influence of model parameters, cost

coefficients and inspection scheme on the optimal policy.

Chapter 2

A Wiener-based degradation model with imperfect maintenance actions and under different observation schemes

In this chapter, technological or industrial equipment that are subject to degradation are considered. These units undergo maintenance actions, which aim to reduce their degradation level. The following sections consider a degradation model with imperfect maintenance effect. The underlying degradation process is a Wiener process with drift. The maintenance effects are described with an Arithmetic Reduction of Degradation ARD_1 model. The system is regularly inspected, during which the degradation levels are measured. Four different observation schemes are considered, allowing degradation levels to be observed between maintenance actions, as well as just before or just after maintenance times. This chapter focuses on studying the estimation of the model parameters under four observation schemes. Maximum likelihood estimators are derived for each scheme. The quality of the estimations and the observation schemes are compared through an extensive simulation and performance study.

The chapter is structured as follows. In Section 2.1, the Wiener-based ARD_1 model and the four selected observation schemes are introduced. The statistical inference of the model based on these observation schemes is examined in Section 2.2. The quality of the estimations and a comparative analysis of the observation schemes are explored in Section 2.3. Concluding remarks are provided in Section 2.4.

2.1 The Wiener-based ARD_1 model

This section presents the degradation model and the observation schemes used in the paper. The underlying degradation process is a Wiener process. The effect of maintenance is an arithmetic reduction of degradation, expressed by the ARD_1 model. Four observation schemes are considered, depending on the observations made (or not) at maintenance times. Finally, the notations used in the paper are presented.

2.1.1 The underlying degradation process

Let $X(t)$ be the degradation level at time t of a system which is not maintained. $X = \{X(t)\}_{t\geq 0}$ is called the underlying degradation process. In this paper, X is assumed to be a Wiener process with drift. This process is commonly used in degradation modeling, especially in order to take into account the possibility of non strictly increasing degradation paths.

Therefore, $\forall t \geq 0, X(t) = \mu\ t + \sigma\ B(t)$ where B is a standard Brownian motion. $\mu > 0$ is a drift parameter and σ^2 is a variance parameter. The Wiener process is such that:

- $X(0) = 0$ almost surely.
- The increments are independent. $\forall s_1 < t_1 < s_2 < t_2$, $X(t_1) - X(s_1)$ and $X(t_2) - X(s_2)$ are independent.
- The increments are normally distributed. $\forall s < t$, $X(t) - X(s)$ has the normal distribution $\mathcal{N}\left(\mu\ (t-s),\ \sigma^2\ (t-s)\right)$. In particular, $X(t) \sim \mathcal{N}(\mu\ t, \sigma^2\ t)$.

2.1.2 The effect of maintenance

The system is observed from time 0 to a certain time τ. Between 0 and τ, k maintenance actions (or repairs) are performed at times $\tau_1 < \tau_2, ..., < \tau_k$. Maintenance durations are assumed to be negligible or not taken into account. To simplify the mathematical writing, let $\tau_0 = 0$ and $\tau_{k+1} = \tau$.

An efficient maintenance is expected to reduce the degradation level. Let $Y(t)$ be the degradation level at time t of the maintained system. $Y = \{Y(t)\}_{t\geq 0}$ is the degradation process of the maintained system. We have to express Y as a function of the underlying degradation process X. In [73], Mercier and Castro used both ARD_1 (Arithmetic Reduction of Degradation) and ARA_1 models. For this last model, they needed to introduce

independent copies $X^{(i)}$ of X. In the present paper, we consider only the ARD_1 model, so only one copy of X is needed.

The ARD_1 assumption is that the effect of maintenance is to reduce the level of degradation of a quantity which is proportional to the level of degradation accumulated since the last maintenance. Let $\rho \in [0,1]$ be the coefficient of proportionality, which is called the maintenance effect parameter.

Before the first maintenance, both X and Y processes are identical:

$$\forall t \in [0, \tau_1[, Y(t) = X(t)$$

Let $Y(\tau_1^-)$ be the degradation level just before the first maintenance action, so that $Y(\tau_1^-) = X(\tau_1)$. The effect of the first maintenance at τ_1 is to reduce the degradation level $Y(\tau_1^-)$ of a quantity $\rho \ \left[Y(\tau_1^-) - Y(0)\right] = \rho Y(\tau_1^-)$. Therefore, the degradation level just after τ_1 is

$$Y(\tau_1^+) = Y(\tau_1^-) - \rho Y(\tau_1^-) = (1-\rho)Y(\tau_1^-) = (1-\rho)X(\tau_1) \tag{2.1}$$

After the first maintenance action, the system is deteriorating according to X and we have

$$\forall\ t \in [\tau_1, \tau_2[,\ Y(t) = Y(\tau_1^+) + X(t) - X(\tau_1) = X(t) - \rho X(\tau_1)$$

Just after the second maintenance action we have

$$\begin{aligned} Y(\tau_2^+) &= Y(\tau_2^-) - \rho[Y(\tau_2^-) - Y(\tau_1^+)] \\ &= X(\tau_2) - \rho X(\tau_1) - \rho[X(\tau_2) - X(\tau_1)] = (1-\rho)X(\tau_2) \end{aligned} \tag{2.2}$$

By recurrence, it follows that $\forall\ t \in [\tau_{j-1}, \tau_j[$

$$Y(t) = Y(\tau_j^+) + [X(t) - X(\tau_j)] = X(t) - \rho X(\tau_j) \tag{2.3}$$

The effect of maintenance at time τ_j is expressed by the degradation jump Z_j^c, difference between the degradation level after and before maintenance

$$Z_j^c = Y(\tau_j^+) - Y(\tau_j^-) = (1-\rho)X(\tau_j) - [X(\tau_j) - \rho X(\tau_{j-1})] = -\rho\left[X(\tau_j) - X(\tau_{j-1})\right] \tag{2.4}$$

2.1.3 Observation schemes

The system is regularly inspected and the degradation levels are measured. Potentially, the degradation level can be measured either at maintenance times (just before and/or just after) and/or between maintenance actions.

Let n_j be the number of observations of the degradation levels on $]\tau_{j-1}, \tau_j[$, i.e. between two successive maintenance times. It is possible that $n_j = 0$. When $n_j \geq 1$, the corresponding observation times are denoted $t_{j,1} < t_{j,2} < ... < t_{j,n_j}$. Let $N = \sum_{j=1}^{k+1} n_j$, i.e. the total number of observations of the degradation levels between maintenance times.

For observations made at maintenance times, $\forall\ j \in \{1, ..., k+1\}$ let us denote $t_{j,n_j+1} = \tau_j = t_{j+1,0}$. Therefore, in $[\tau_{j-1}, \tau_j]$, we have potentially n_j+2 observations, at times $\tau_{j-1} = t_{j,0} < t_{j,1} < t_{j,2} < ... < t_{j,n_j} < t_{j,n_j+1} = \tau_j$. The subscript j in these notations means that τ_j corresponds to the last observed maintenance time. Consequently,

$$Y(t_{j+1,0}) = Y(\tau_j^+) \text{ and } Y(t_{j,n_j+1}) = Y(\tau_j^-)$$

The observations are the levels of degradation $Y(t_{j,i})$ at times $t_{j,i}$, $\forall\ j \in \{1, ..., k+1\}$, $\forall i \in \{0, ..., n_j + 1\}$. Considering the independence of increments in the Wiener process, the quantities of interest are the observed increments of degradation. The time intervals between observations are denoted $\Delta t_{j,i} = t_{j,i} - t_{j,i-1}, \forall\ j \in \{1, ..., k+1\}, \forall i \in \{1, ..., n_j + 1\}$. The degradation increments are denoted $\Delta Y_{j,i} = Y(t_{j,i}) - Y(t_{j,i-1}), \forall\ j \in \{0, ..., k\}, \forall i \in \{1, ..., n_j + 1\}$.

The ideal situation is when all the degradation measures can be made, at maintenance times (before and after) and between maintenance times. This situation of complete measurements is called "complete observation scheme" in the following. In this case, the jumps $Z_j^c = Y(\tau_j^+) - Y(\tau_j^-)$ are observed.

Figure 2.1 represents an example of trajectory of the degradation process for the complete observation scheme. In this example, maintenance actions are done periodically each 5 time units. Each point is an observed degradation level. The blue lines are the successive mean degradation paths after maintenance actions.

In Figure 2.1, $\forall\ j \in \{1, ..., k+1\}$, $t_{j,n_j+1} = \tau_j = t_{j+1,0}$. $Y(\tau_j^-)$ and $Y(\tau_j^+)$ are respectively the degradation levels that happen just before and just after the j^{th} maintenance. Thus, $Y(\tau_j^-)$ is observed just before $Y(\tau_j^+)$ at time τ_j . In the same way, $Y(t_{j,n_j+1})$ is observed just before $Y(t_{j+1,0})$.

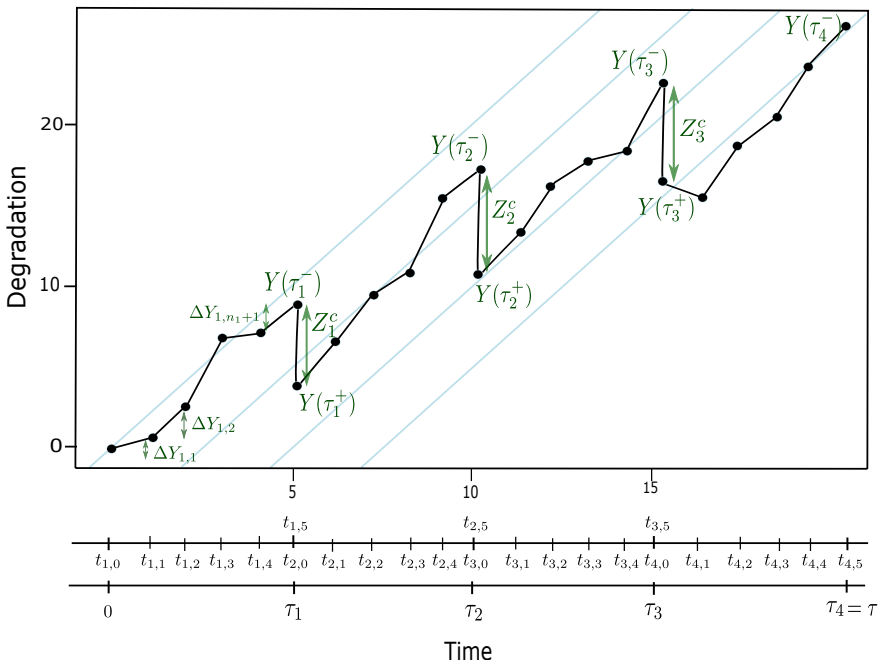

Figure 2.1: A trajectory of the degradation process and notations used

In practice, it may happen that it is not possible to observe all or part of the degradation levels at maintenance times. In this case of incomplete measurements, the real degradation jumps Z_j^c cannot be observed. Instead, other kinds of jumps are observed, which will be defined in next section. In this paper, we consider the complete observation scheme as well as three incomplete observation schemes. So four observation schemes are studied. In the observation scheme m, the observed jump around the j^{th} maintenance is denoted Z_j^s.

- *Complete observation scheme*: The degradation levels are observed just before and just after each maintenance action.
- *Second observation scheme*: The degradation levels are observed just before each maintenance action but not just after.
- *Third observation scheme*: The degradation levels are observed just after each maintenance action but not just before.
- *General observation scheme*: The degradation levels are not observed neither just before nor just after each maintenance action.

A summary of all the notations used in the paper is given hereafter.

2.2 Statistical inference

The aim of this section is to estimate the three parameters of the Wiener-based ARD_1 model under the four observation schemes. Let us recall that μ is a drift parameter, σ^2 is a variance parameter and ρ is the maintenance effect parameter.

We use the maximum likelihood method, from the observation of the degradation process on $[0, \tau]$. The four observation schemes described previously lead to different writings of the likelihood and therefore to different estimators of the parameters.

There are two kinds of observations, the increments of degradation and the observed jumps around maintenance times. Therefore, the likelihood $L(\mu, \sigma^2, \rho)$ has two parts. Thanks to the independence of the increments of the Wiener process, the part linked to degradation increments is the product of the densities of these increments. The part linked to degradation jumps is more complex and will be studied in each observation scheme.

Finally, a general expression of the likelihood is

$$L(\mu, \sigma^2, \rho) = \left[\prod_j \prod_i f_{\Delta Y_{j,i}}(\Delta y_{j,i}) \right] \prod_j f_{Z_j^s | \mathcal{O}^s_{\tau_j^-}}(z_j^s) \tag{2.5}$$

where $\mathcal{O}^s_{\tau_j^-}$ is the history of the observed degradation process just before τ_j, i.e. the σ-algebra generated by the increments and observed jumps before the j^{th} maintenance for the observation scheme s. Moreover, the increments $\Delta Y_{j,i}$ have a normal distribution $\mathcal{N}(\mu \Delta t_{j,i} \ , \ \sigma^2 \Delta t_{j,i})$. Therefore, the main problem is to determine in each scheme the conditional distribution of the observed degradation jumps Z_j^s given the past.

2.2.1 Complete observation scheme

In this complete observation scheme, the degradation levels are both observed just before and just after each maintenance action. A simulated trajectory of the degradation process is presented in Figure 2.2. The black points are the observed degradation levels. In this example, the maintenance actions are made periodically each 5 time units and the observations of the degradation levels between maintenance actions are made periodically each 1 time unit. The values of the parameters are $\mu = 2$, $\sigma^2 = 2$ and $\rho = 0.5$. $k = 3$ maintenance actions are done, $n = 24$ observations of the degradation levels are made and $\forall \ j \in \{1, 2, 3, 4\}$, $n_j = 4$. The first degradation level $y(t_{1,0}) = 0$ is considered as an observation.

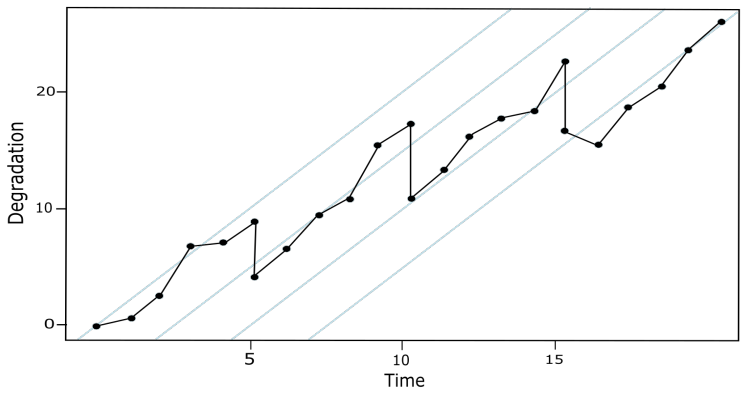

Figure 2.2: Complete scheme: a trajectory of the degradation process

All the degradation increments $\Delta Y_{j,i}$ are observed, $\forall\, j \in \{1, ..., k+1\}$, $\forall\, i \in \{1, ..., n_j + 1\}$. $\forall\, j \in \{1, ..., k\}$, the real degradation jumps Z_j^s are observed. Therefore, the likelihood (2.5) is:

$$L_1(\mu, \sigma^2, \rho) = \left[\prod_{j=1}^{k+1} \prod_{i=1}^{n_j+1} f_{\Delta Y_{j,i}}(\Delta y_{j,i})\right] \prod_{j=1}^{k} f_{Z_j^c | \mathcal{O}^1_{\tau_j^-}}(z_j^c) \tag{2.6}$$

Here $\forall j \in \{1, ..., k\}$,
$\mathcal{O}^1_{\tau_j^-} = \{\Delta y_{1,1}, ..., \Delta y_{1,n_1+1}, z_1^1, \Delta y_{2,1}, ..., , \Delta y_{j-1,n_{j-1}+1}, z_{j-1}^1, \Delta y_{j,1}, ..., \Delta y_{j,n_j+1}\}$
From (2.4), we have for all j:

$$Z_j^c = -\rho\,[X(\tau_j) - X(\tau_{j-1})] = -\rho \sum_{i=1}^{n_{j-1}+1} \Delta Y_{j,i} \tag{2.7}$$

Thus, given $\mathcal{O}^1_{\tau_j^-}$, Z_j^c is completely known. $Z_j^c \mid \mathcal{O}^1_{\tau_j^-}$ follows a Dirac distribution:

$$f_{Z_j^c | \mathcal{O}^1_{\tau_j^-}}(z_j^c) = \mathbb{1}_{\left\{z_j^c = -\rho \sum_{i=1}^{n_{j-1}+1} \Delta y_{j,i}\right\}}$$

Therefore, the model is meaningful, under this complete observation scheme, only if all the quantities $\frac{z_j^c}{\sum_{i=1}^{n_{j-1}+1} \Delta y_{j,i}}$ are equal (equal to $-\rho$). This seems obviously very unlikely in practical situations. So in the following, we will not consider the estimation of ρ. μ and σ^2 are estimated by maximizing the likelihood

$$L_1\left(\mu, \sigma^2\right) = \prod_{j=1}^{k+1} \prod_{i=1}^{n_j+1} \frac{1}{\sqrt{2\pi\sigma^2 \Delta t_{j,i}}} \exp\left(-\frac{(\Delta y_{j,i} - \mu \Delta t_{j,i})^2}{2\sigma^2 \Delta t_{j,i}}\right) \tag{2.8}$$

Straightforward computations lead to the maximum likelihood estimators of μ and σ^2

$$\hat{\mu} = \frac{\sum_{j=1}^{k+1} \sum_{i=1}^{n_j+1} \Delta Y_{j,i}}{\sum_{j=1}^{k+1} \sum_{i=1}^{n_j+1} \Delta t_{j,i}} = \frac{1}{\tau}\left[Y(\tau) - \sum_{j=1}^{k} Z_j^c\right] \tag{2.9}$$

$$\hat{\sigma}^2 = \frac{1}{N+k+1} \sum_{j=1}^{k+1} \sum_{i=1}^{n_j+1} \frac{(\Delta Y_{j,i} - \hat{\mu}\Delta t_{j,i})^2}{\Delta t_{j,i}} \tag{2.10}$$

Note that $\hat{\mu} = X(\tau)/\tau$, so $\hat{\mu}$ is an unbiased estimator of μ. Furthermore $\tilde{\sigma}^2 = \dfrac{N+k+1}{N+k}\hat{\sigma}^2$ is an unbiased estimator of σ^2 (proof in Appendix A.2)

2.2.2 Second observation scheme

In this scheme, the degradation levels just before maintenance actions $Y(\tau_j^-)$ are observed, but the degradation levels just after maintenance actions $Y(\tau_j^+)$ are not observed. This situation is illustrated in Figure 2.3. In this figure, we have used the same trajectory of the degradation process as in Figure 2.2, but we considered that the degradation levels just after maintenance actions $Y(\tau_j^+)$ are not observed. The jumps at maintenance times and the first degradation increments after maintenance are not observed, so they are represented with dotted lines. The values of the parameters μ, σ^2, ρ, the number of maintenance actions k and the number of observations between maintenance actions $\{n_j\}_{0\leq j\leq 3}$ are the same as in Figure 2.2, but the number of observed data is now $n = 21$.

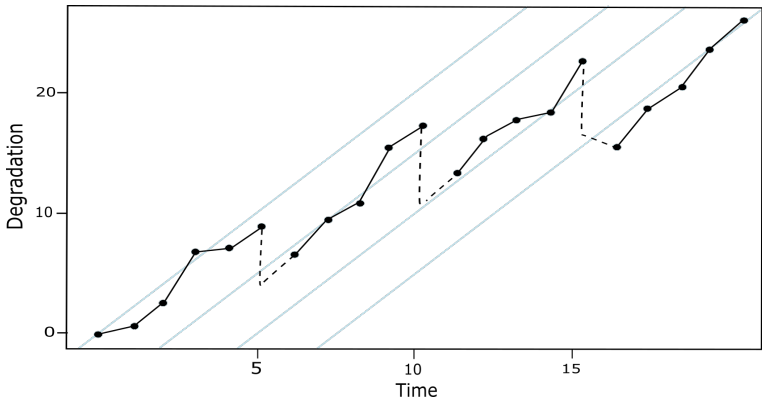

Figure 2.3: Second scheme: a trajectory of the degradation process

The studies in [87, 54] assume that only the degradation levels just before maintenance actions are observed. This corresponds to this second observation scheme in the particular

case where $\forall j$, $n_j = 0$. In this case, the observed jumps are the only observations

$$Z_j^2 = Y(\tau_{j+1}^-) - Y(\tau_j^-) = X(\tau_{j+1}) - X(\tau_j) - \rho\ [X(\tau_j) - X(\tau_{j-1})]$$

which have the $\mathcal{N}\left(\mu(\tau_{j+1} - \tau_j) - \mu\rho(\tau_j - \tau_{j-1})\ ,\ \sigma^2(\tau_{j+1} - \tau_j) + \sigma^2\rho^2(\tau_j - \tau_{j-1})\right)$ distribution.

Note that the $\Delta Y_{j,1}\ \forall j \in \{2, .., k+1\}$ are not observed but the first increment $\Delta Y_{1,1}$ is observed. Thus, the history of the process at τ_j^- is $\forall j \in \{1, ..., k\}$,

$\mathcal{O}^2_{\tau_j^-} = \{\Delta y_{1,1}, \Delta y_{1,2}, ..., \Delta y_{1,n_1+1}, z_1^2, \Delta y_{2,2}, ..., \Delta y_{j-1,n_{j-1}+1}, z_{j-1}^2, \Delta y_{j,2}, ..., \Delta y_{j,n_j+1}\}$

The real degradation jumps $Z_j^c = Y(\tau_j^+) - Y(\tau_j^-)$ are not observed. Instead, the observed jump around the j^{th} maintenance is

$$\begin{aligned} Z_j^2 &= Y(t_{j+1,1}) - Y(\tau_j^-) = Y(t_{j+1,1}) - Y(\tau_j^+) + Y(\tau_j^+) - Y(\tau_j^-) \\ &= \Delta Y_{j+1,1} + Z_j^c = \Delta Y_{j+1,1} - \rho \sum_{i=1}^{n_j+1} \Delta Y_{j,i} \\ &= \Delta Y_{j+1,1} - \rho \Delta Y_{j,1} - \rho \sum_{i=2}^{n_j+1} \Delta Y_{j,i} \end{aligned} \tag{2.11}$$

In the likelihood, we need to compute the conditional PDF of Z_j^2 given $\mathcal{O}^2_{\tau_j^-}$. Since $\Delta Y_{j,1}$ is not independent of $\mathcal{O}^2_{\tau_j^-}$, the computation of this conditional distribution could be complex.

However, the computation can be simplified in this case because, thanks to the properties of the ARD_1 model, the missing value $Y(\tau_j^+)$ can be computed as a function of the already observed values and ρ.

At time zero, $Y(\tau_0) = 0$. From (2.1), $Y(\tau_1^+) = (1-\rho)\ Y(\tau_1^-)$. From (2.2),

$$Y(\tau_2^+) = Y(\tau_2^-) - \rho\ \left[Y(\tau_2^-) - Y(\tau_1^+)\right] = (1-\rho)Y(\tau_2^-) + \rho\ (1-\rho)\ Y(\tau_1^-)$$

By recurrence, it follows that $\forall\ j \in \{1, ..., k\}$

$$Y(\tau_j^+) = (1-\rho) \sum_{i=0}^{j} \rho^{j-i}\ Y(\tau_i^-) \tag{2.12}$$

Therefore, $\forall\ j \in \{1, ..., k\}$, the observed jump Z_j^2 can be written

$$Z_j^2 = \Delta Y_{j+1,1} + Y(\tau_j^+) - Y(\tau_j^-) = \Delta Y_{j+1,1} + (1-\rho)\sum_{i=0}^{j} \rho^{j-i}\ Y(\tau_i^-) - Y(\tau_j^-)$$

$$= \Delta Y_{j+1,1} - \rho Y(\tau_j^-) + (1-\rho)\sum_{i=0}^{j-1} \rho^{j-i}\ Y(\tau_i^-) \tag{2.13}$$

Equation (2.13) is much easier to use than (2.11) because $\Delta Y_{j,1}$ is independent of $\mathcal{O}^2_{\tau_j^-}$ and conditionnally to $\mathcal{O}^2_{\tau_j^-}$, the $Y(\tau_i^-)$ for $i \leq j$ are observed. So the conditional distribution of Z_j^2 given $\mathcal{O}^2_{\tau_j^-}$ is the $\mathcal{N}\left(\mu\ \Delta t_{j+1,1} - \rho\ y(\tau_j^-) + (1-\rho)\ \sum_{i=1}^{j-1} \rho^{j-i}\ y(\tau_i^-),\ \sigma^2 \Delta t_{j+1,1}\right)$ distribution.

Finally, the likelihood for the second observation scheme is

$$L_2\left(\mu, \sigma^2, \rho\right) = \left[\prod_{j=1}^{k+1} \prod_{i=1+\mathbb{1}_{j>1}}^{n_j+1} f_{\Delta Y_{j,i}}(\Delta y_{j,i})\right] \prod_{j=1}^{k} f_{Z_j^2|\mathcal{O}^2_{\tau_j^-}}\left(z_j^2\right) \tag{2.14}$$

From Equation (2.13), for all j, $z_j^2 - \mu\ \Delta t_{j+1,1} + \rho\ y(\tau_j^-) - (1-\rho)\ \sum_{i=1}^{j-1} \rho^{j-i}\ y(\tau_i^-) = y(t_{j+1,1}) - \mu\ \Delta t_{j+1,1} - (1-\rho)\ \sum_{i=1}^{j} \rho^{j-i}\ y(\tau_i^-)$. Therefore, the log-likelihood is derived as

$$\ln L_2\left(\mu, \sigma^2, \rho\right) = -\frac{N+k+1}{2} \ln \sigma^2 + c_1 - \frac{1}{2\sigma^2}\left[\sum_{j=1}^{k+1} \sum_{i=1+\mathbb{1}_{j>1}}^{n_j+1} \frac{\left(\Delta y_{j,i} - \mu \Delta t_{j,i}\right)^2}{\Delta t_{j,i}}\right.$$
$$\left. + \sum_{j=1}^{k} \frac{1}{\Delta t_{j+1,1}} \left(y(t_{j+1,1}) - \mu \Delta t_{j+1,1} - (1-\rho)\sum_{i=0}^{j} \rho^{j-i} y(\tau_i^-)\right)^2\right] \tag{2.15}$$

where c_1 is a constant.

Deriving the log-likelihood, the maximum likelihood estimators $\hat{\mu}$, $\hat{\sigma}^2$ and $\hat{\rho}$ are obtained as the solutions of the likelihood equations system, as follows.

$$\hat{\mu} = \frac{1}{\tau}\left[Y(\tau) + \hat{\rho}\sum_{j=1}^{k} Y(\tau_j^-) - (1-\hat{\rho})\sum_{j=1}^{k}\sum_{i=0}^{j-1}\hat{\rho}^{j-i}Y(\tau_i^-)\right] \tag{2.16}$$

Moreover, let us notice that $\sum_{j=1}^{k}\sum_{i=0}^{j-1}\hat{\rho}^{j-i}Y(\tau_i^-) = \sum_{i=1}^{k-1}\sum_{j=i+1}^{k}\hat{\rho}^{j-i}Y(\tau_i^-)$ and

$$\begin{aligned}(1-\hat{\rho})\sum_{i=1}^{k-1}\left(\sum_{j=i+1}^{k}\hat{\rho}^{j-i}\right)Y(\tau_i^-) &= \sum_{i=1}^{k-1}\left(\sum_{j=i+1}^{k}\hat{\rho}^{j-i} - \sum_{j=i+1}^{k}\hat{\rho}^{j-i+1}\right)Y(\tau_i^-)\\ &= \sum_{i=1}^{k-1}(\hat{\rho}-\hat{\rho}^{k-i+1})Y(\tau_i^-)\end{aligned}$$

Since $Y(\tau) + \hat{\rho}\sum_{j=1}^{k} Y(\tau_j^-) = Y(\tau_{k+1}^-) + \hat{\rho}Y(\tau_k^-) + \hat{\rho}\sum_{j=1}^{k-1} Y(\tau_j^-)$ then,

$$Y(\tau) + \hat{\rho}\sum_{j=1}^{k} Y(\tau_j^-) - (1-\hat{\rho})\sum_{j=1}^{k}\sum_{i=1}^{j-1}\hat{\rho}^{j-i}\,Y(\tau_i^-) = Y(\tau_{k+1}^-) + \hat{\rho}\,Y(\tau_k^-) + \sum_{i=1}^{k-1}\hat{\rho}^{k-i+1}\,Y(\tau_i^-)$$

$$\text{Thus, } \hat{\mu} = \frac{1}{\tau}\sum_{i=1}^{k+1}\hat{\rho}^{k-i+1}\,Y(\tau_i^-) \tag{2.17}$$

$$\hat{\sigma}^2 = \frac{1}{N+k+1}\left[\sum_{j=1}^{k+1}\sum_{i=1+\mathbb{1}_{j>1}}^{n_j+1}\frac{(\Delta Y_{j,i} - \hat{\mu}\,\Delta t_{j,i})^2}{\Delta t_{j,i}} + \sum_{j=1}^{k}\frac{\left(Y(t_{j+1,1}) - \hat{\mu}\,\Delta t_{j+1,1} - (1-\hat{\rho})\sum_{i=0}^{j}\hat{\rho}^{j-i}Y(\tau_i^-)\right)^2}{\Delta t_{j+1,1}}\right] \tag{2.18}$$

$$\sum_{j=1}^{k} \frac{1}{\Delta t_{j+1,1}} \left[\sum_{i=0}^{j} \hat{\rho}^{j-i-1} Y(\tau_i^-)[(1-\hat{\rho})(j-i) - \hat{\rho}] \right] \left[Y(t_{j+1,1}) - \hat{\mu}\Delta t_{j+1,1} - (1-\hat{\rho}) \sum_{i=0}^{j} \hat{\rho}^{j-i} Y(\tau_i^-) \right] = 0 \tag{2.19}$$

These estimators can equivalently be obtained using the profile likelihood method. The maximum likelihood estimator $\hat{\rho}$ is equal to $\arg\max_\rho \ln L_2(\hat{\mu}(\rho), \hat{\sigma}^2(\rho), \rho)$ where $\hat{\mu}(\rho)$ and $\hat{\sigma}^2(\rho)$ are obtained using Equations (2.17) and (2.18) replacing $\hat{\rho}$ and $\hat{\mu}$ by ρ and $\hat{\mu}(\rho)$. Using Equations (2.15) and (2.18), one can easily show that the profile log-likelihood can be written

$$\ln\ L_2(\hat{\mu}(\rho), \hat{\sigma}^2(\rho), \rho) = -\frac{N+k+1}{2} \left[\ln\ \hat{\sigma}^2(\rho) + 1 \right] + c_1$$

Then, the maximum likelihood estimator of ρ can be viewed as the value of ρ which minimizes the estimated variance of the underlying degradation process when ρ is supposed to be known.

Biases of these estimators are computed in Appendix A.2.

2.2.3 Third observation scheme

In this scheme, the degradation levels just after maintenances $Y(\tau_j^+)$ are observed, but the degradation levels just before maintenance actions $Y(\tau_j^-)$ are not observed. This situation is illustrated in Figure 2.4. As for Figure 2.3, we have used the same trajectory of the degradation process as in Figure 2.2, but we considered that the degradation levels just before maintenance actions $Y(\tau_j^-)$ are not observed. This is illustrated by dotted lines in Figure 2.4. In order to keep the notations homogeneous, we also assume that the last degradation level $Y(\tau)$ is not observed, so the last observation is $Y(t_{k+1,n_{k+1}})$. The values of μ, σ^2, ρ, k and $\{n_j\}_{1 \leq j \leq 4}$ are the same as before, but the number of observed data is now $n = 20$.

Here, none of the $\Delta Y_{j,n_j+1}$ $\forall j \in \{1, .., k\}$ are observed. In this case, the history of the process at τ_j^- is also the history of the process at t_{j,n_j}: $\forall j \in \{1, ..., k\}$,
$\mathcal{O}^3_{\tau_j^-} = \mathcal{O}^3_{t_{j,n_j}} = \{\Delta y_{1,1}, ..., \Delta y_{1,n_1}, z_1^3, \Delta y_{2,1}, ..., \Delta y_{j-1,n_{j-1}}, z_{j-1}^3, \Delta y_{j,1}, ..., \Delta y_{j,n_j}\}$
The real degradation jumps $Z_j^c = Y(\tau_j^+) - Y(\tau_j^-)$ are not observed. Instead, the observed

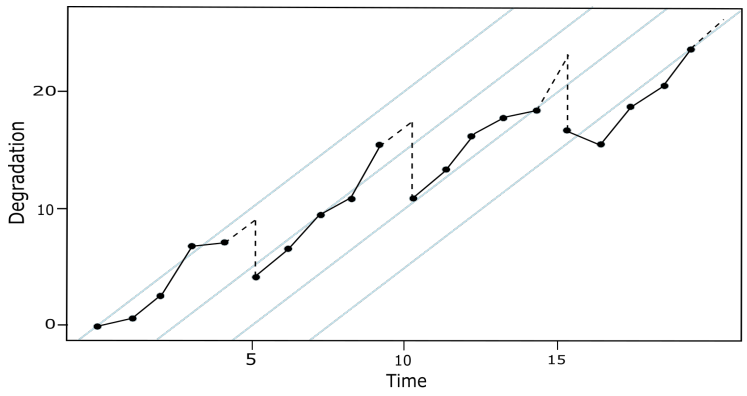

Figure 2.4: Third scheme: a trajectory of the degradation process

jump around the j^{th} maintenance is

$$\begin{aligned} Z_j^3 &= Y(\tau_j^+) - Y(t_{j,n_j}) = Y(\tau_j^+) - Y(\tau_j^-) + Y(\tau_j^-) - Y(t_{j,n_j}) \\ &= Z_j^c + \Delta Y_{j,n_j+1} = -\rho \sum_{i=1}^{n_j+1} \Delta Y_{j,i} + \Delta Y_{j,n_j+1} \\ &= -\rho \sum_{i=1}^{n_j} \Delta Y_{j,i} + (1-\rho)\ \Delta Y_{j,n_j+1} \end{aligned} \tag{2.20}$$

$\Delta Y_{j,n_j+1}$ is independent of $\mathcal{O}^3_{\tau_j^-}$. So the conditional distribution of Z_j^3 given $\mathcal{O}^3_{\tau_j^-}$ is the $\mathcal{N}\left(\mu(1-\rho)\Delta t_{j,n_j+1} - \rho \sum_{i=1}^{n_j} \Delta y_{j,i}\ ,\ \sigma^2(1-\rho)^2 \Delta t_{j,n_j+1}\right)$ distribution.
Finally, the likelihood for the third observation scheme is

$$L_3\left(\mu, \sigma^2, \rho\right) = \left[\prod_{j=1}^{k+1} \prod_{i=1}^{n_j} f_{\Delta Y_{j,i}}(\Delta y_{j,i})\right] \prod_{j=1}^{k} f_{Z_j^3 | \mathcal{O}^3_{t_{j,n_j}}}(z_j^3) \tag{2.21}$$

The log-likelihood is derived as

$$\ln L_3\left(\mu,\sigma^2,\rho\right) = -\frac{N+k}{2}\ln\sigma^2 + c_2 - k\ln(1-\rho) - \frac{1}{2\sigma^2}\left[\sum_{j=1}^{k+1}\sum_{i=1}^{n_j}\frac{(\Delta y_{j,i}-\mu\Delta t_{j,i})^2}{\Delta t_{j,i}}\right.$$
$$\left. + \frac{1}{(1-\rho)^2}\sum_{j=1}^{k}\frac{1}{\Delta t_{j,n_j+1}}\left(z_j^3 - \mu(1-\rho)\Delta t_{j,n_j+1} + \rho\sum_{i=1}^{n_j}\Delta y_{j-1,i}\right)^2\right] \tag{2.22}$$

where c_2 is a constant.

Deriving the log-likelihood, the maximum likelihood estimators $\hat{\mu}$ and $\hat{\sigma^2}$ are obtained as the solutions of the likelihood equations system, as follows.

$$\hat{\mu} = \frac{1}{t_{k+1,n_{k+1}}}\left[\sum_{j=1}^{k+1}\sum_{i=1}^{n_j}\Delta Y_{j,i} \;+\; \frac{1}{1-\hat{\rho}}\sum_{j=1}^{k}\left(Z_j^3 + \hat{\rho}\sum_{i=1}^{n_j}\Delta Y_{j,i}\right)\right] \tag{2.23}$$

$$\hat{\sigma^2} = \frac{1}{N+k}\left[\sum_{j=1}^{k+1}\sum_{i=1}^{n_j}\frac{(\Delta Y_{j,i}-\hat{\mu}\;\Delta t_{j,i})^2}{\Delta t_{j,i}} + \sum_{j=1}^{k}\frac{\left(Z_j^3 - \hat{\mu}\;(1-\hat{\rho})\Delta t_{j,n_j+1} + \hat{\rho}\sum\limits_{i=1}^{n_j}\Delta Y_{j,i}\right)^2}{(1-\rho)^2\Delta t_{j,n_j+1}}\right] \tag{2.24}$$

One can show that $\hat{\mu}$ can also be written (see Appendix A.1)

$$\hat{\mu} = \frac{1}{t_{k,n_k}}\left[Y(t_{k,n_k}) + \frac{\hat{\rho}}{1-\hat{\rho}}Y(\tau_k^+)\right]$$

For $\hat{\rho}$, the derivation of the log-likelihood leads to an expression which is too complex to be given here. Therefore we use directly the profile likelihood method. As in the previous sub-section, $\hat{\rho} = argmax_\rho \ln L_3\;(\hat{\mu}(\rho),\hat{\sigma}^2(\rho),\rho)$, where the profile log-likelihood is

$$\ln L_3\;(\hat{\mu}(\rho),\hat{\sigma}^2(\rho),\rho) = -\frac{1}{2}(N+k)\left[\ln\;\hat{\sigma}^2(\rho)+1\right] - k\;\ln\;(1-\rho) + c_2 \tag{2.25}$$

where $\hat{\mu}(\rho)$ and $\hat{\sigma}^2(\rho)$ are obtained similarly as in the previous sub-section.

By analogy with [87, 54] one could assume that only the degradation levels just after maintenance actions are observed. This corresponds to this third observation scheme where $\forall j$, $n_j = 0$. In this case, the observed jumps are the unique observations

$$Z_j^3 = Y(\tau_j^+) - Y(\tau_{j-1}^+) = (1-\rho)\Delta Y_{j,1}$$

which have the $\mathcal{N}\left(\mu(1-\rho)(\tau_j - \tau_{j-1})\ ,\ \sigma^2(1-\rho)^2(\tau_j - \tau_{j-1})\right)$ distribution.
Therefore, different triplets (μ, σ^2, ρ) will lead to the same observations, so the model is not identifiable. Note that this problem does not appear for the second observation scheme.
Biases of these estimator are detailed in Appendix A.2.

2.2.4 General observation scheme

In this last scheme, neither $Y(\tau_j^-)$ nor $Y(\tau_j^+)$ are observed. This situation is illustrated in Figure 2.5. As before, the last observation is $Y(t_{k,n_k})$. The values of μ, σ^2, ρ, k and $\{n_j\}_{1 \leq j \leq 4}$ are the same as before, but the number of observed data is now $n = 17$.

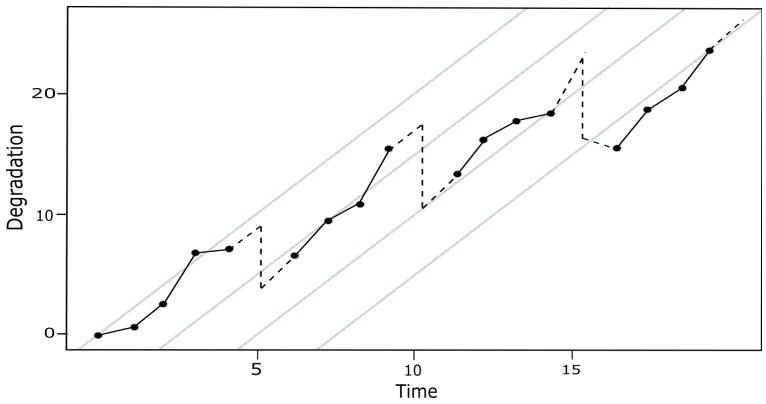

Figure 2.5: General observation scheme : a trajectory of the degradation process

It is assumed that we have at least one observation between two successive maintenance actions : $\forall\ j \in \{1, ..., k+1\}$, $n_j \geq 1$. Here, neither the $\Delta Y_{j,1}$ (except the first one) nor the $\Delta Y_{j,n_j+1}$ are observed. In this case, the history of the process at τ_j^- or t_{j,n_j} is $\forall j \in \{1, ..., k\}$,
$\mathcal{O}^g_{\tau_j^-} = \mathcal{O}^g_{t_{j,n_j}} = \{\Delta y_{1,1}, ..., \Delta y_{1,n_1}, z_1^g, \Delta y_{2,2}, ..., \Delta y_{j-1,n_{j-1}}, z_{j-1}^g, \Delta y_{j,2}, ..., \Delta y_{j,n_j}\}$
The real degradation jumps $Z_j^c = Y(\tau_j^+) - Y(\tau_j^-)$ are not observed. Instead, the observed

jump around the j^{th} maintenance action is

$$\begin{aligned} Z_j^g &= Y(t_{j+1,1}) - Y(t_{j,n_j}) = Y(t_{j+1,1}) - Y(\tau_j^+) + Y(\tau_j^+) - Y(\tau_j^-) + Y(\tau_j^-) - Y(t_{j,n_j}) \\ &= \Delta Y_{j+1,1} + Z_j^c + \Delta Y_{j,n_j+1} \\ &= \Delta Y_{j+1,1} - \rho \sum_{i=1}^{n_j+1} \Delta Y_{j,i} + \Delta Y_{j,n_j+1} \\ &= \Delta Y_{j+1,1} - \rho \sum_{i=2}^{n_j} \Delta Y_{j,i} - \rho\ \Delta Y_{j,1} + (1-\rho)\Delta Y_{j,n_j+1} \end{aligned} \tag{2.26}$$

$\Delta Y_{j+1,1}$ and $\Delta Y_{j,n_j+1}$ are independent of $\mathcal{O}^g_{t_{j,n_j}}$. But Z_j^g and Z_{j-1}^g share the same non observed increment $\Delta Y_{j,1}$, so $\Delta Y_{j,1}$ is not independent of $\mathcal{O}^g_{t_{j,n_j}}$. Therefore, the conditional distribution of Z_j^g given $\mathcal{O}^g_{t_{j,n_j}}$ is not easy to derive.
In fact, it is easier here to use the joint distribution of the observed jumps given the observed increments. Let $\mathcal{O}_g$ be the set of all observed increments

$$\mathcal{O}^g = \left\{\Delta y_{0,1}, \{\Delta y_{j,i}\}_{1\leq j\leq k+1,\ 2\leq i\leq n_j}\right\}$$

The likelihood can be written

$$L_g\left(\mu, \sigma^2, \rho\right) = \left[\prod_{j=1}^{k+1} \prod_{i=1+\mathbb{1}_{j>0}}^{n_j} f_{\Delta Y_{j,i}}\left(\Delta y_{j,i}\right)\right] f_{Z^g|\mathcal{O}^g}\left(z_1^g, z_2^g, ..., z_k^g\right) \tag{2.27}$$

where $f_{Z^g|\mathcal{O}^g}$ is the conditional PDF of the observed jumps given the observed increments. Since the Z_j^g are linear combinations of independent normal random variables, $f_{Z^g|\mathcal{O}^g}$ is the PDF of a Gaussian vector. Therefore, we have to compute the expectation and covariance matrix of this vector.
From (2.26), the conditional expectation of Z_j^g is, $\forall\ j \in \{1, ..., k\}$

$$\mathbb{E}\left[Z_j^g \mid \mathcal{O}^g\right] = \mu u_j(\rho) - v_j(\rho) \tag{2.28}$$

where $\forall j$,

$$u_j(\rho) = \Delta t_{j+1,1} - \rho \Delta t_{j,1} \mathbb{1}_{j>1} + (1-\rho)\Delta t_{j,n_j+1}$$
$$v_j(\rho) = \rho \sum_{i=1+\mathbb{1}_{j>1}}^{n_j} \Delta y_{j,i}$$

From (2.26), the conditional variance of Z_j^g is, $\forall\ j \in \{1, ..., k\}$

$$\mathbb{V}ar\left[Z_j^g \mid \mathcal{O}^g\right] = \sigma^2 s_j(\rho) \tag{2.29}$$

where $\forall j$,

$$s_j(\rho) = \Delta t_{j+1,1} + \rho^2 \Delta t_{j,1} \mathbb{1}_{j>1} + (1-\rho)^2 \Delta t_{j,n_j+1}$$

The conditional covariance of (Z_{j-1}^g, Z_j^g) is, $\forall\ j \in \{2, ..., k\}$

$$\begin{aligned} Cov\left(Z_{j-1}^g,\ Z_j^g \mid \mathcal{O}^g\right) = \ & Cov(\Delta Y_{j,1} - \rho \sum_{i=2}^{n_{j-1}} \Delta y_{j-1,i} - \rho\ \Delta Y_{j-1,1} + (1-\rho)\Delta Y_{j-1,n_{j-1}+1}, \\ & \Delta Y_{j+1,1} - \rho \sum_{i=2}^{n_j} \Delta y_{j,i} - \rho\ \Delta Y_{j,1} + (1-\rho)\Delta Y_{j,n_j+1}) \\ = \ & Cov(-\rho\ \Delta Y_{j,1}\ ,\ \Delta Y_{j,1}) = -\rho\ \mathbb{V}ar[\Delta Y_{j,1}] = -\rho\ \sigma^2 \Delta t_{j,1} \end{aligned} \tag{2.30}$$

Let us define $u(\rho)^t = (u_1(\rho), u_2(\rho), ..., u_k(\rho))$ and similarly $v(\rho)^t$ and $s(\rho)^t$.
Finally, the conditional distribution of Z^g given $\mathcal{O}^g$ is the multivariate normal distribution $\mathcal{N}(\mu\ u(\rho) - \rho\ v(\rho)\ ,\ \sigma^2\ \Sigma(\rho))$ where

$$\Sigma(\rho) = \begin{pmatrix} s_1(\rho) & -\rho\Delta t_{2,1} & 0 & \cdots & \cdots & \cdots & \cdots & 0 \\ -\rho\Delta t_{2,1} & s_2(\rho) & -\rho\Delta t_{3,1} & 0 & & & & \\ 0 & -\rho\Delta t_{3,1} & s_3(\rho) & -\rho\Delta t_{4,1} & 0 & & & \\ \vdots & & \ddots & \ddots & \ddots & \ddots & \ddots & \vdots \\ & & & & 0 & -\rho\Delta t_{k-2,1} & s_{k-1}(\rho) & -\rho\Delta t_{k-1,1} \\ 0 & \cdots & \cdots & \cdots & \cdots & 0 & -\rho\Delta t_{k-1,1} & s_k(\rho) \end{pmatrix}$$

The log-likelihood is derived as

$$\ln\ L_g\left(\mu,\sigma^2,\rho\right) = -\frac{N}{2}\ln\sigma^2 + c_3 - \ln\sqrt{\det\Sigma(\rho)}$$
$$-\frac{1}{2\sigma^2}\left[(z^g-\mu u(\rho)+v(\rho))^t\ \Sigma(\rho)^{-1}\ (z^g-\mu u(\rho)+v(\rho)) \quad +\sum_{j=1}^{k+1}\sum_{i=1+\mathbb{1}_{j>1}}^{n_j}\frac{(\Delta y_{j,i}-\mu\Delta t_{j,i})^2}{\Delta t_{j,i}}\right] \tag{2.31}$$

where c_3 is a constant.

Deriving the log-likelihood, the maximum likelihood estimators $\hat{\mu}$ and $\hat{\sigma^2}$ are obtained as the solutions of the likelihood equations system, as follows.

$$\hat{\mu} = \frac{u^t(\hat{\rho})\ \Sigma^{-1}(\hat{\rho})\ z^g + u^t(\hat{\rho})\ \Sigma^{-1}(\hat{\rho})\ v(\hat{\rho}) + \sum_{j=1}^{k+1}\sum_{i=1+\mathbb{1}_{j>1}}^{n_j}\Delta Y_{j,i}}{u^t(\hat{\rho})\Sigma^{-1}(\hat{\rho})u(\hat{\rho}) + \sum_{j=1}^{k+1}\sum_{i=1+\mathbb{1}_{j>1}}^{n_j}\Delta t_{j,i}} \tag{2.32}$$

$$\hat{\sigma^2} = \frac{1}{N}\left[(z^g-\hat{\mu}\ u(\hat{\rho})+v(\hat{\rho}))^t\ \Sigma^{-1}(\hat{\rho})\ (z^g-\hat{\mu}\ u(\hat{\rho})+v(\hat{\rho})) + \sum_{j=1}^{k+1}\sum_{i=1+\mathbb{1}_{j>1}}^{n_j}\frac{(\Delta Y_{j,i}-\hat{\mu}\Delta t_{j,i})^2}{\Delta t_{j,i}}\right] \tag{2.33}$$

As in the previous sub-section, the profile log-likelihood is derived as

$$\ln\ L_g\left(\hat{\mu}(\rho),\hat{\sigma}^2(\rho),\rho\right) = -\frac{N}{2}(1+\ln\hat{\sigma}^2(\rho)) + c_3 - \ln\sqrt{\det\Sigma(\rho)} \tag{2.34}$$

Therefore, $\hat{\rho} = \underset{\rho}{argmin}\left[\frac{N}{2}\ln\hat{\sigma}^2(\rho) + \ln\sqrt{\det\Sigma(\rho)}\right]$
Biases of these estimators are detailed in Appendix A.2.

2.3 Quality and comparison of the estimators

This section presents the results of an experimental study which aims to assess the quality of the proposed estimators and to compare the four observation schemes.

Several situations are studied in order to assess the influence on the estimation quality of

- the number n_j and location of observations between two successive maintenance actions,
- the number of maintenance actions k ,
- the maintenance efficiency parameter ρ.

For each situation, the same 5000 simulated trajectories of the degradation process are used for each observation scheme. In each case, the model parameters ρ, μ and σ^2 are estimated.

In this section, the figures represent the boxplots of the distributions of the estimations for each parameter. The observation schemes are represented from left to right by colours (complete: green, 2: orange, 3: blue, general: magenta). The red dotted lines represent the true value of the parameters. Let us remind that there is no estimation of ρ for the complete observation scheme.

For the complete observation scheme, the degradation levels are observed periodically each one time unit. In the first two sub-sections, the three other observation schemes are obtained by removing some observations from the complete scheme (see Figures 2.2 to 2.5). The effect of this loss of information on the quality on the estimators is studied.

In the third sub-section, for each situation, the total number of observations n is the same for the four observation schemes. It allows to compare the quality of estimation for each observation scheme for a given size of data.

For a given situation, the $\{n_j\}_{j\in\{1,\dots,k+1\}}$ are all equal and the maintenance times τ_j are periodic. The underlying degradation process is the same in each case with $\mu = 2$ and $\sigma^2 = 5$. The different features used for the simulations are given in Table 2.1.

Table 2.1: Summary of the different features used for the simulations

Situation	Figure	μ	σ^2	ρ	n_j	k	n	Maintenance period
1	2.6	2	5	0.5	2	3	-	6
2	2.7	2	5	0.5	5	3	-	6
3	2.8	2	5	0.5	2	7	-	6
4	2.9	2	5	0.1	2	7	-	6
5	2.10	2	5	0.9	2	7	-	6
6	2.12	2	5	0.5	-	7	16	10
7	2.13	2	5	0.5	-	7	16	10

2.3.1 Influence of the number of observations

In situations 1 to 3 (Figures 2.6 to 2.8), the maintenance efficiency parameter ρ is the same, which allows to assess the effect of

- the number of observations between two successive maintenance actions, by comparing Figure 2.6 (n_j= 2) and Figure 2.7 (n_j= 5),
- the number of maintenance actions, by comparing Figure 2.6 ($k = 3$) and Figure 2.8 ($k = 7$),
- the loss of information linked to the observation schemes, by comparing the boxplots inside each figure.

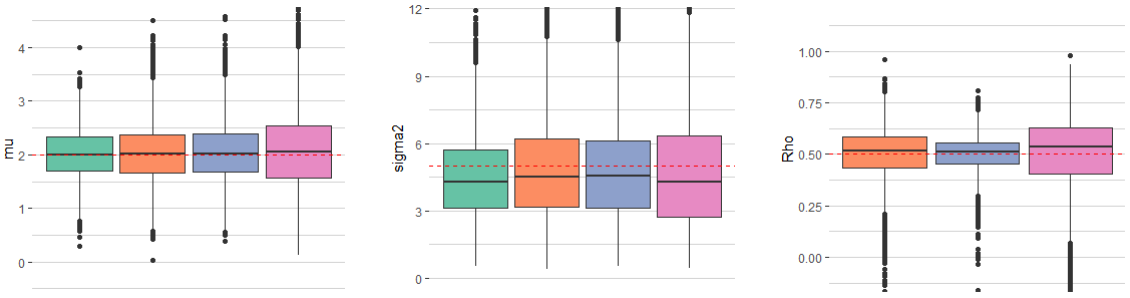

Figure 2.6: Estimation of μ, σ^2 and ρ, situation 1

For μ and σ^2, the best estimations are obtained for the complete scheme, and the worst for the general scheme . The quality of estimations in scheme 2 and 3 are equivalent. This

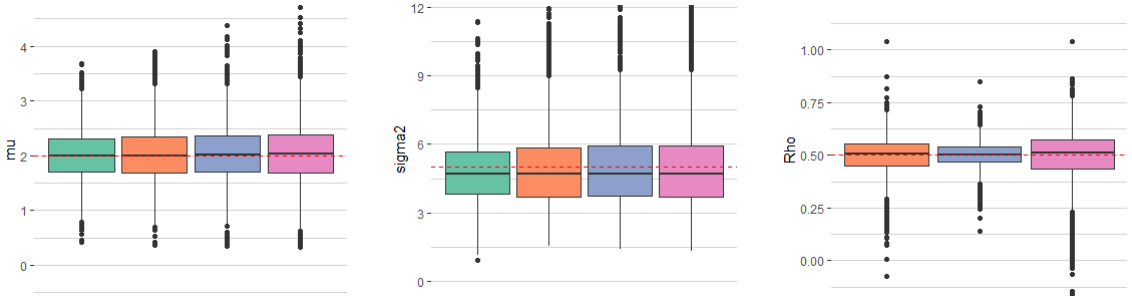

Figure 2.7: Estimation of μ, σ^2 and ρ, situation 2

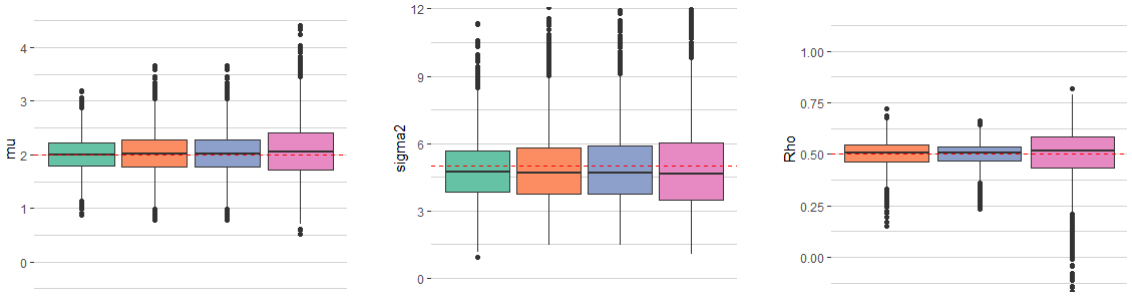

Figure 2.8: Estimation of μ, σ^2 and ρ, situation 3

result was expected and is linked to the total number of observation in each scheme, given in Table 2.2. The boxplots confirm the negative bias of $\hat{\sigma}^2$, previously proved for the complete scheme. Similar bias seem to hold for the three other schemes.

For ρ, the worst estimations are obtained as expected for the general scheme. The estimations for scheme 3 are significantly better than for scheme 2. From a practical point of view, it is not surprising that ρ is better estimated when the effect of maintenance on the degradation level is immediately observed.

Table 2.2: Total number of observations, n

	Observation scheme			
Situation	1	2	3	4
1	16	13	12	9
2	28	25	24	21
3	32	25	24	17

The bigger the number of observations, the better the quality of estimations, whether the degradation levels are observed at maintenance times or between maintenance times. For the general scheme, the estimations are better in situation 2 than in situation 3. Therefore, one could believe that it is better to increase the number of observations between maintenance actions than the number of maintenance actions. However, Table 2.2 shows that the total number of observations is bigger in situation 2 than in situation 3. Finally, to increase the quality of estimations, the main point seems to increase the number of observations whatever they are.

2.3.2 Influence of the value of the maintenance efficiency parameter ρ

In this sub-section, situations 3 to 5 (Figures 2.8 to 2.10) are compared, for which all the features of the simulations are equal except the value of ρ : $\rho \in \{0.5,\ 0.1,\ 0.9\}$. Note that the number of observations in each scheme is the same for the three situations (see situation 3 in Table 2.2), so the comparison of the situations will reflect only the impact of the value of ρ.

The comparison of the quality of estimations between the four observation schemes leads to the same conclusions as in the previous section. The change of the value of ρ has no impact on the estimations of μ and σ^2. The closer the value of ρ is to 1, the better it is estimated.

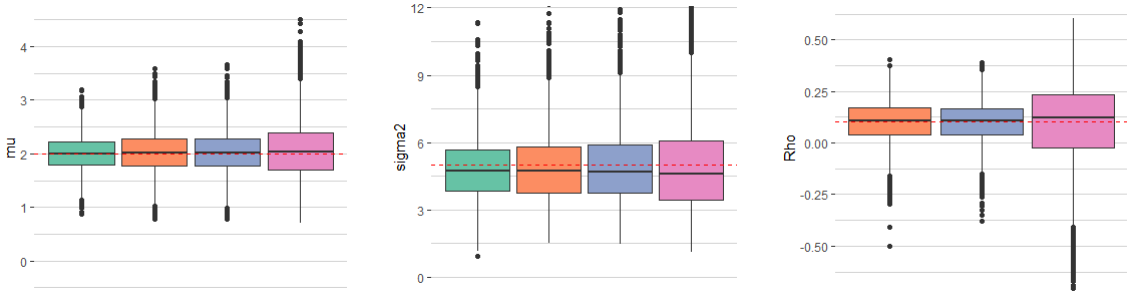

Figure 2.9: Estimation of μ, σ^2 and ρ, situation 4

2.3.3 Influence of the observations locations

In the previous sub-sections, we have noticed that, as expected, the quality of the estimations grows with the total number of observations n. Therefore, in the following, we compare

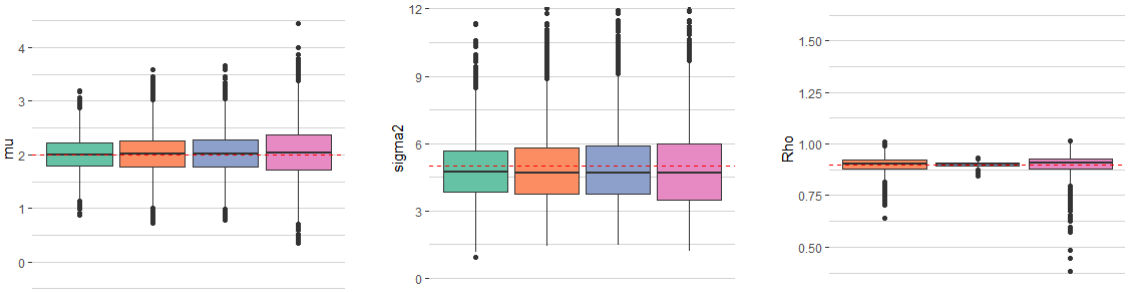

Figure 2.10: Estimation of μ, σ^2 and ρ, situation 5

the quality of estimations between schemes with the same total number of observations.

Starting from a sequence of observations following the complete scheme, we build observation sequences according to schemes 2,3 and the general scheme with the same number of observations, where the observation times are either close to the maintenance times (situation 6) or far from the maintenance times (situation 7). Moreover, we choose to have a minimal number of observations between maintenance actions ($n_j \in \{1, 2, 3\}$) in order that the impact of the locations of the observations with respect to maintenance times be clearly seen.

Observation backgrounds

Situation 6 for which the observation times are close to maintenance times is illustrated in Figure 2.12. Situation 7 for which the observation times are far from maintenance times is illustrated in Figure 2.13. In both situations, $n = 16$ degradation levels are observed in every scheme. The observations locations in situations 6 and 7 are described hereafter and illustrated in Figure 2.11.

1. Complete observation scheme, $n_j = 0$.
   The degradation levels are only observed at the maintenance times.

2. Second observation scheme, $n_j = 1$.

   - the observed degradation levels are close to the missing values at maintenance times, $t_{j+1,1} = \tau_j + \frac{1}{10}(\tau_{j+1} - \tau_j)$ (Situation 6, Figure 2.12)
   - the observed degradation levels are located at the middle time between two successive maintenance actions , $t_{j+1,1} = \tau_j + \frac{1}{2}(\tau_{j+1} - \tau_j)$ (Situation 7, Figure 2.13)

3. Third observation scheme, $n_j = 1$.

   - the observed degradation levels are close to the missing values at maintenance times , $t_{j+1,1} = \tau_{j+1} - \frac{1}{10}(\tau_{j+1} - \tau_j)$ (Situation 6, Figure 2.12)
   - the observed degradation levels are located at the middle time between two successive maintenance actions , $t_{j+1,1} = \tau_j + \frac{1}{2}(\tau_{j+1} - \tau_j)$ (Situation 7, Figure 2.13)

4. General observation scheme, $n_j = 2$

   - the observed degradation levels are close to the missing values at maintenance times, $t_{j+1,1} = \tau_j + \frac{1}{10}(\tau_{j+1} - \tau_j)$ and $t_{j+1,2} = \tau_{j+1} - \frac{1}{10}(\tau_{j+1} - \tau_j)$ (Situation 6, Figure 2.12)
   - the observed degradation levels are further to the maintenance times, $t_{j+1,1} = \tau_j + \frac{1}{3}(\tau_{j+1} - \tau_j)$ and $t_{j+1,2} = \tau_{j+1} - \frac{1}{3}(\tau_{j+1} - \tau_j)$ (Situation 7, Figure 2.13)

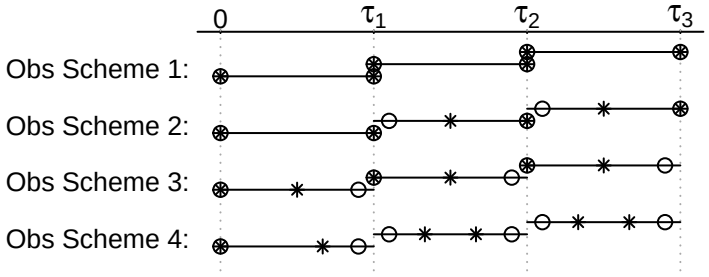

Figure 2.11: Locations of the observations of the degradation under situation 6 (circles) and 7 (stars)

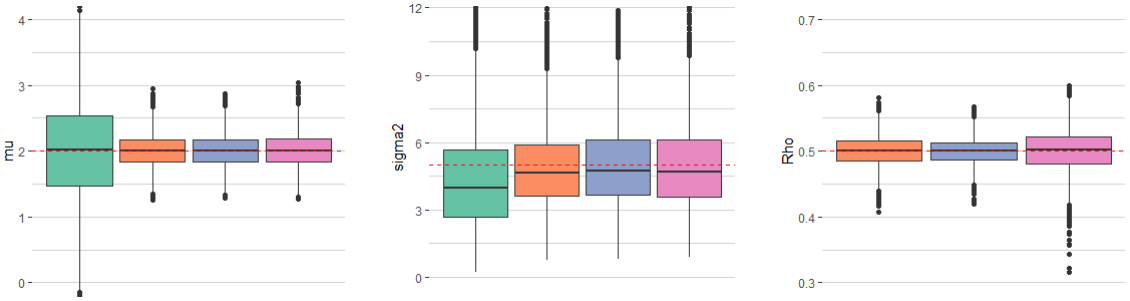

Figure 2.12: Estimation of μ, σ^2 and ρ, situation 6

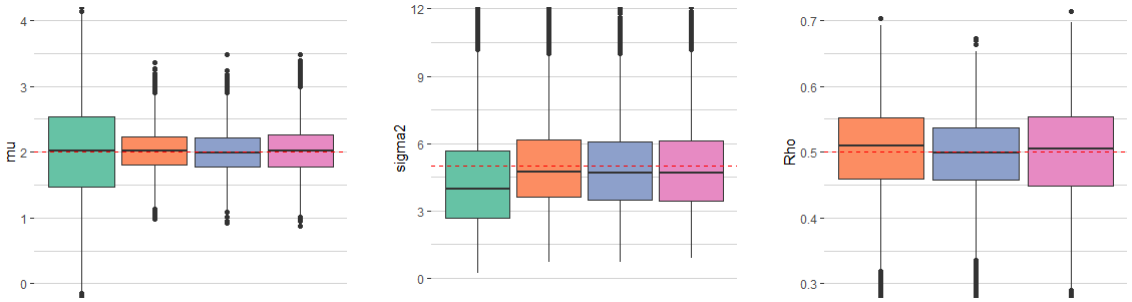

Figure 2.13: Estimation of μ, σ^2 and ρ, situation 7

Quality of the Estimations

The most striking result from Figures 2.12 and 2.13 is that the estimations of μ and σ^2 are noticeably worse for the complete scheme than for the other schemes in both situations. This can be explained by the fact that, in the complete scheme with $n_j = 0$, the observations consist of the degradation increments $\Delta Y_{j,1}$ and the degradation jumps $Z_j^c = -\rho\ \Delta Y_{j,1}$. Therefore, only half of the observations brings useful information for estimating μ and σ^2.

Moreover, it appears that the estimations of ρ are better in situation 6 than in situation 7. It reflects the fact that in order to estimate the maintenance efficiency, it is recommended to observe the degradation levels close to the maintenance actions. As before, the best scheme for the estimation of ρ is scheme 3.

2.4 Conclusion on the Wiener-based degradation model

This chapter examined studied statistical inference for a Wiener-based degradation model with ARD_1 imperfect maintenance actions under four distinct observation schemes. For each scheme, the maximum likelihood estimators of the three model parameters have been derived. Through a simulation study, the impact of the number and placement of observations between successive maintenance actions, the count of maintenance actions, and maintenance efficiency on estimation quality has been investigated. As expected, estimation quality improves with an increased number of observations. An interesting finding is that the best estimation of ρ is obtained for the third observation scheme. It means that if only a limited number of observations is possible, it is recommended to perform them just after each maintenance.

The study reveals that the ARD_1 model encounters certain drawbacks concerning inference matters. The model is not well suited to practical situations involving the complete observation scheme. To avoid these issues another Wiener-based degradation model with imperfect maintenance is considered in the next chapter.

Chapter 3

Modeling and inference for a degradation process with partial maintenance effects

This chapter proposes a novel approach to modeling imperfect maintenance in degradation models, under the assumption that maintenance impacts only a part of the degradation process. In the existing literature, concerning degradation model, maintenance effects are generally assumed to affect the entire degradation process. However, in practical scenarios, maintenance actions are often performed only on specific components of the system and consequently have an effect only on a part of the degradation process. For instance, within the framework of railway infrastructure management and track geometry maintenance, longitudinal leveling by tamping (i.e. compacting the ballast to correct the track geometry) can be considered as a partial repair : they do restore in part the track geometry, but since the ballast itself is not replaced and rail fastenings are not tightened, this operation does not results in a as-good-as new state for the track level [71]. Another example is a vehicle's braking system, where maintenance actions are generally performed only on the break pads and not on the whole disc. More generally, when a system is made of several components, maintenance often consists in replacing only a smaller group of components [91, 58]. This is called partial replacement. Maintenance is perfect for the replaced components, but is imperfect for the whole system. While this situation has been discussed to justify the relevance of imperfect maintenance models, these models typically do not directly incorporate the partial replacement assumption. An exception is the partial repair model based on superimposed renewal processes proposed in [65]. Therefore, for modeling degradation, it

appears pertinent to consider that maintenance can affect only a part of the degradation process.

More precisely, the global degradation process is the sum of two dependent Wiener processes with drift. Maintenance has an ARD_1-type effect (Arithmetic Reduction of Degradation), as introduced in [73], on only one of these processes. It reduces the degradation level of a quantity which is proportional to the amount of degradation of this process accumulated since the last maintenance. Two particular cases of the model are explored: the perturbed ARD_1 and the partial replacement models. The system undergoes regular inspections, during which degradation levels are measured. The conventional ARD_1 model is a specific case of this newly proposed full model. Two distinct observation schemes are considered. In the complete scheme, the degradation levels are measured both between maintenance actions and at maintenance times (just before and just after). In the general scheme, the degradation levels are measured only between maintenance actions but can be observed as close as possible from maintenance times. At first sight, the complete observation scheme seems the most natural and reasonable. However, it may not be possible to implement this ideal scheme in practice, for various technological and engineering reasons. This is for example the case if the measurement devices and technical crew for inspection are not the same as the technical devices and crew for maintenance, such as for railway assets monitoring and maintenance, where inspections and maintenance actions cannot be performed at the same time because of an incompressible maintenance intervention delay [71]. In such cases, it is necessary to model the observation procedures in a more realistic way (accounting for delays between the inspections and the maintenance actions, or non-periodic inspections). This can be done in the general observation scheme. Besides, a measurement at a maintenance time is a limit case of a measurement between maintenance times, when the measurement (inspection) time tends to the maintenance time. Therefore, all the possible observations schemes (as the 4 schemes considered in [62]) are limit cases of the general scheme. That is why it is called general. Thereafter, the maximum likelihood estimation of the model parameters is studied for both observation schemes in both particular models. The quality of the estimators is assessed through a simulation study.

The chapter is organized as follows. The new degradation model is presented in Section 3.1. The statistical inference is studied in Section 3.2 for the perturbed ARD_1 and partial replacement models, under both observation schemes. The results of the simulation study are presented in Section 3.3. Finally, concluding comments are given and some prospects are raised in Section 3.4.

3.1 A degradation model with partial maintenance effects

This section presents the proposed degradation model, for which maintenance affects only a part of the degradation process. The model is described in Section 3.1.1. An alternative parameterization is proposed in Section 3.1.2. Some particular cases are listed in Section 3.1.3 and an identifiability issue is raised in Section 3.1.4.

3.1.1 Model description

The assumptions of the proposed model are given below.

- The degradation process is made of two parts $X^U = \{X^U(t)\}_{t\geq 0}$ and $X^M = \{X^M(t)\}_{t\geq 0}$.
- Between two maintenances, the degradation process evolves as the sum of the underlying degradation processes X^U and X^M.
- Maintenance only affects X^M.
- Maintenance effect is of the ARD_1-type [73]: at maintenance times, the degradation level is reduced of a quantity which is proportional to the amount of degradation of X^M accumulated since the last maintenance action.
- X^U and X^M are dependent Wiener processes with drift, or $(X^U, X^M)^T$ is a bivariate Wiener process with drift. Therefore, their increments are independent and $(X^U(t), X^M(t))^T$ is a Gaussian vector:

$$\begin{pmatrix} X^U(t) \\ X^M(t) \end{pmatrix} \sim \mathcal{N}\left(\begin{pmatrix} \mu_U \\ \mu_M \end{pmatrix} t,\, \Sigma_{UM} t \right) \tag{3.1}$$

  where $\Sigma_{UM} = \begin{pmatrix} \sigma_U^2 & c_{UM} \\ c_{UM} & \sigma_M^2 \end{pmatrix}$.

  μ_U, μ_M are the drift parameters, σ_U^2, σ_M^2 are the variance parameters, and c_{UM} is a covariance parameter. Note that the coefficient of correlation between $X_U(t)$ and $X_M(t)$ is

$$Corr(X_U(t), X_M(t)) = \frac{c_{UM} t}{\sqrt{\sigma_U^2 t\, \sigma_M^2 t}} = \frac{c_{UM}}{\sigma_U \sigma_M} = r_{UM} \in [-1, 1].$$

Therefore, the coefficient of correlation does not depend on time.

The system is maintained at times $(\tau_1, \tau_2, ...)$. Let $Y(t)$ be the degradation level at time t of a maintained system, with $Y(0) = 0$. Let $Y(\tau_j^-)$ be the degradation level just before the j^{th} maintenance at time τ_j and $Y(\tau_j^+)$ be the degradation level just after τ_j.

Before the first maintenance action, the degradation level Y of the system evolves as the sum of X^U and X^M.

$$\forall\ t \in [0, \tau_1[,\ Y(t) = X^U(t) + X^M(t).$$

Just before the first maintenance, $Y(\tau_1^-) = X^U(\tau_1) + X^M(\tau_1)$.

At time τ_1, an ARD_1-type maintenance is performed that only affects X^M. The maintenance effect is to reduce the degradation level of a quantity proportional to the amount of degradation of X^M accumulated since the origin. Let ρ be the coefficient of proportionality, which expresses the efficiency of maintenance.

$$Y(\tau_1^+) = Y(\tau_1^-) - \rho\left[X^M(\tau_1) - X^M(0)\right] = X^U(\tau_1) + (1-\rho)X^M(\tau_1)$$

Between τ_1 and τ_2, the system is degrading as a non-maintained system.

$$\begin{aligned} \forall\ t \in [\tau_1, \tau_2[,\quad Y(t) &= Y(\tau_1^+) + X^U(t) + X^M(t) - X^U(\tau_1) - X^M(\tau_1) \\ &= X^U(t) + X^M(t) - \rho X^M(\tau_1) \end{aligned}$$

At τ_2, an ARD_1-type maintenance is performed.

$$Y(\tau_2^+) = Y(\tau_2^-) - \rho\left[X^M(\tau_2) - X^M(\tau_1)\right] = X^U(\tau_2) + (1-\rho)X^M(\tau_2)$$

By recurrence, it is easy to show that the degradation process of the maintained system is defined as follows.

$$\forall j \geq 1,\ Y(\tau_j^-) = X^U(\tau_j) + X^M(\tau_j) - \rho X^M(\tau_{j-1}) \tag{3.2}$$

$$Y(\tau_j^+) = X^U(\tau_j) + (1-\rho)X^M(\tau_j) \tag{3.3}$$

$$\forall\ t \in [\tau_{j-1}, \tau_j[,\ Y(t) = X^U(t) + X^M(t) - \rho X^M(\tau_{j-1}) \tag{3.4}$$

The effect of a maintenance action is represented by a jump of the degradation level.

Let Z_j^c be the observed jump at the j^{th} maintenance time.

$$Z_j^c = Y(\tau_j^+) - Y(\tau_j^-) = -\rho \ \left[X^M(\tau_j) - X^M(\tau_{j-1})\right] \tag{3.5}$$

From the properties of the Wiener process X^M, the Z_j^c are independent random variables and their respective distributions are, $\forall j \geq 1$:

$$Z_j^c \sim \mathcal{N}\left(-\rho\mu_M\Delta\tau_j \ , \ \rho^2\sigma_M^2\Delta\tau_j\right). \tag{3.6}$$

where $\Delta\tau_j = \tau_j - \tau_{j-1}$. Note that the jumps are not independent of the previous degradation increments.

The distribution of the degradation increments inside each inter-maintenance interval can also be easily derived from (3.4):

$$\forall\ j \geq 1,\ \forall\ \tau_{j-1} < s < t < \tau_j,\ Y(t) - Y(s) = X^U(t) - X^U(s) + X^M(t) - X^M(s).$$

Therefore, the distribution of the increments is given by, $\forall\ j \geq 1,\ \forall\ \tau_{j-1} < s < t < \tau_j$:

$$Y(t) - Y(s) \sim \mathcal{N}\left((\mu_U + \mu_M)(t-s),\ (\sigma_U^2 + \sigma_M^2 + 2c_{UM})(t-s)\right). \tag{3.7}$$

The independence of increments of the bivariate process (X^U,X^M) implies the independence of increments of Y.

3.1.2 An alternative parameterization

From a statistical perspective, the model parameters will have to be estimated from field data. The observed data are degradation increments and degradation jumps, whose distributions are given by (3.6) and (3.7). Therefore, in order to simplify the writings in statistical inference, it appears relevant to introduce an alternative parameterization of the model. Let

$$X^S(t) = X^U(t) + X^M(t) \tag{3.8}$$

X^S is the global underlying degradation process of the unmaintained system and X^M is the part of this process which is affected by maintenance actions. $(\ X^S(t), X^M(t))^T$ is a

linear transform of the Gaussian vector $(X^U(t), X^M(t))^T$:

$$\begin{pmatrix} X^S(t) \\ X^M(t) \end{pmatrix} = A \begin{pmatrix} X^U(t) \\ X^M(t) \end{pmatrix}, \quad \text{where } A = \begin{pmatrix} 1 & 1 \\ 0 & 1 \end{pmatrix}.$$

So $(X^S(t), X^M(t))^T$ is still a Gaussian vector. From usual results on random vectors, its mean is

$$A\, \mathbb{E} \begin{pmatrix} X^U(t) \\ X^M(t) \end{pmatrix} = \begin{pmatrix} \mu_U + \mu_M \\ \mu_M \end{pmatrix} t$$

and its covariance matrix is

$$A\Sigma_{UM} t A^T = \begin{pmatrix} \sigma_U^2 + \sigma_M^2 + 2c_{UM} & c_{UM} + \sigma_M^2 \\ c_{UM} + \sigma_M^2 & \sigma_M^2 \end{pmatrix} t.$$

Therefore, let us introduce new parameters μ_S, μ_M, σ_S^2, σ_M^2, c_{SM}, r_{SM}, such that $(X^S(t), X^M(t))^T$ is a Gaussian vector with mean $(\mu_S, \mu_M)^T t$ and covariance matrix $\Sigma_{SM} t$, where $\Sigma_{SM} = \begin{pmatrix} \sigma_S^2 & c_{SM} \\ c_{SM} & \sigma_M^2 \end{pmatrix}$ and $r_{SM} = c_{SM}/(\sigma_S \sigma_M)$. The links between the first parameterization (U, M) and the second parameterization (S, M) are given in Table 3.1.

Table 3.1: Links between the two model parameterizations

	(X^U, X^M)	(X^S, X^M)
Drift	$\mu_U = \mu_S - \mu_M$	$\mu_S = \mu_U + \mu_M$
Variance	$\sigma_U^2 = \sigma_S^2 + \sigma_M^2 - 2c_{SM}$	$\sigma_S^2 = \sigma_U^2 + \sigma_M^2 + 2\, c_{UM}$
Covariance	$c_{UM} = c_{SM} - \sigma_M^2$	$c_{SM} = c_{UM} + \sigma_M^2$
Correlation	$r_{UM} = \dfrac{r_{SM}\sigma_S - \sigma_M}{\sqrt{\sigma_S^2 + \sigma_M^2 - 2\, r_{SM}\sigma_S\sigma_M}}$	$r_{SM} = \dfrac{r_{UM}\sigma_U + \sigma_M}{\sqrt{\sigma_U^2 + \sigma_M^2 + 2\, r_{UM}\sigma_U\sigma_M}}$

To simplify writings, let $\forall\ \ell \in \{S, M\}$, $\Delta X_j^\ell = X^\ell(\tau_j) - X^\ell(\tau_{j-1})$ be the increment of the degradation process ℓ ($\ell \in \{S, M\}$) between the $j-1^{th}$ and the j^{th} maintenance action.

In the new parameterization, the degradation level and jumps are defined as follows.

$$\forall\ j \geq 1,\ \forall\ t \in [\tau_{j-1}, \tau_j[, \quad Y(t) = X^S(t) - \rho\ X^M(\tau_{j-1}). \tag{3.9}$$

$$\forall j \geq 1, \quad Z_j^c = -\rho\ \left[X^M(\tau_j) - X^M(\tau_{j-1})\right] = -\rho\ \Delta X_j^M. \tag{3.10}$$

The distributions of the degradation increments and jumps are:

$$\forall\ j \geq 1,\ \forall\ \tau_{j-1} \leq s < t \leq \tau_j,\quad Y(t) - Y(s) \sim \mathcal{N}\left(\mu_S(t-s),\ \sigma_S^2(t-s)\right). \tag{3.11}$$

$$\forall\ j \geq 1,\quad Z_j^c \sim \mathcal{N}\left(-\rho\mu_M\Delta\tau_j\ ,\ \rho^2\sigma_M^2\Delta\tau_j\right). \tag{3.12}$$

From (3.11) an (3.12), it can be seen that parameters (μ_S, σ_S^2) are closely linked to degradation increments between maintenance actions while parameters $(\mu_M, \sigma_M^2, \rho)$ are closely linked to degradation jumps, so to maintenance efficiency. This remark will be useful in Section 3.2 for the estimation of these parameters.

Finally, the distribution of the degradation level at time t can be easily computed from (3.9):

$$Y(t) \sim \mathcal{N}\left(\mu_S t - \rho\mu_M\tau_{j-1}\ ,\ \sigma_S^2 t + \rho^2\sigma_M^2\tau_{j-1} - 2\rho r_{SM}\sigma_S\sigma_M\tau_{j-1}\right)$$

The same degradation trajectory under both parameterizations is presented in Figure 3.1. The observed degradation process Y is represented with the underlying processes X^U and X^M on the left figure and with X^S and X^M on the right figure. This trajectory has been simulated using the following parameters : $\mu_U = 4$, $\mu_M = 2$, $\sigma_U^2 = 10$, $\sigma_M^2 = 7$, $r_{UM} = 0.8$, $\rho = 0.7$, which is equivalent to $\mu_S = 6$, $\mu_M = 2$, $\sigma_S^2 = 30.39$, $\sigma_M^2 = 7$, $r_{SM} = 0.94$, $\rho = 0.7$.

In this example, four maintenance actions are periodically performed at times $\{3, 6, 9, 12\}$. The underlying processes are simulated using consecutive degradation increments on a time increment equals to 0.001. In the first parameterization, between maintenance actions, the degradation process Y (in black) evolves as the sum of X^U (in green) and X^M (in blue). In the second parameterization, Y evolves as X^S (in red) between maintenances. The correlation between the underlying degradation processes clearly appears in this figure. The maintenance effect is also clearly visible for the first three maintenances. For the fourth one at $\tau_4 = 12$, the maintenance effect is not visible because the amount of degradation accumulated for process X^M between $\tau_3 = 9$ and $\tau_4 = 12$ is very small.

3.1.3 Specific cases

The model defined by Section 3.1.2 will be called hereafter the full model. Some interesting specific cases of the full model can be considered.

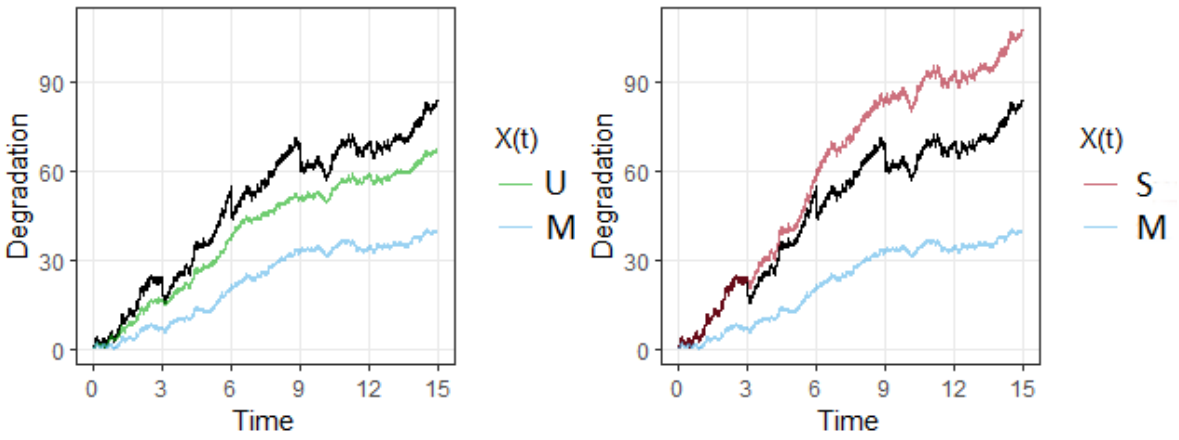

Figure 3.1: Degradation trajectories of $Y(t)$ (in black) with (X^U, X^M) (in green and blue) in the left figure and (X^S,X^M) (in red and blue) in the right figure.

- **ABAO**. When $\rho = 0$, $Y(t) = X^S\ (t) = X^U(t) + X^M(t)$. Maintenance has no effect on the system, the system after maintenance is As Bad As Old (ABAO).

- **Usual ARD$_1$ model**. The new model is equivalent to the usual Wiener-based ARD$_1$ model [73, 62] when the whole degradation process is affected by maintenance actions. This is the case for $X^U(t) = 0, \forall\ t \geq 0$, i.e. $\mu_U = \sigma_U^2 = c_{UM} = 0$. In this case, $X^S = X^M$ so $\mu_S = \mu_M$, $\sigma_S^2 = \sigma_M^2 = c_{SM}$ and $r_{SM} = 1$. In this situation, $\rho = 1$ entails a perfect maintenance action.

- **Perturbed ARD$_1$ model**. When $\mu_S = \mu_M$ or $\mu_U = 0$, X^U, which can depend on the degradation process, is a white noise. So the degradation process Y can be considered as a usual Wiener-based ARD$_1$ model perturbed by this white noise.

- **Partial replacement**. In the usual ARD$_1$ model, $\rho = 1$ means that the system is renewed, or As Good As New (AGAN), after each maintenance. Here, $\rho = 1$ means that maintenance deletes all the amount of degradation of X^M accumulated since the last maintenance. Globally, maintenance is not perfect ($Y(\tau_j^+) = X^U(\tau_j) \neq 0$) but can be considered as optimal. This corresponds to the situation where maintenance consists in replacing a part of the system components, but not the whole system. This situation is particularly interesting in practice and will be studied in Section 3.2.

- When X^U and X^M are independent, $r_{UM} = 0$ so $r_{SM} = \frac{\sigma_M}{\sqrt{\sigma_U^2+\sigma_M^2}}$. Therefore X^S and X^M are dependent and positively correlated.
- When X^S and X^M are independent, $r_{SM} = 0$ so $r_{UM} = -\frac{\sigma_M}{\sqrt{\sigma_S^2+\sigma_M^2}}$. Therefore X^U and X^M are dependent and negatively correlated.
- $r_{UM} = 1 \Rightarrow r_{SM} = 1$. A perfect positive correlation under the (U, M) parameterization entails a perfect positive correlation under the (S, M) parameterization.
- $r_{SM} = 1 \Rightarrow \ r_{UM} = \frac{\sigma_S-\sigma_M}{\sqrt{(\sigma_S-\sigma_M)^2}} \Rightarrow \ r_{UM} = \{-1, 1\}$. A perfect positive correlation under the (S, M) parameterization entails a perfect correlation under the (U, M) parameterization, which can be either positive or negative.

3.1.4 Identifiability

The definition of the model in (3.9) to (3.12) shows that two different sets of parameters $(\mu_M, \sigma_M^2, \rho)$ and $(\tilde{\mu}_M, \tilde{\sigma}_M^2, \tilde{\rho})$ such that $\rho\mu_M = \tilde{\rho}\tilde{\mu}_M$ and $\rho\sigma_M = \tilde{\rho}\tilde{\sigma}_M$ define the same model.

More precisely, $X^S(t)$ and $X^M(t)$ can be written $X^S(t) = \mu_S t + \sigma_S B^S(t)$ and $X^M(t) = \mu_M t + \sigma_M B^M(t)$, where B^S and B^M are dependent standard Brownian motions. Let $\tilde{X}^M(t) = \tilde{\mu}_M t + \tilde{\sigma}_M B^M(t)$, where $\tilde{\mu}_M = \rho\mu_M/\tilde{\rho}$ and $\tilde{\sigma}_M = \rho\sigma_M/\tilde{\rho}$. We have $\tilde{X}^M(t) = \rho X^M(t)/\tilde{\rho}$ and $\tilde{\rho}\tilde{X}^M(t) = \rho X^M(t)$. Therefore, the degradation process $\tilde{Y}(t) = X^S(t) - \tilde{\rho}\tilde{X}^M(t)$ is exactly the same as $Y(t) = X^S(t) - \rho X^M(t)$. Moreover, it is easy to show that $Cov(X^S(t), \tilde{X}^M(t)) = \rho c_{SM} t/\tilde{\rho} = \tilde{c}_{SM} t$ and $\tilde{r}_{SM} = \tilde{c}_{SM}/\sigma_S\tilde{\sigma}_M = r_{SM}$.

So finally, $\forall\tilde{\rho} \in]0, 1]$ the sets of parameters $(\mu_S, \mu_M, \sigma_S^2, \sigma_M^2, r_{SM}, \rho)$ and $(\mu_S, \rho\mu_M/\tilde{\rho}$, $\sigma_S^2, \rho^2\sigma_M^2/\tilde{\rho}^2,\ r_{SM}, \tilde{\rho})$ define the same model. Although it is less visible, the same problem also appears using the (U, M) parameterization.

Hence, the full model is not identifiable. Therefore, in Section 3.2, constraints will be imposed in order to estimate the parameters of identifiable models: the perturbed ARD_1 and partial replacement models.

In order to study statistical inference in the following section, the model's likelihood is first derived for the full model.

3.2 Statistical Inference

Let $\Theta = (\mu_S, \mu_M, \sigma_S^2, \sigma_M^2, r_{SM}, \rho)$ be the set of model parameters under the second parameterization. This section studies the statistical estimation of these parameters from field data. The system is assumed to be regularly inspected and degradation levels $Y_{j,i}$ are measured. Two observation schemes (i.e. two ways of collecting data) are considered, the complete scheme and the general scheme. For both schemes, the parameters are estimated by the maximum likelihood method. Each scheme leads to a different writing of the likelihood and then to different estimations of the parameters. The observation schemes are described in Section 3.2.1. The general expressions of the likelihoods are determined in Section 3.2.2. Due to the identifiability issue raised in Section 3.1.4, the estimation is made in Section 3.2.3 only for the perturbed ARD_1 and partial replacement models under both observation schemes.

3.2.1 Observation schemes

The considered system is observed in a time interval $[0, \tau]$. In this interval, k maintenances are performed at times $\tau_1, \ldots, \tau_k$. Let us denote $\tau_0 = 0$ and $\tau_{k+1} = \tau$.

$\forall\ j \in \{1, ..., k+1\}$, let n_j be the number of observations of the degradation level in $]\tau_{j-1}, \tau_j[$. The degradation levels are observed at times $t_{j,i}$, where $t_{j,i}$ is the time of the i^{th} observation in $]\tau_{j-1}, \tau_j[\ \forall\ i \in \{1, ..., n_j\}$. If observations are made at the maintenance times (just before and/or just after), the corresponding observation times are denoted $t_{j,n_j+1} = \tau_j = t_{j+1,0}$. Let $\Delta t_{j,i} = t_{j,i} - t_{j,i-1}$ be the time elapsed between two successive observations.

Complete observation scheme

In the complete scheme, the degradation levels are measured both between maintenance actions and at maintenance times (just before and just after). In Figure 3.2, a degradation trajectory is simulated for $\mu_S = 10$, $\mu_M = 5$, $\sigma_S^2 = 30$, $\sigma_M^2 = 20$, $r_{SM} = 0.7$, $\rho = 0.8$. In this example, degradation levels are periodically observed and represented by black dots. Maintenance actions are periodically performed at times $\{3, 6, 9, 12\}$. The two underlying processes X^S and X^M are respectively depicted by the red and blue lines. The observed degradation increments of the system are represented by the black line.

Due to the properties of the Wiener process, it is more convenient to consider that

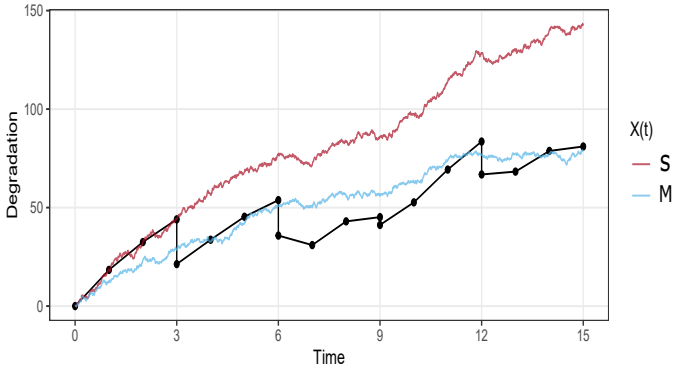

Figure 3.2: Observations of the degradation levels of the maintained system (in black) under the complete observation scheme

the degradation increments (instead of degradation levels) are observed. Therefore, in the complete scheme, the observations are made of:

- The degradation increments $\Delta Y^c_{j,i} = Y(t_{j,i}) - Y(t_{j,i-1}) = X^S(t_{j,i}) - X^S(t_{j,i-1})$, for $1 \leq j \leq k+1$ and $1 \leq i \leq n_j + 1$. They are independent and their respective distributions are $\Delta Y^c_{j,i} \sim \mathcal{N}\left(\mu_S \Delta t_{j,i},\ \sigma_S^2 \Delta t_{j,i}\right)$.
- The degradation jumps $Z^c_j = Y(\tau_j^+) - Y(\tau_j^-) = -\rho\ \left[X^M(\tau_j) - X^M(\tau_{j-1})\right] = -\rho\, \Delta X^M_j$, for $1 \leq j \leq k$. They are not independent of the observations prior to τ_j. The set of all these observations is denoted:

$$\mathcal{O}^c_{\tau_j^-} = \{\Delta y^c_{1,1}, ..., \Delta y^c_{1,n_1+1}, z^c_1, \Delta y^c_{2,1}, ..., \Delta y^c_{j-1,n_{j-1}+1}, z^c_{j-1}, \Delta y^c_{j,1}, ..., \Delta y^c_{j,n_j+1}\}$$

The likelihood function is the joint PDF of the j^{th} jump given all the observations before τ_j. Therefore, the likelihood function in the complete scheme, denoted $L_c(\Theta)$, is given by

$$L_c(\Theta) = \prod_{j=1}^{k+1} \prod_{i=1}^{n_j+1} f_{\Delta Y^c_{j,i}}\left(\Delta y^c_{j,i}\right) \prod_{j=1}^{k} f_{Z^c_j | \mathcal{O}^c_{\tau_j^-}}(z^c_j) \tag{3.13}$$

where $f_{Z^c_j | \mathcal{O}^c_{\tau_j^-}}$ is the conditional PDF of the j^{th} jump given all the observations before τ_j. The expression of this likelihood is developed in Section 3.2.2.

In [62], this observation scheme has been considered for a usual ARD_1 Wiener-based degradation model (first observation scheme in [62]). In this model, the value of a jump is

proportional to the amount of degradation accumulated since the last maintenance action. Thus, under the complete observation scheme, the sizes of the jumps are deterministic given the previous observations. This is very unlikely in practice. Here, $Z_j^c = -\rho\ \Delta X_j^M$ and the ΔX_j^M are not observed, so the problem of the ARD_1 model does not occur. Therefore, the proposed model is more realistic than the ARD_1 model for the complete observation scheme.

General observation scheme

In the general scheme, the degradation levels are measured only between maintenance actions. In Figure 3.3, a degradation trajectory is simulated for the same parameters as in Figure 3.2. In this example, contrary to Figure 3.2, the observations are not periodic and the numbers of observations between two successive maintenances are not constant. As in Figure 3.2, every black dot represents an observated degradation level. Dotted lines correspond to the unobserved degradation increments around maintenance times. The two underlying processes X^S and X^M are respectively depicted by the red and blue lines. The observed degradation increments of the system are represented by the black line.

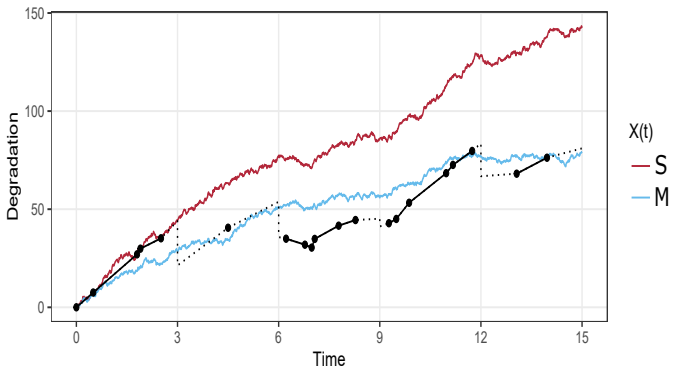

Figure 3.3: Observations of the degradation levels of the maintained system (in black) under the general observation scheme

In this case, neither $Y(\tau_j^-)$ nor $Y(\tau_j^+)$ are observed. Therefore, the true degradation jumps Z_j^c are also not observed. The observation around the j^{th} maintenance time τ_j is the difference between the first observed degradation level after τ_j and the last observed degradation level before τ_j:

$$\forall j \geq 1,\ Z_j^g = Y(t_{j+1,1}) - Y(t_{j,n_j}) \tag{3.14}$$

Therefore, in the general scheme, the observations are made of:

- The degradation increments $\Delta Y^c_{j,i}$, for $2 \leq j \leq k$ and $2 \leq i \leq n_j$, and $1 \leq i \leq n_1$ for $j = 1$. Indeed, with respect to the complete scheme, the first and last degradation increments of each interval are no longer observed, except the very first one $\Delta Y^c_{1,1}$. As before, they are independent and their respective distributions are $\Delta Y^c_{j,i} \sim \mathcal{N}\left(\mu_S \Delta t_{j,i},\ \sigma_S^2 \Delta t_{j,i}\right)$.
- The new jumps $Z^g_j = Y(t_{j+1,1}) - Y(t_{j,n_j})$, for $1 \leq j \leq k$. They are not independent of the observations prior to t_{j,n_j}. The set of all these observations is denoted:

$$\mathcal{O}^g_{t_{j,n_j}} = \{\Delta y^c_{1,1}, ..., \Delta y^c_{1,n_1}, Z^g_1, \Delta y^c_{2,2}, ..., \Delta y^c_{j-1,n_{j-1}}, Z^g_{j-1}, \Delta y^c_{j,2}, ..., \Delta y^c_{j,n_j}\}$$

Therefore, the likelihood function in the general scheme, denoted $L_g(\Theta)$, is given by

$$L_g(\Theta) = \prod_{j=1}^{k+1} \prod_{i=1+\mathbb{1}_{j>1}}^{n_j} f_{\Delta Y^c_{j,i}}\left(\Delta y^c_{j,i}\right) \prod_{j=1}^{k} f_{Z^g_j | \mathcal{O}^g_{t_{j,n_j}}}\left(z^g_j\right) \tag{3.15}$$

The expression of this likelihood is developed in Section 3.2.2.

3.2.2 Derivation of the likelihood

Complete observation scheme

In order to write the likelihood (3.13), the only difficulty is to derive the conditional distributions of the jumps $Z^c_j = -\rho\ \Delta X^M_j$ given $\mathcal{O}^c_{\tau_j^-}$.

We have $\Delta X^M_j = X^M(\tau_j) - X^M(\tau_{j-1}) = \sum_{i=1}^{n_j+1} \Delta X^M_{j,i}$ and $\Delta X^S_j = X^S(\tau_j) - X^S(\tau_{j-1}) = \sum_{i=1}^{n_j+1} \Delta X^S_{j,i}$. $\Delta X^M_{j,i}$ is independent of all observed degradation increments before τ_j, except $\Delta X^S_{j,i} = \Delta Y^c_{j,i}$. So finally, the conditional distribution of Z_j given $\mathcal{O}^c_{\tau_j^-}$ is simply the conditional distribution of $-\rho\ \Delta X^M_j$ given $\Delta X^S_j = \Delta y^c_j$.

$(\Delta X^M_j, \Delta X^S_j)^T$ is a Gaussian vector:

$$\begin{pmatrix} \Delta X^M_j \\ \Delta X^S_j \end{pmatrix} \sim \mathcal{N}\left(\begin{pmatrix} \mu_M \\ \mu_S \end{pmatrix} \Delta\tau_j,\ \begin{pmatrix} \sigma_M^2 & c_{SM} \\ c_{SM} & \sigma_S^2 \end{pmatrix} \Delta\tau_j \right) \tag{3.16}$$

The following lemma [57] gives the conditional distributions of the components of a Gaussian vector.

Let $\begin{pmatrix} A \\ B \end{pmatrix}$ be a Gaussian vector such that $\begin{pmatrix} A \\ B \end{pmatrix} \sim \mathcal{N}(\mu, \Sigma)$, where $\mu = \begin{pmatrix} \mu_A \\ \mu_B \end{pmatrix}$ and $\Sigma = \begin{pmatrix} \Sigma_A & \Sigma_{AB} \\ \Sigma_{BA} & \Sigma_B \end{pmatrix}$. Then, the conditional distribution of U given $[B = b]$ is multivariate normal $\mathcal{N}(\tilde{\mu}, \tilde{\Sigma})$ where $\tilde{\mu} = \mu_A + \Sigma_{AB}\Sigma_B^{-1}(b - \mu_B)$ and $\tilde{\Sigma} = \Sigma_A - \Sigma_{AB}\Sigma_B^{-1}\Sigma_{BA}$.
So the distribution of ΔX_j^M given ΔX_j^S can be derived thanks to the lemma given in 3.2.2, with $A = \Delta X_j^M$, $B = \Delta X_j^S$, $\mu_A = \mu_M \Delta\tau_j$, $\mu_B = \mu_S \Delta\tau_j$, $\Sigma_A = \sigma_M^2 \Delta\tau_j$, $\Sigma_B = \sigma_S^2 \Delta\tau_j$, and $\Sigma_{AB} = c_{SM}\Delta\tau_j$.

Straightforward computations lead to the desired conditional distribution:

$$Z_j^c \mid \mathcal{O}^c_{\tau_j^-} \sim \mathcal{N}\left(-\rho\big(\mu_M \Delta\tau_j + r_{SM}\frac{\sigma_M}{\sigma_S}\,(\Delta y_j^c - \mu_S \Delta\tau_j)\big)\ ,\ \rho^2 \Delta\tau_j\ \sigma_M^2\big(1 - r_{SM}^2\big)\right) \tag{3.17}$$

Hence, the log-likelihood for the complete observation scheme is:

$$\begin{aligned} \ln L_c(\Theta) = -\frac{1}{2}\Bigg(&\sum_{j=1}^{k+1}\sum_{i=1}^{n_j+1} \ln(2\pi\sigma_S^2 \Delta t_{j,i}) + \frac{\big(\Delta y_{j,i}^c - \mu_S \Delta t_{j,i}\big)^2}{\sigma_S^2 \Delta t_{j,i}} \\ &+ \sum_{j=1}^{k} \ln(2\pi\rho^2 \Delta\tau_j \sigma_M^2(1 - r_{SM}^2)) + \frac{\big(z_j^c + \rho\mu_M \Delta\tau_j + \rho r_{SM}\frac{\sigma_M}{\sigma_S}(\Delta y_j^c - \mu_S \Delta\tau_j)\big)^2}{\rho^2 \Delta\tau_j \sigma_M^2(1 - r_{SM}^2)}\Bigg) \end{aligned} \tag{3.18}$$

General observation scheme

In order to write the likelihood (3.15), the only difficulty is to derive the conditional distribution of the observed jump around the j^{th} maintenance Z_j^g given $\mathcal{O}^g_{t_{j,n_j}}$. $\forall\ j \in \{1, ..., k\}$,

we have:

$$\begin{aligned} Z_j^g &= Y(t_{j+1,1}) - Y(t_{j,n_j}) \\ &= Y(t_{j+1,1}) - Y(\tau_j^+) + Y(\tau_j^+) - Y(\tau_j^-) + Y(\tau_j^-) - Y(t_{j,n_j}) \\ &= \Delta Y_{j+1,1}^c + Z_j^c + \Delta Y_{j,n_j+1}^c \\ &= \Delta X_{j+1,1}^S - \rho\, \Delta X_j^M + \Delta X_{j,n_j+1}^S \\ &= \Delta X_{j+1,1}^S - \rho\, \Delta X_{j,1}^M \mathbb{1}_{j>1} - \rho \sum_{i=1+\mathbb{1}_{j>1}}^{n_j} \Delta X_{j,i}^M - \rho\, \Delta X_{j,n_j+1}^M + \Delta X_{j,n_j+1}^S \end{aligned} \tag{3.19}$$

In this sum:

- $\Delta X_{j+1,1}^S$ is not observed and is independent of $\mathcal{O}_{t_{j,n_j}}^g$.
- $\Delta X_{j,1}^M \mathbb{1}_{j>1}$ is not observed. It depends on $\Delta X_{j,1}^S \mathbb{1}_{j>1}$, which is also not observed, but involved in Z_j^g.
- $\sum_{i=1+\mathbb{1}_{j>1}}^{n_j} \Delta X_{j,i}^M$ is not observed but depends on $\sum_{i=1+\mathbb{1}_{j>1}}^{n_j} \Delta X_{j,i}^S$, which is observed.
- $\Delta X_{j,n_j+1}^M$ and $\Delta X_{j,n_j+1}^S$ are not observed, are independent of $\mathcal{O}_{t_{j,n_j}}^g$, but are dependent one from each other.

Finally, the conditional distribution of Z_j^g given $\mathcal{O}_{t_{j,n_j}}^g$ is the conditional distribution of Z_j^g given $\left(\sum_{i=1+\mathbb{1}_{j>1}}^{n_j} \Delta X_{j,i}^S,\ Z_{j-1}^g \right)$. This distribution will be obtained by using again the lemma of Appendix 3.2.2, starting from the Gaussian vector $\left(Z_j^g,\ \sum_{i=1+\mathbb{1}_{j>1}}^{n_j} \Delta X_{j,i}^S,\ Z_{j-1}^g \right)$.

To simplify writings, let us denote:

- $\Delta t_j^g = \sum_{i=1+\mathbb{1}_{j>1}}^{n_j} \Delta t_{j,i}$ the elapsed time between the first and last observation on the j^{th} inter-maintenance interval. For $j \geq 2$, $\Delta t_j^g = t_{j,n_j} - t_{j,1}$. For $j = 1$, $\Delta t_1^g = t_{1,n_1}$.
- $\Delta Y_j^g = \sum_{i=1+\mathbb{1}_{j>1}}^{n_j} \Delta X_{j,i}^S$ the total increment of degradation observed on the j^{th} inter-maintenance interval. The Gaussian vector of interest can now be written $\left(Z_j^g,\ \Delta Y_j^g,\ Z_{j-1}^g \right)$.

The expectation of the Gaussian vector is given by:

$$\begin{aligned}\mu_{Z_j^g} &= \mathbb{E}[Z_j^g] = \mathbb{E}[\Delta Y_{j+1,1}^c] + \mathbb{E}[Z_j^c] + \mathbb{E}[\Delta Y_{j,n_j+1}^c] \\ &= \mu_S(\Delta t_{j+1,1} + \Delta t_{j,n_j+1}) - \rho\mu_M\Delta\tau_j. \qquad (3.20)\\ \mathbb{E}[\Delta Y_j^g] &= \mu_S\Delta t_j^g. \qquad (3.21)\end{aligned}$$

For the covariance matrix, one has to compute:

$$\begin{aligned}\sigma_{Z_j^g}^2 &= \mathbb{V}ar[Z_j^g] \\ &= \mathbb{V}ar[\Delta X_{j+1,1}^S - \rho\ \Delta X_{j,1}^M \mathbb{1}_{j>1} - \rho \sum_{i=1+\mathbb{1}_{j>1}}^{n_j} \Delta X_{j,i}^M - \rho\ \Delta X_{j,n_j+1}^M + \Delta X_{j,n_j+1}^S] \\ &= \mathbb{V}ar[\Delta X_{j+1,1}^S] + \rho^2\ \mathbb{V}ar[\Delta X_{j,1}^M \mathbb{1}_{j>1}] + \rho^2\ \mathbb{V}ar[\sum_{i=1+\mathbb{1}_{j>1}}^{n_j} \Delta X_{j,i}^M] \\ &\quad + \rho^2\ \mathbb{V}ar[\Delta X_{j,n_j+1}^M] + \mathbb{V}ar[\Delta X_{j,n_j+1}^S] - 2\rho\ \mathbb{C}ov(\Delta X_{j,n_j+1}^S, \Delta X_{j,n_j+1}^M) \\ &= \sigma_S^2\Delta t_{j+1,1} + \rho^2\sigma_M^2\Delta t_{j,1}\mathbb{1}_{j>1} + \rho^2\sigma_M^2 \sum_{i=1+\mathbb{1}_{j>1}}^{n_j} \Delta t_{j,i} \\ &\quad + \rho^2\sigma_M^2\Delta t_{j,n_{j+1}} + \sigma_S^2\Delta t_{j,n_j+1} - 2\rho c_{SM}\Delta t_{j,n_j+1} \\ &= \sigma_S^2(\Delta t_{j,n_j+1} + \Delta t_{j+1,1}) + \rho^2\sigma_M^2\Delta\tau_j - 2\rho\ r_{SM}\sigma_S\sigma_M\ \Delta t_{j,n_j+1}. \qquad (3.22)\end{aligned}$$

$$\begin{aligned}\mathbb{V}ar[\Delta Y_j^g] &= \sigma_S^2\Delta t_j^g. \qquad (3.23)\\ \mathbb{C}ov(Z_j^g, Z_{j-1}^g) &= \mathbb{C}ov(-\rho\Delta X_{j,1}^M, \Delta X_{j,1}^S) = -\rho c_{SM}\Delta t_{j,1}. \qquad (3.24)\\ \mathbb{C}ov(Z_j^g, \Delta Y_j^g) &= \mathbb{C}ov(-\rho\sum_{i=1}^{n_j}\Delta X_{j,i}^M, \sum_{i=1+\mathbb{1}_{j>1}}^{n_j} \Delta X_{j,i}^S) = -\rho c_{SM}\Delta t_j^g. \qquad (3.25)\\ \mathbb{C}ov(\Delta Y_j^g, Z_{j-1}^g) &= \mathbb{C}ov(\sum_{i=1+\mathbb{1}_{j>1}}^{n_j} \Delta X_{j,i}^S, \Delta X_{j,1}^S) = 0. \qquad (3.26)\end{aligned}$$

Finally, $\forall j \in \{2, ..., k\}$, the distribution of the Gaussian vector $\left(Z_j^g,\ \Delta Y_j^g,\ Z_{j-1}^g\right)$ is

given by:

$$\begin{pmatrix} Z_j^g \\ \Delta Y_j^g \\ Z_{j-1}^g \end{pmatrix} \sim \mathcal{N}\left(\begin{pmatrix} \mu_{Z_j^g} \\ \mu_S \Delta t_j^g \\ \mu_{Z_{j-1}^g} \end{pmatrix} , \begin{pmatrix} \sigma^2_{Z_j^g} & -\rho r_{SM}\sigma_S\sigma_M \Delta t_j^g & -\rho r_{SM}\sigma_S\sigma_M \Delta t_{j,1} \\ -\rho r_{SM}\sigma_S\sigma_M \Delta t_j^g & \sigma_S^2 \Delta t_j^g & 0 \\ -\rho r_{SM}\sigma_S\sigma_M \Delta t_{j,1} & 0 & \sigma^2_{Z_{j-1}^g} \end{pmatrix} \right) \tag{3.27}$$

The distribution of Z_j^g given $(\Delta Y_j^g, Z_{j-1}^g)$ can be derived thanks to the lemma given in Appendix 3.2.2, with $A = Z_j^g$, $B = \begin{pmatrix} \Delta Y_j^g \\ Z_{j-1}^g \end{pmatrix}$, $\mu_A = \mu_{Z_j^g}$, $\mu_B = \begin{pmatrix} \mu_S \Delta t_j^g \\ \mu_{Z_{j-1}^g} \end{pmatrix}$, $\Sigma_A = \sigma^2_{Z_j^g}$, $\Sigma_{AB} = (-\rho r_{SM}\sigma_S\sigma_M \Delta t_j^g, -\rho r_{SM}\sigma_S\sigma_M \Delta t_{j,1})$, $\Sigma_{BA} = \Sigma_{AB}^T$ and $\Sigma_B = \begin{pmatrix} \sigma_S^2 \Delta t_j^g & 0 \\ 0 & \sigma^2_{Z_{j-1}^g} \end{pmatrix}$.

After computations, the desired conditional distribution is obtained:

$$Z_j^g \mid \mathcal{O}^g_{t_{j,n_j}} \sim \mathcal{N}\Bigg(\mu_{Z_j^g} - \frac{\rho\, r_{SM}\sigma_M}{\sigma_S}\big(\Delta y_j^g - \mu_S \Delta t_j^g\big) - \frac{\rho\, r_{SM}\sigma_S\sigma_M \Delta t_{j,1}\mathbb{1}_{j>1}}{\sigma^2_{Z_{j-1}^g}}\big(z_{j-1}^g - \mu_{Z_{j-1}^g}\big), \\ \sigma^2_{Z_j^g} - \rho^2 r_{SM}^2 \sigma_S^2 \sigma_M^2 \left(\frac{\Delta t_j^g}{\sigma_S^2} + \frac{\Delta t_{j,1}^2 \mathbb{1}_{j>1}}{\sigma^2_{Z_{j-1}^g}} \right) \Bigg) \tag{3.28}$$

Finally, the log-likelihood for the general observation scheme is:

$$\begin{aligned} \ln L_g(\Theta) = -\frac{1}{2}\Bigg(& \sum_{j=1}^{k+1} \sum_{i=1+\mathbb{1}_{j>0}}^{n_j} \ln(2\pi\sigma_S^2 \Delta t_{j,i}) + \frac{(\Delta y_{j,i}^c - \mu_S \Delta t_{j,i})^2}{\sigma_S^2 \Delta t_{j,i}} \\ & + \sum_{j=1}^{k} \ln\left(2\pi \left(\sigma^2_{Z_j^g} - \rho^2 r_{SM}^2 \sigma_S^2 \sigma_M^2 \big(\frac{\Delta t_j^g}{\sigma_S^2} + \frac{\Delta t_{j,1}^2 \mathbb{1}_{j>1}}{\sigma^2_{Z_{j-1}^g}} \big) \right) \right) \\ & + \frac{\left(z_j^g - \mu_{Z_j^g} + \frac{\rho\, r_{SM}\sigma_M}{\sigma_S}\big(\Delta y_j^g - \mu_S \Delta t_j^g\big) + \frac{\rho\, r_{SM}\sigma_S\sigma_M \Delta t_{j,1}\mathbb{1}_{j>1}}{\sigma^2_{Z_{j-1}^g}}\big(z_{j-1}^g - \mu_{z_{j-1}^{(2)}}\big) \right)^2}{\sigma^2_{Z_j^g} - \rho^2 r_{SM}^2 \sigma_S^2 \sigma_M^2 \big(\frac{\Delta t_j^g}{\sigma_S^2} + \frac{\Delta t_{j,1}^2 \mathbb{1}_{j>1}}{\sigma^2_{Z_{j-1}^g}} \big)} \Bigg) \end{aligned} \tag{3.29}$$

Let us recall that this second observation scheme has been called general because the complete scheme is a limit case of this scheme when t_{j,n_j} and $t_{j+1,1}$ tend to τ_j. In this case, $\Delta t_{j+1,1}$ and $\Delta t_{j,n_j+1}$ tend to 0, Δt_j^g tends to $\Delta\tau_j$ and Δy_j^g tends to ΔY_j^c. Under these

assumptions, it is easy to check that the conditional distribution in the general case (3.28) converges to the conditional distribution in the complete case (3.17).

3.2.3 Estimation for the perturbed ARD_1 and partial replacement models

The identifiability issue raised in Section 3.1.4 leads that the parameters $\Theta = (\mu_S, \mu_M, \sigma_S^2, \sigma_M^2, \rho, r_{SM})$ of the full model cannot be estimated. But if some constraints are imposed, the model may become identifiable. Therefore, we will consider in the following the parameter estimation for two specific models introduced in Section 3.1.3, the perturbed ARD_1 and partial replacement models.

- **Perturbed ARD_1**. The degradation process is an ARD_1 model perturbed by a white noise. This corresponds to the case $\mu_S = \mu_M = \mu$. Therefore, the model parameters in this case are $\Theta_1 = (\mu, \sigma_S^2, \sigma_M^2, \rho, r_{SM})$. The log-likelihoods in the complete and general observation schemes are respectively $\ln L_c^{PA}(\Theta_1) = \ln L_c(\mu, \mu, \sigma_S^2, \sigma_M^2, \rho, r_{SM})$ and $\ln L_g^{PA}(\Theta_1) = \ln L_g(\mu, \mu, \sigma_S^2, \sigma_M^2, \rho, r_{SM})$, which can be computed using (3.18) and (3.29).
- **Partial replacement**. The maintenance is optimal since it deletes all the amount of removable degradation accumulated since the last maintenance. This corresponds to the case $\rho = 1$. Therefore, the model parameters in this case are $\Theta_2 = (\mu_S, \mu_M, \sigma_S^2, \sigma_M^2, r_{SM})$. The log-likelihoods in the complete and general observation schemes are respectively $\ln L_c^{PR}(\Theta_2) = \ln L_c(\mu_S, \mu_M, \sigma_S^2, \sigma_M^2, 1, r_{SM})$ and $\ln L_g^{PR}(\Theta_2) = \ln L_g(\mu_S, \mu_M, \sigma_S^2, \sigma_M^2, 1, r_{SM})$, which can be computed using (3.18) and (3.29).

3.3 Simulation study

This section presents the results of a simulation study which aims to assess the quality of the estimators. In order to analyze the impact on the estimation quality of the parameters values, the number of maintenance actions and the number of observations, several situations are considered and compared to each other. Through a study of the impact on observation locations, it is also possible to compare the complete and general observation schemes.

Only the Perturbed ARD_1 and Partial replacement model are considered. Maintenance actions and degradation measurements are supposed to be periodically performed. A situation is defined by the values of the model parameters, the number of observations

between maintenance actions (n_j), the number of maintenance actions (k), the total number of observations (n), and the maintenance period. For each situation, 5000 degradation trajectories are simulated. The five model's parameters are estimated by maximizing the log-likelihoods (3.18) and (3.29) with the Nelder-Mead method. To obtain good estimation results, the initial parameter values of this algorithm have to be carefully chosen. The employed technique is described in Appendix A.3. The results are presented through box-plots of the empirical distribution of each estimator.

3.3.1 Quality of parameter estimation for the complete observation scheme

Perturbed ARD_1 model

For the Perturbed ARD_1 model, 8 situations are considered, described in Table 3.2. For each situation, 5000 degradation trajectories are simulated. For each trajectory, maintenances are performed every 3 time units. The boxplots of the estimators are presented in Figure 3.4.

Table 3.2: Simulation situations for the Perturbed ARD_1 model

Situation	μ	σ_S^2	σ_M^2	ρ	r_{SM}	n_j	k	n
1	5	10	7	0.5	0.7	2	4	20
2	5	10	7	0.5	0.7	0	9	20
3	5	10	7	0.5	0.7	5	2	21
4	5	10	7	0.5	0.7	2	49	200
5	5	10	7	0.5	0.1	2	4	20
6	5	10	20	0.5	0.7	2	4	20
7	5	10	7	0.2	0.7	2	4	20
8	5	10	7	0.8	0.7	2	4	20

- Situation 1 is the reference situation, with an average maintenance efficiency ($\rho = 0.5$), a quite high correlation between the underlying degradation processes ($r_{SM} = 0.7$), $k = 4$ maintenance actions and n_j= 2 observations of the degradation level between each maintenance.
- Situation 2 has the same parameters and the same amount of data, but with more maintenances and no observations between maintenances. Since we have more information on the jumps and less information between maintenance, σ_M^2 and ρ are better estimated and σ_S^2 is less well estimated. μ and r_{SM} are also better estimated.

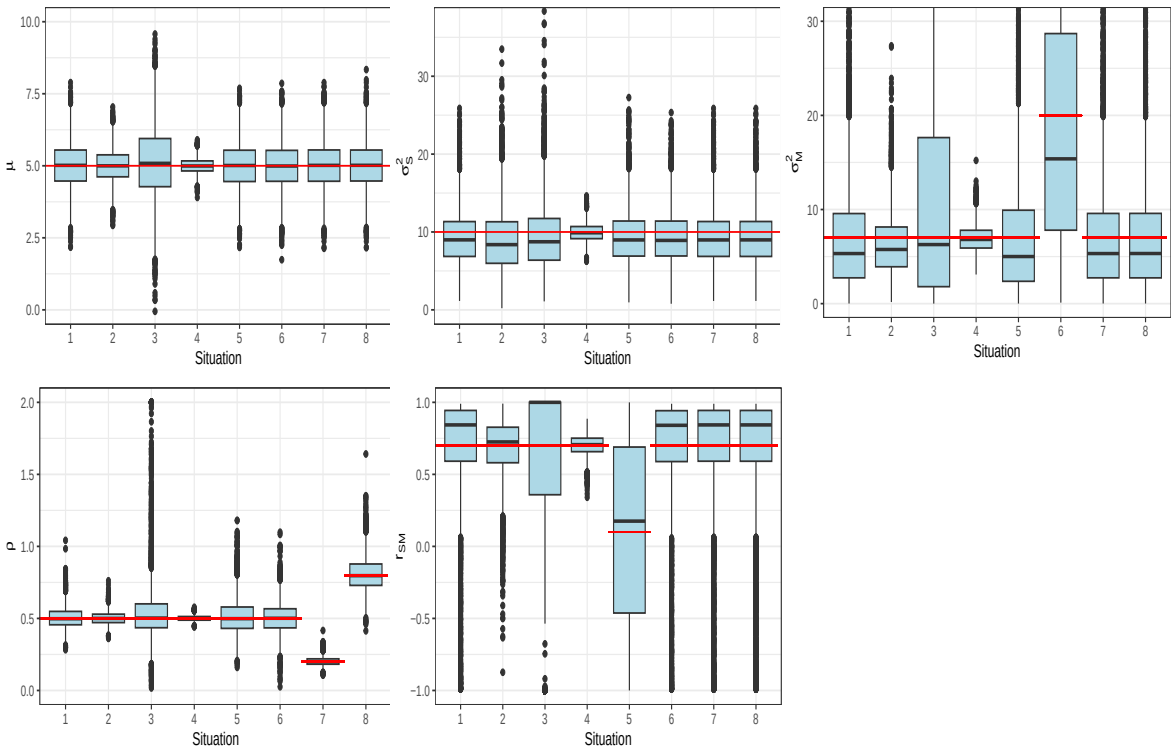

Figure 3.4: Estimations of the parameters of the Perturbed ARD_1 model for the complete observation scheme

- Situation 3 is the dual of the previous one, with less maintenances and more observations between maintenances. Logically, all the estimations are degraded, except that of σ_S^2.
- Situation 4 is similar to situation 1, with much more data. As expected, the estimation quality of all estimators increases with the number of data.
- Situation 5 is similar to situation 1, except that the coefficient of correlation is much smaller ($r_{SM} = 0.1$). The box-plot shows that it is difficult to estimate a so small coefficient of correlation. The estimations of other parameters are not affected except ρ, which is slightly less well estimated as in Situation 1.
- Situation 6 is similar to situation 1, except that the second variance is much larger ($\sigma_M^2 = 20$). Unsurprisingly, only the estimation of σ_M^2 is affected.
- Situation 7 is similar to situation 1, except that the maintenance efficiency is much smaller ($\rho = 0.2$). It appears that the estimation of ρ is improved and the the estimations of other parameters are not affected.
- Situation 8 is similar to situation 1, except that the maintenance efficiency is much larger ($\rho = 0.8$). Only the estimation of ρ is slightly degraded.

These results and other simulations not reported here lead us to draw the following conclusions. The parameters are generally well estimated, even for a rather small amount of data. σ_S^2 and σ_M^2 are slightly underestimated and r_{SM} is overestimated. A higher number of maintenances improve the estimation of the parameters linked to the jumps σ_M^2, ρ and r_{SM}. A higher number of observed degradation levels between maintenances improves the estimation of σ_S^2. It is difficult to estimate r_{SM} when its value is close to 0 or 1. The variances of the estimators of σ_M^2 and ρ increase when the true parameter values increase.

Partial replacement model

For the Partial replacement model, 6 situations are considered, described in Table 3.3. The boxplots of the estimators are presented in Figure 3.5. The results are completely similar to those of the Perturbed ARD_1 model. Whereas drifts theoretical values are different, the estimations quality of μ_S and μ_M remains comparable.

Table 3.3: Simulation situations for the Partial replacement model

Situation	μ_S	μ_M	σ_S^2	σ_M^2	r_{SM}	n_j	k	n
1	10	5	10	7	0.7	2	4	20
2	10	5	10	7	0.7	0	9	20
3	10	5	10	7	0.7	5	2	21
4	10	5	10	7	0.7	2	49	200
5	10	5	10	7	0.1	2	4	20
6	10	5	10	20	0.7	2	4	20

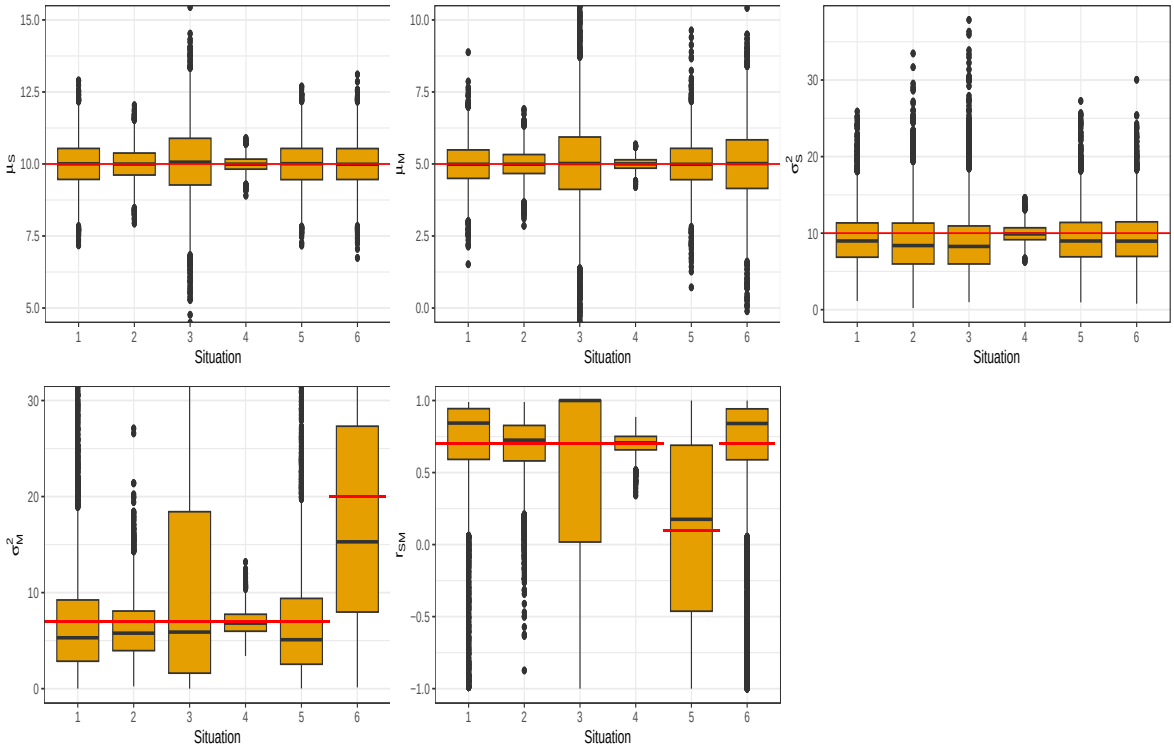

Figure 3.5: Estimations of the parameters of the Partial replacement model for the complete observation scheme

3.3.2 Impact of the observations locations and the observation schemes

The aim of this section is to look if the observations locations between two successive maintenance actions can have an impact on the estimation quality. To that aim, degradation levels are not necessarily periodically observed. Five situations are considered, described in Table 3.4 and illustrated in Figure 3.6. The total numbers of data are equivalent in all situations. The considered model is the Perturbed ARD_1 model.

Table 3.4: Simulation situations for assessing the impact of observations locations

Observation scheme	Situation	μ	σ_S^2	σ_M^2	ρ	r_{SM}	n_j	k	n
c	1	5	10	7	0.5	0.7	0	9	20
g	2	5	10	7	0.5	0.7	2	9	21
g	3	5	10	7	0.5	0.7	2	9	21
g	4	5	10	7	0.5	0.7	2	9	21
g	5	5	10	7	0.5	0.7	2	9	21

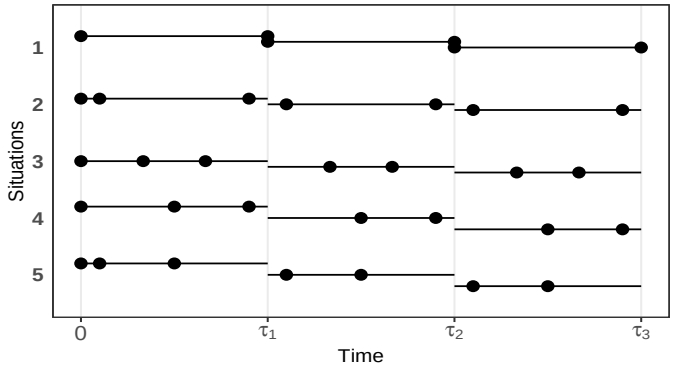

Figure 3.6: Observations location for the five considered situations and the first three maintenance times.

- In situation 1, the data are collected under the complete observation scheme, with no observed degradation levels between maintenances.
- In situation 2, the data are collected under the general observation scheme. Two degradation levels are measured in each interval, and the measurement times are close to the maintenance times. Here, the degradation measurements are not periodic: $\forall\ j \in \{1, ..., 9\},\ t_{j,n_j} = \tau_j - \frac{1}{5}$ and $t_{j+1,1} = \tau_j + \frac{1}{5}$.

- In situation 3, the data are collected under the general observation scheme. Two degradation levels are measured in each interval, and the measurement times are periodically spaced in the intervals between maintenances.
- In situation 4, the data are collected under the general observation scheme. Two degradation levels are measured in each interval, and the measurement times are just before the maintenance times. Here, the degradation measurements are not periodic: $\forall\ j \in \{1, ..., 9\},\ t_{j,n_j} = \tau_j - \frac{1}{5}$ and $t_{j+1,1} = \tau_j + \frac{1}{2}$.
- In situation 5, the data are collected under the general observation scheme. Two degradation levels are measured in each interval, and the measurement times are just after the maintenance times. Here, the degradation measurements are not periodic: $\forall\ j \in \{1, ..., 9\},\ t_{j,n_j} = \tau_j - \frac{1}{2}$ and $t_{j+1,1} = \tau_j + \frac{1}{5}$.

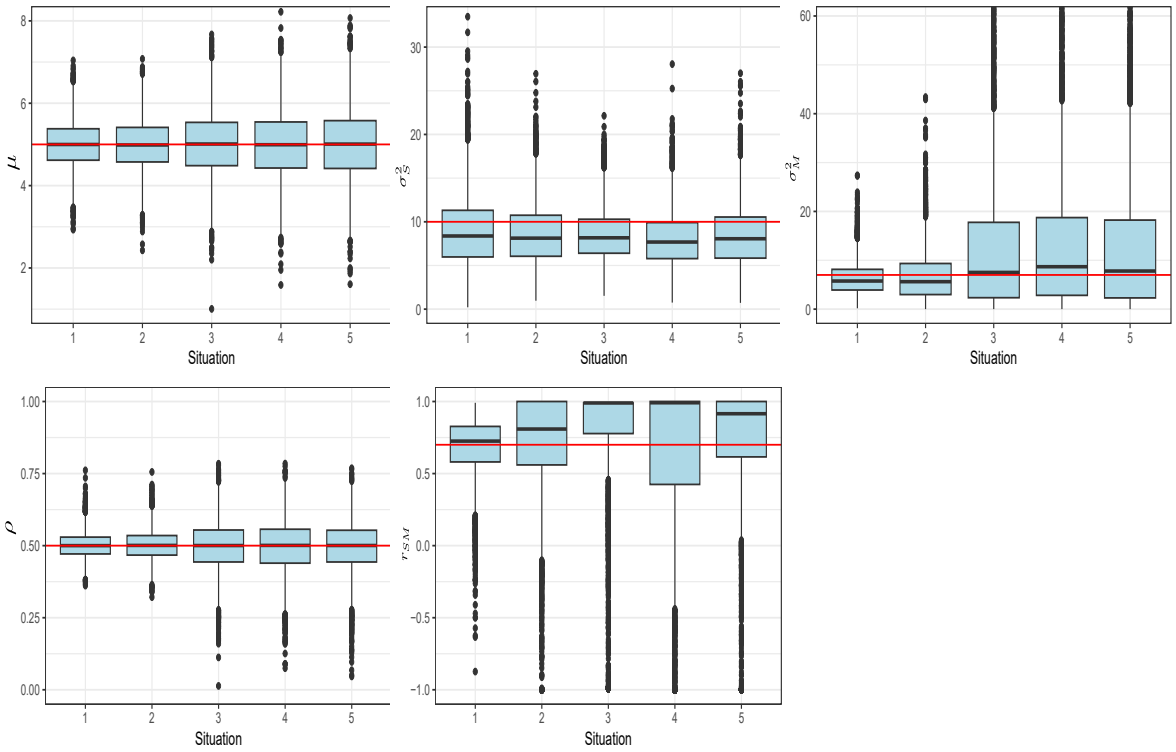

Figure 3.7: Estimations of the parameters of the Perturbed ARD_1 model for the situations of Table 3.4

The boxplots of the estimators are presented in Figure 3.7. This figure shows that the best estimations are obtained for situation 1, except for σ_S^2. It means that in order to estimate the parameters mainly linked to the maintenance effect, it is better to observe degradation levels at maintenance times. Conversely, for parameter σ_S^2 mainly linked to the intrinsic degradation, it is recommended to observe degradation levels between maintenances.

The results for situation 2 are closer to the results of situation 1 than those of situation 3. This illustrates the fact that Situation 1 is a limit case of situation 2, or that the complete observation scheme is a limit case of the general observation scheme. In this case, the observed jumps in the general scheme Z_j^g are close to the real jumps Z_j^c.

The estimations in situation 4 and 5 are comparable except for the correlation coefficient r_{SM}, which is better estimated when degradation levels are observed just after maintenance actions.

The estimation quality is slightly better in situation 5 compared to situation 4. Measuring degradation levels just after maintenance actions improves the estimations quality. In the usual ARD_1 model, the best estimations are not obtained for the complete observation scheme [62]. On the contrary, for the proposed model, the complete observation scheme provides the best estimation.

3.4 Conclusion on the new degradation model with partial maintenance effects and perspectives

This chapter has introduced a new degradation model with imperfect maintenance, which assumes that maintenance effect only affects a part of the degradation process. Two particular models of interest have been studied, the Perturbed ARD_1 and the Partial replacement models. The parameters of these models have been estimated under two different observation schemes. The quality of estimation has been assessed through a simulation study and the impact of different features of the model and data has been analyzed. A first prospect of this study is to derive the theoretical properties of the estimators.

In the future, decision making techniques could be carried out in order to establish optimal maintenance policies. Generally, it is assumed that a failure occurs when the degradation process hits for the first time a given degradation threshold. For usual Wiener processes, it is well known that the first hitting time is inverse Gaussian distributed [52]. For the new degradation model presented in this article, the first hitting time's distribution is not inverse Gaussian anymore but appears to be more complex as the degradation trajectory is discontinuous at maintenance times. So an interesting prospect of this work is the determination of this distribution.

In 3.4, a preliminary step is given, through an empirical estimate of this distribution's PDF. Maintenance effects seem to cause the multimodal shape of the distribution. Due to the maintenance effect, the risk of failure is higher before a maintenance than after. Further studies could be carried out in the future in order to determine the theoretical distribution of the first hitting time for this degradation model.

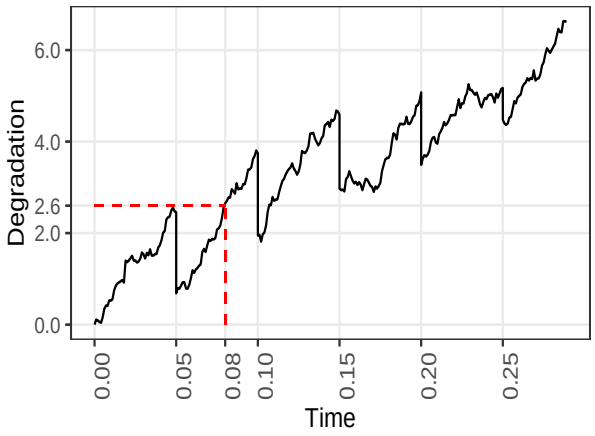

Figure 3.8: An example of a simulated degradation trajectory

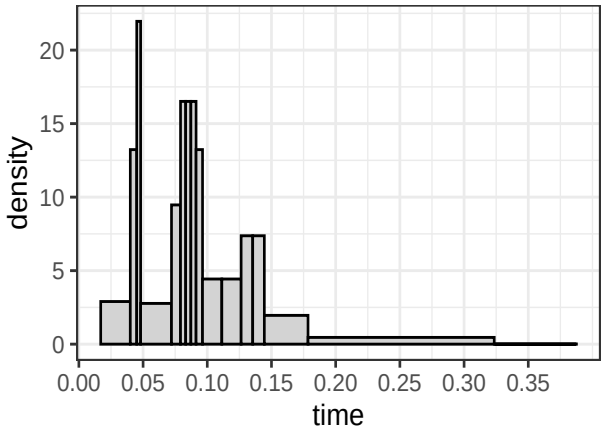

Figure 3.9: Empirical distribution of the first passage time

Degradation trajectories are simulated for the proposed model and first hitting times are collected. An example of a simulated trajectory and observed hitting time is given in Figure 3.8. An histogram of the obtained values is plotted in Figure 3.9.
It appears that the first hitting time is multimodal distributed. In Figure 3.9, the modes of the empirical PDF are clearly close to the maintenance times. In fact, the multimodal shape of the distribution is a consequence of the maintenance effect on the degradation.

Chapter 4

An inspection/replacement policy for a degrading system with imperfect partial repair effects

This chapter focuses on a cost modeling and optimization of a maintenance policy based on the previously studied Wiener-based degradation model with partial maintenance effects. To distinguish those imperfect maintenance actions with partial effects from other maintenance types, they are referred to as repairs. In this chapter, the proposed maintenance policy involves inspections, repairs (or imperfect maintenances), and as-good-as-new (AGAN) replacements. These replacements can be either corrective (if performed after a failure) or preventive (triggered when the degradation level exceeds a certain threshold). The inter-inspection time and the preventive replacement threshold are optimized by minimizing the average maintenance cost. This average cost is determined by using the Markov-renewal properties of the degradation process of the maintained system. Two methods are considered to compute the average cost and obtain the optimal policy. The study also explores the impact of specific cost coefficients and model parameters on the optimal maintenance policy.

In Section 4.1, a description on the studied degradation model is recalled and the maintenance assumptions are exposed. Based on these assumptions, a maintenance policy is formulated and optimized in Section 4.2 based on the average maintenance cost. To minimize this cost and determine the optimal maintenance policy, two different methods are introduced. Subsequently, numerical results are discussed in Section 4.3, in order to analyze the potential influence of predefined cost coefficients and model parameters on the optimal

maintenance policy.

4.1 Description of the Wiener-based degradation model

Given its suitability for practical situations, the Wiener-based degradation model with partial maintenance effects, as described previously in Chapter 3, is employed in this chapter to model degradation and establish a maintenance policy.

4.1.1 Degradation process under periodic repair

Let us recall some main assumptions about the used degradation process in this chapter. The system's degradation is divided into two components: $X^U = X^U(t)_{t\geq 0}$, the unmaintainable part of the degradation and $X^M = X^M(t)_{t\geq 0}$, the maintainable part. Between repairs, the degradation process evolves as the sum of these two underlying processes. Repairs exclusively impact the X^M component of the system's degradation. Furthermore, the repair effect is characterized as an ARD_1-type process, as detailed in [73]. The underlying processes X^U and X^M are Wiener processes with drift. Their parameters are respectively defined by the drift parameters μ_U, μ_M, the variance parameters σ_U^2, σ_M^2, and the covariance parameter c_{UM}. Notably, the coefficient of correlation between $X_U(t)$ and $X_M(t)$, denoted as r_{UM}, is constant over time and $r_{UM} \in [-1, 1]$. As written in the previous chapter, ρ represents the repair efficiency parameter. In the following sections, repairs are supposed to be efficient, i.e. $\rho \in [0, 1]$. $\forall j \in \mathbb{N}^*$, τ_j are the periodic maintenance times, such that $\widetilde{\tau} = \tau_j - \tau_{j-1}$. Let $Y(t)$ be the degradation level of the maintained system at time t. Let $X^S(t)$ represents the evolution of the degradation between two inspections, i.e. the sum of the underlying processes X^U and X^M. It is assumed that $Y(0) = 0$ and $\forall\, t \in [\tau_{j-1}, \tau_j[,\ \forall\, j \in \{1, ..., k\},\ Y(t) = X^U(t) + X^M(t) - \rho X^M(\tau_{j-1}) = X^S(t) - \rho X^M(\tau_{j-1})$, where X^S represents the evolution of the degradation between two maintenance actions, i.e. the sum of the underlying Wiener processes X^U and X^M.

4.1.2 Maintenance assumptions and maintenance policy structure

The type of maintenance action is determined by periodic inspections (conducted with period $\widetilde{\tau}$), each one performed immediately before each repair or replacement, both of which are instantaneous. The inspected degradation level just before each maintenance $\forall\, j \in \{1, ...k\}$, $Y(\tau_j^-)$, at time τ_j, is considered to decide between a repair (as described in

the previous section) or an as-good-as-new replacement. Two degradation thresholds are defined: M as the preventive replacement threshold and L as the corrective replacement (or failure) threshold. M is set by the "maintenance decision maker" whereas L is not a maintenance decision variable ans is assumed to be given in this study. $\forall\ j \in \{1, ..., k\}$, over $[\tau_{j-1}, \tau_j[$, the following rules apply:

- If there exists a time $t\ \in [\tau_{j-1}, \tau_j[$ such that $Y(t) > L$, then a failure occurs when degradation first exceeds the threshold L over the interval $[\tau_{j-1},\ \tau_j[$, leading to temporary unavailability. The whole system undergoes a corrective replacement at the next maintenance time τ_j, such that $Y(\tau_j^+) = 0$.

  Failures are not self-declared: An inspection needs to be performed at the next maintenance time to witness this breakdown and carry out the replacement.

  If degradation does not exceed the threshold L over $[\tau_{j-1},\ \tau_j[$, then either a repair or a preventive replacement is performed at time τ_j according to the following rules.

- If $Y(\tau_j^-) < M$, a repair is carried out, such that $Y(\tau_j^+) = X^S(\tau_j) + (1-\rho)X^M(\tau_j)$.

- If $M \leq Y(\tau_j^-) \leq L$, a preventive replacement is performed, such that $Y(\tau_j^+) = 0$. Let us notice that, if a failure occurs exactly at the scheduled maintenance time (which is a zero probability event), no unavailability time is considered, and a preventive maintenance is performed.

Under these assumptions, each inspection is instantaneously followed by either repair or replacement. Consequently, the j^{th} maintenance time, denoted as τ_j, represents j periodic inspection times such that $\tau_j = j\widetilde{\tau}$ where $\widetilde{\tau}$ is the inspection period.

An example of a degradation trajectory including two system life cycles is presented in Figure 4.1. The inter-inspection time $\widetilde{\tau}$ is set to 40, M is 700, and L is 1000. As the employed degradation model is Wiener-based, degradation can decrease on some time intervals. Inspections are depicted by circles and lead either to a repair or a preventive replacement. Corrective maintenances due to failures are only conducted at inspection times. In Figure 4.1, one failure is observed at time 230, leading to corrective replacement conducted at the next inspection times $\tau_6 = 240$.

The preventive replacement threshold M and the inspection period $\widetilde{\tau}$ are the decision variables for the considered maintenance policy. Each type of maintenance action, including inspection, repair, preventive and corrective replacement, involves a specific maintenance

cost. The asymptotic maintenance cost per time unit is assessed, and an optimal maintenance policy is considered by minimizing this cost.

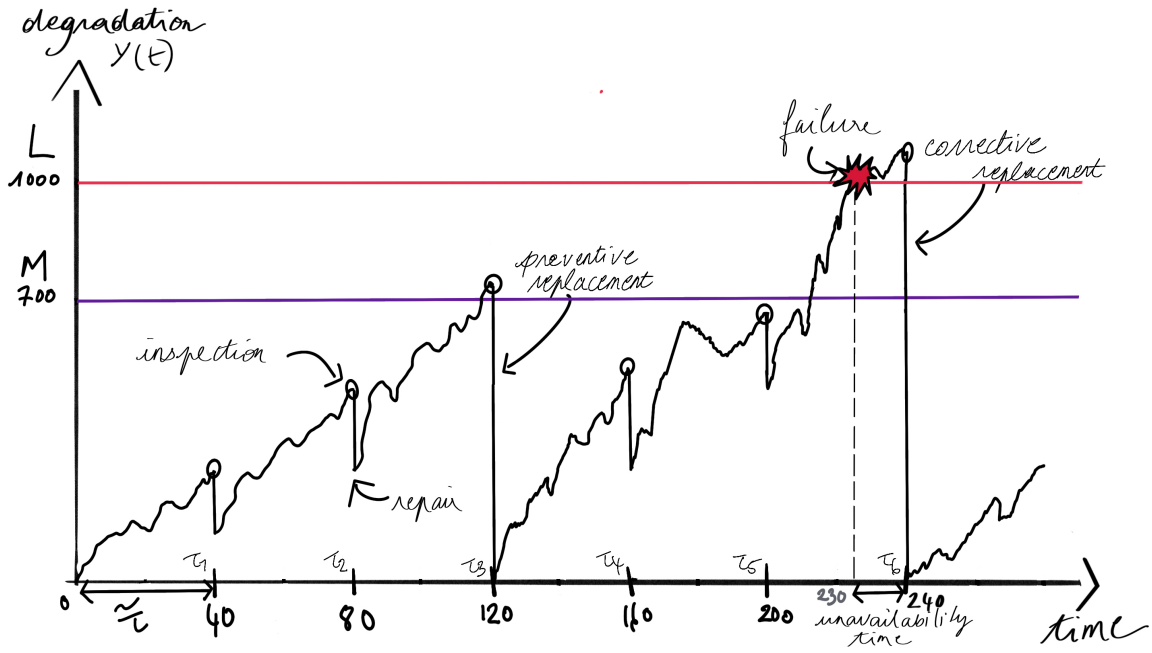

Figure 4.1: Evolution of a degradation trajectory $Y(t)$ under maintenance assumptions

4.2 Maintenance cost assessment using two different methods

In this section, the asymptotic maintenance cost per time unit is defined according to the maintenance assumptions described in the previous section. Two distinct approaches are suggested for evaluating this cost.

4.2.1 Maintenance cost modeling

As mentioned earlier, each type of maintenance action entails a maintenance cost. Here, the global cost at time t is determined by the total unavailability time and the number of inspections, repairs, preventive and corrective replacements carried out within the time interval $[0, t]$.

A cost coefficient is associated to each type of maintenance. Let c_I, c_R, c_P, c_C be respectively the cost coefficient for inspections, repairs, preventive replacements, corrective

replacements and c_D be the the cost rate per time unit for unavailability. The number of these different types of maintenance actions over the interval $[0,t]$ can be defined as follows.

- $N_R(t)$, the number of repairs over $[0,t]$ is equal to $\sum_{j=1}^{\lfloor \frac{t}{\tau} \rfloor} \mathbb{1}_{\{Y(\tau_j^-)<M\} \cap \{\sup_{s\in[\tau_{j-1},\tau_j[} Y(s)\leq L\}}$.
- $N_P(t)$, the number of preventive replacements over $[0,t]$, is equal to $\sum_{j=1}^{\lfloor \frac{t}{\tau} \rfloor} \mathbb{1}_{\{M\leq Y(\tau_j^-)\leq L\} \cap \{\sup_{s\in[\tau_{j-1},\tau_j[} Y(s)\leq L\}}$.
- $N_C(t)$, the number of corrective replacements over $[0,t]$, is equal to $\sum_{j=1}^{\lfloor \frac{t}{\tau} \rfloor} \mathbb{1}_{\{\sup_{s\in[\tau_{j-1},\tau_j[} Y(s)>L\}}$.

Furthermore, after each failure, the system is no longer available until the next inspection time. The total unavailability time must also be taken into consideration in the global maintenance cost. Thus, this global maintenance cost at time t, denoted $c(t)$, is incurred by inspections, repairs, replacements and system unavailability and verifies

$$c(t) = (c_I + c_R)\ N_R(t) + (c_I + c_P)\ N_P(t) + (c_I + c_C)\ N_C(t) + c_D \sum_{j=1}^{\lfloor \frac{t}{\tau} \rfloor} (\tau_j - S_j) \quad (4.1)$$

where S_j represents the time at which a potential failure occurs over the interval $[\tau_{j-1}, \tau_j[$. Considering that the system keeps degrading itself after failure, it follows that $\forall\ j \geq 1$,

$$S_j = \begin{cases} \tau_j, & \text{if } \sup_{s\in[\tau_{j-1},\tau_j[} Y(s) \leq L \\ \inf\{s \in\ [\tau_{j-1}, \tau_j[\ \mid Y(s) > L\}, & \text{otherwise.} \end{cases}$$

Let us notice that if $\sup_{s\in[\tau_{j-1},\tau_j[} Y(s) \leq L$, no failure occurs over $[\tau_{j-1}, \tau_j[$. On the contrary, if $\sup_{s\in[\tau_{j-1},\tau_j[} Y(s) > L$, the system fails involving an unavailability time. For example, in Figure 4.1, the observed value of S_5 is $\tau_5 = 200$ and the observed value of S_6 is 230, which differs from $\tau_6 = 240$ because the system failed between τ_5 and τ_6.

In order to assess the performance of the maintenance policy, we use the asymptotic cost per time unit $\lim_{t\to+\infty} \frac{c(t)}{t}$. Thereafter, two different approaches are introduced in order to compute this asymptotic maintenance cost per time unit. The first method relies only on numerical simulations of multiple system life cycles, while the second, named the hybrid method, resorts to the semi-regenerative Markov process properties of the maintained

degradation process to derive analytic expressions and it incorporates both numerical evaluation of these expressions and stochastic simulation for the cost computation. Let us first depict the mathematical properties of the maintenance based degradation process used in both cases.

4.2.2 Two mathematical approaches for considering the maintenance-based degradation process

There are two equivalent approaches to apprehend the maintenance-based degradation process in order to assess the asymptotic maintenance cost per time unit.

Considering regenerative life cycles

The first approach consists in considering the evolution of the system degradation between two AGAN replacements, i.e. over a regenerative life cycle. Let T denote the random variable that represents the life cycle duration of the system. The link between T and the considered degradation model can be expressed using the following notations:

- R_j^p is the random variable equal to 1 when the j^{th} inspection is followed by a preventive replacement and 0 otherwise, $R_j^p = \mathbb{1}_{\{M \leq Y(\tau_j^-) \leq L, \sup_{s \in [\tau_{j-1}, \tau_j[} Y(s) \leq L\}}$.
- R_j^c is the random variable equal to 1 when the j^{th} inspection is followed by a corrective replacement and 0 otherwise, $R_j^c = \mathbb{1}_{\{\sup_{s \in [\tau_{j-1}, \tau_j[} Y(s) > L\}}$.
- R_j is the random variable equal to 1 when the j^{th} inspection is followed by a replacement and 0 otherwise, $R_j = \mathbb{1}_{\{R_j^p = 1\}} + \mathbb{1}_{\{R_j^c = 1\}}$ and $R_0 = 0$.
- Q_ℓ is the index of the inspection time which corresponds to the ℓ^{th} replacement, such that $Q_\ell = \{inf j \in \mathbb{N} | j > Q_{\ell-1}; R_j = 1\}$ and $Q_0 = 0$.
- Given the previous expressions, $\{\tau_{Q_\ell}\}_{\ell \geq 0}$ are the replacement times, i.e. times at which a replacement is carried out on the system. For instance, in Figure 4.1, the observed replacement indexes are $Q_1 = 3$ and $Q_2 = 6$ and the replacement times are $\tau_{Q_1} = \tau_3$ and $\tau_{Q_2} = \tau_6$.
- $\Delta\tau_{Q_\ell}$ represents the random duration of the ℓ^{th} life cycle of a system, such that $\Delta\tau_{Q_\ell} = \tau_{Q_\ell} - \tau_{Q_{\ell-1}}$. $\{\Delta\tau_{Q_\ell}\}_{\ell \geq 1}$ are independent and identically distributed as the random variable T.

Considering a semi-regenerative Markov process

The second approach consists in considering the evolution of the system degradation between two inspections. In fact, $\{Y(t)\}_{t\geq 0}$ is a semi-regenerative Markov process taking values in $\mathbb{R}$, whose semi-regenerative instants are $\{\tau_j\}_{j\geq 0}$. Let $(Y(\tau_j^+))_{j\geq 1} = (Y_j)_{j\geq 1}$ be the embedded Markov chain taking values in $\mathbb{R}$. After each replacement, degradation is completely reset to zero and the following progression of the degradation is independent of prior events. Likewise, after each repair, the degradation only advances based on the system's condition right after that specific maintenance time. Thus, between two repairs, the studied model can be described by a semi-regenerative Markov process (or Markov renewal) [20, 36, 21]. As a matter of fact, $\forall t \in [0, \widetilde{\tau}[,\ \forall\ j \geq 0$,

$$(Y(t+\tau_j)|Y_0 = y_0, ..., Y_j = y_j) \text{ is similarly distributed as } (Y(t)|Y(0) = y_j) \text{ indeed,}$$
$$Y(t+\tau_j) - Y_j = Y(t+\tau_j) - Y(\tau_j^+) = X^S(t+\tau_j) - X^S(\tau_j) = \Delta X^S(t)$$

Therefore, $Y(t)$ is a semi-regenerative Markov process, and τ_j represents its semi-regenerative instants.

Let us notice that, as illustrated in Figure 4.2, degradation can decrease over some time intervals due to the considered Wiener underlying processes. The consequences of this property may not be immediately intuitive: Although $\rho \in [0, 1]$, degradation levels after repair can be greater than degradation levels right before repair, meaning that $Y(\tau_j^-) \leq Y(\tau_j^+)$. Despite maintenance assumption, $Y(\tau_j^+)$ does not belong to $[0, M[$ since in reality $Y_i \in \mathbb{R}$. These properties arise because the maintenance effect $Y(\tau_j^-) - Y(\tau_j^+) = \rho\left(X^M(\tau_j) - X^M(\tau_{j-1})\right)$ can potentially increase the degradation (even if $\rho \in [0, 1]$) due to the fact that the underlying Wiener process X^M is not necessarily increasing.

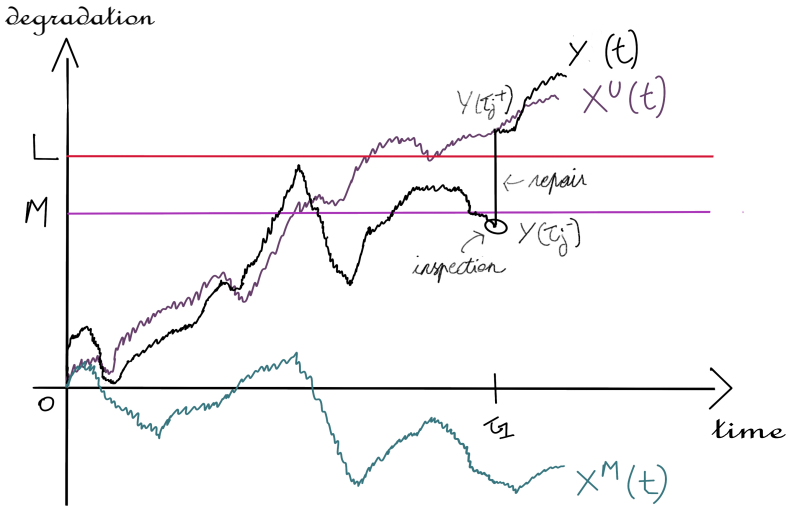

Figure 4.2: Example of degradation, denoted as $Y(t)$ and its underlying Wiener processes $X^U(t)$ and $X^M(t)$ over $[0, \tau_1]$. In this specific scenario, the degradation level before repair is lower than the degradation level after repair

4.2.3 Maintenance cost assessment based on life cycles simulations

After both preventive and corrective replacements, the entire system is renewed, causing the degradation level to reset to zero instantly after replacement. Consequently, a new life cycle of the system begins. From practical point of view, it is reasonable to assume that the regenerative period is finite, and then $\mathbb{E}[T] < +\infty$. Moreover, the maintenance cost function $(t \to c(t))$ defined in the previous section, is positive (all the cost coefficients are positive), increasing $(c(0) = 0)$ and for any $0 \leq s \leq t,\ c(t) - c(s) = c(t - s)$.
Thus, according to the renewal theory [20], the long run average maintenance cost, or the maintenance cost rate in loose terms, can be expressed as below.

$$\lim_{t\to\infty} \frac{c(t)}{t} = \frac{\mathbb{E}[c(T)]}{\mathbb{E}[T]}$$

The stochastic behavior of the degradation over different life cycles are independent and

identical. Then, the following expression holds true for all $\ell \geq 1$, specifically when $\ell = 1$.

$$\begin{aligned}\frac{\mathbb{E}[c(T)]}{\mathbb{E}[T]} =& \frac{1}{\mathbb{E}[T]} \Bigg[(c_I + c_R)\ \mathbb{E}\left[Q_1 - 1\right] \\ &+ (c_I + c_P)\ \mathbb{P}(\sup_{s \in [0, \tau_{Q_1}[} Y(s) \leq L) \\ &+ (c_I + c_C)\ \mathbb{P}(\sup_{s \in [0, \tau_{Q_1}[} Y(s) > L) + c_D\ \mathbb{E}\left[\tau_{Q_1} - S_{Q_1}\right] \Bigg] \end{aligned} \tag{4.2}$$

where:

- $\mathbb{E}\left[Q_1 - 1\right]$ is the expectation of the number of repairs within a life cycle. Given that Q_1 represents the number of inspections within one cycle, and the last inspection is followed by a replacement, it follows that $Q_1 - 1$ repairs are carried out over one life cycle.
- $\mathbb{P}(\sup_{s \in [0, \tau_{Q_1}[} Y(s) \leq L)$ is the probability that the system life cycle ends with a preventive replacement.
- $\mathbb{P}(\sup_{s \in [0, \tau_{Q_1}[} Y(s) > L)$ is the probability that the system life cycle concludes with a corrective replacement.
- $\mathbb{E}\left[\tau_{Q_1} - S_{Q_1}\right]$ is the expectation of the unavailability time over τ_{Q_1}.

Determining an analytic expression of these probabilities and expectations proves to be challenging due to their dependence on the stochastic variable Q_1, representing the number of inspections before replacement. Consequently, the expected cost will be assessed by stochastic simulations of the realizations (i.e. Monte Carlo simulations) over multiple life cycles. Let N_{cyc} be the predefined number of life cycles, chosen high enough to ensure convergence in the frequencies of maintenances and replacements, such that,

- $\mathbb{E}[Q_1 - 1]$ is estimated by $\frac{1}{N_{cyc}} \sum_{\ell=1}^{N_{cyc}} (Q_\ell - Q_{\ell-1} - 1)$
- $\mathbb{P}(\sup_{s \in [0, \tau_{Q_1}[} Y(s) \leq L)$ is estimated by $\frac{1}{N_{cyc}} \sum_{\ell=1}^{N_{cyc}} R_\ell^p$
- $\mathbb{P}(\sup_{s \in [0, \tau_{Q_1}[} Y(s) > L)$ is estimated by $\frac{1}{N_{cyc}} \sum_{\ell=1}^{N_{cyc}} R_\ell^c$

- $\mathbb{E}[\tau_{Q_1} - S_{Q_1}]$ is estimated by $\frac{1}{N_{cyc}} \sum_{\ell=1}^{N_{cyc}} (\tau_{Q_\ell} - S_{Q_\ell})$
- $\mathbb{E}[T]$ is defined by $\frac{1}{N_{cyc}} \sum_{\ell=1}^{N_{cyc}} (\tau_{Q_\ell} - \tau_{Q_{\ell-1}})$

4.2.4 Maintenance cost assessment using semi-regenerative process properties

The long run average maintenance cost can also be written using the semi-regenerative Markov property of the maintenance-based degradation process $Y(t)$, considering $\widetilde{\tau}$ as the semi-regenerative period.

Let us assume that :

- $\mathbb{E}[T^2] < +\infty$
- $\mathbb{E}[c(T)] < +\infty$
- $\mathbb{E}[Tc(T)] < +\infty$
- π_∞ is the unique stationary probability for the Markov chain $(Y_j)_{j\geq 1}$

Given these assumptions and according to [20], the long run average maintenance cost verifies

$$\lim_{t\to\infty} \frac{c(t)}{t} = \frac{\mathbb{E}_\pi[c(\widetilde{\tau})]}{\widetilde{\tau}} = \frac{\int_{\mathbb{R}} \mathbb{E}[c(\widetilde{\tau})|Y(0) = y]\pi_\infty(y)dy}{\widetilde{\tau}} \tag{4.3}$$

To solve this equation, two quantities need to be computed: the conditional expectation $\mathbb{E}[c(\widetilde{\tau})|Y(0) = y]$ and the stationary distribution $\pi_\infty(y)$. First, let us have a look on this conditional expectation.

Analytic formulation of the conditional expectation expressed in the long run average maintenance cost

As the degradation level over the interval $[0, \widetilde{\tau}]$ depends on the degradation level at time zero and considering that Y can now be seen as a semi-regenerative Markov process, the conditional expectation $\mathbb{E}[c(\widetilde{\tau})|Y(0) = y]$ can be computed using the Equation (4.1) for $t = \widetilde{\tau}$.

Consequently, the Equation (4.4) is deduced.

$$\mathbb{E}_\pi[c(\widetilde{\tau})|Y(0)=y] = (c_I + c_R)\; p_1(y,\widetilde{\tau}) + (c_I + c_P)\; p_2(y,\widetilde{\tau}) + (c_I + c_C)\; p_3(y,\widetilde{\tau}) + c_D\; q_4(y,\widetilde{\tau}) \tag{4.4}$$

where the quantities $p_1(y,\widetilde{\tau})$, $p_2(y,\widetilde{\tau})$, $p_3(y,\widetilde{\tau})$ and $q_4(y,\widetilde{\tau})$ refer to:

- $p_1(y,\widetilde{\tau}) = \mathbb{E}[N_R(\widetilde{\tau})|Y(0)=y] = \mathbb{P}\left(Y(\widetilde{\tau}^-) < M,\ \sup_{s\in[0,\widetilde{\tau}[} Y(s) \leq L \mid Y(0)=y\right)$ is the conditional probability of a repair occurring after $\widetilde{\tau}$
- $p_2(y,\widetilde{\tau}) = \mathbb{E}[N_P(\widetilde{\tau})|Y(0)=y] = \mathbb{P}\left(M \leq Y(\widetilde{\tau}^-) \leq L,\ \sup_{s\in[0,\widetilde{\tau}[} Y(s) \leq L \mid Y(0)=y\right)$ is the conditional probability of a preventive replacement being carried out after $\widetilde{\tau}$
- $p_3(y,\widetilde{\tau}) = \mathbb{E}[N_C(\widetilde{\tau})|Y(0)=y] = \mathbb{P}\left(\sup_{s\in[0,\widetilde{\tau}[} Y(s) > L \mid Y(0)=y\right)$ is the conditional probability of a corrective replacement occurring after $\widetilde{\tau}$
- $q_4(y,\widetilde{\tau}) = \mathbb{E}\left[\widetilde{\tau} - S_1 |\ Y(0)=y\right]$ where S_1, initially defined in Section 4.2, represents the first time at which the degradation exceeds the corrective threshold L.

Then, the conditional expectation expressed in Equation (4.3) verifies

Proposition 4.2.1 *The following proposition gives an analytic expression of the quantities involved in Equation (4.4).*

- $$p_1(y,\widetilde{\tau}) = \left[\Phi\left(\frac{M-y-\mu_S\widetilde{\tau}}{\sigma_S\sqrt{\widetilde{\tau}}}\right) - \exp\left(2\frac{\mu_S(L-y)}{\sigma_S^2}\right)\Phi\left(\frac{M-y-\mu_S\widetilde{\tau}-2(L-y)}{\sigma_S\sqrt{\widetilde{\tau}}}\right)\right]\mathbb{1}_{\{y\leq L\}}$$
- $$p_2(y,\widetilde{\tau}) = \left[\Phi\left(\frac{L-y-\mu_S\widetilde{\tau}}{\sigma_S\sqrt{\widetilde{\tau}}}\right) - \exp\left(2\frac{\mu_S(L-y)}{\sigma_S^2}\right)\Phi\left(\frac{-(L-y)-\mu_S\widetilde{\tau}}{\sigma_S\sqrt{\widetilde{\tau}}}\right) - \Phi\left(\frac{M-y-\mu_S\widetilde{\tau}}{\sigma_S\sqrt{\widetilde{\tau}}}\right) + \exp\left(2\frac{\mu_S(L-y)}{\sigma_S^2}\right)\Phi\left(\frac{M-y-\mu_S\widetilde{\tau}-2(L-y)}{\sigma_S\sqrt{\widetilde{\tau}}}\right)\right]\mathbb{1}_{\{y\leq L\}}$$
- $$p_3(y,\widetilde{\tau}) = \left[\Phi\left(\frac{\mu_S\widetilde{\tau}-(L-y)}{\sigma_S\sqrt{\widetilde{\tau}}}\right) + \Phi\left(-\frac{\mu_S\widetilde{\tau}+(L-y)}{\sigma_S\sqrt{\widetilde{\tau}}}\right)\exp\left(\frac{2\mu_S(L-y)}{\sigma_S^2}\right)\right]\mathbb{1}_{\{y\leq L\}} + \mathbb{1}_{\{y>L\}}$$

- $q_4(y,\widetilde{\tau}) = \Bigg[\left(\widetilde{\tau} - \dfrac{L-y}{\mu_S}\right)\Phi\left(\dfrac{\mu_S\widetilde{\tau} - (L-y)}{\sigma_S\sqrt{\widetilde{\tau}}}\right)$
$+\left(\widetilde{\tau} + \dfrac{L-y}{\mu_S}\right)\Phi\left(-\dfrac{\mu_S\widetilde{\tau} + L - y}{\sigma_S\sqrt{\widetilde{\tau}}}\right)\exp\left(\dfrac{2\mu_S(L-y)}{\sigma_S^2}\right)\Bigg]\mathbb{1}_{\{y\leq L\}} + \widetilde{\tau}\mathbb{1}_{\{y>L\}}$

where Φ represents the cumulative distribution function (CDF) of a standard Gaussian distribution.

Proof 4.2.1 *First, let us note that if $Y(0) > L$ then $\sup_{s\in[0,\widetilde{\tau}[} Y(s) > L$ and consequently $p_1(y,\widetilde{\tau}) = p_2(y,\widetilde{\tau}) = 0$, $p_3(y,\widetilde{\tau}) = 1$ and $q_4(y,\widetilde{\tau}) = \widetilde{\tau}$. Therefore, in the following proof only the case where $y \leq L$ is considered. Additionally, using the semi-regenerative Markov model, let us recall that the evolution of the degradation level, $\forall\ s \in [0,\widetilde{\tau}[$, verifies*

$$\begin{aligned} Y(s) &= X^S(s) - \rho X^M(0) \\ &= X^S(s) - X^S(0) + X^S(0) - \rho X^M(0) \\ &= \Delta X^S(s) + Y(0) \\ \text{Then,}\quad Y(\widetilde{\tau}^-) &= \Delta X^S(\widetilde{\tau}) + Y(0) \end{aligned}$$

And in particular, since $(Y(\widetilde{\tau}^-)|Y(0) = 0)$ follows a Gaussian $\mathcal{N}(\mu_S\widetilde{\tau}, \sigma_S^2\widetilde{\tau})$, then, for $y \leq L$,

$$\begin{aligned} p_1(y,\widetilde{\tau}) =& \mathbb{P}\left(Y(\tau^-) < M,\ \sup_{s\in[0,\widetilde{\tau}[} Y(s) \leq L \mid Y(0) = y\right) = \mathbb{P}\left(\Delta X^S(\widetilde{\tau}) < M - y,\ \sup_{s\in[0,\widetilde{\tau}[} \Delta X^S(s) \leq L - y\right) \\ =& \int_{-\infty}^{M-y} \mathbb{P}\left(\sup_{s\in[0,\widetilde{\tau}[} \Delta X^S(s) \leq L - y \mid \Delta X^S(\widetilde{\tau}) = x\right) f_{\Delta X^S(\widetilde{\tau})}(x)dx \end{aligned}$$

According to lemma 1.17 in [52] p. 34,

$$\mathbb{P}\left(\sup_{s\in[0,\widetilde{\tau}[} \Delta X^S(s) > L - y \mid \Delta X^S(\widetilde{\tau}) = x\right) = \begin{cases} 1 & \text{if } x > L - y \\ \exp\left(-2\frac{(L-y)(L-y-x)}{\sigma_S^2\widetilde{\tau}}\right) & \text{alternatively} \end{cases}$$

Therefore,

$$p_1(y,\widetilde{\tau}) = \Phi\left(\frac{M-y-\mu_S\widetilde{\tau}}{\sigma_S\sqrt{\widetilde{\tau}}}\right) - \frac{1}{\sigma_S\sqrt{2\pi\widetilde{\tau}}}\int_{-\infty}^{M-y}\exp\left(-\frac{1}{2\sigma_S^2\widetilde{\tau}}\big((x-\mu_S\widetilde{\tau})^2+4(L-y)(L-y-x)\big)\right)dx$$

Let us remark that $(x-\mu_S\widetilde{\tau})^2+4(L-y)(L-y-x) = \big(x-\mu_S\widetilde{\tau}-2(L-y)\big)^2-4\mu_S\widetilde{\tau}(L-y)$ *then,*

$$p_1(y,\widetilde{\tau}) = \Phi\left(\frac{M-y-\mu_S\widetilde{\tau}}{\sigma_S\sqrt{\widetilde{\tau}}}\right) - \exp\left(2\frac{\mu_S(L-y)}{\sigma_S^2}\right)\Phi\left(\frac{M-y-\mu_S\widetilde{\tau}-2(L-y)}{\sigma_S\sqrt{\widetilde{\tau}}}\right)$$

This expression of $p_1(y,\widetilde{\tau})$ *remains true for* $M=L$ *and can be directly used to obtain the following expression of* $p_2(y,\widetilde{\tau})$
It follows that

$$\begin{aligned}p_2(y,\widetilde{\tau}) =& \mathbb{P}\left(M-y\le\Delta X^S(\widetilde{\tau})\le L-y,\ \sup_{s\in[0,\widetilde{\tau}[}\Delta X^S(s)-y\le L-y\right)\\ =&\Phi\left(\frac{L-y-\mu_S\widetilde{\tau}}{\sigma_S\sqrt{\widetilde{\tau}}}\right)-\exp\big(2\frac{\mu_S(L-y)}{\sigma_S^2}\big)\Phi\left(\frac{-(L-y)-\mu_S\widetilde{\tau}}{\sigma_S\sqrt{\widetilde{\tau}}}\right)\\ &-\Phi\left(\frac{M-y-\mu_S\widetilde{\tau}}{\sigma_S\sqrt{\widetilde{\tau}}}\right)+\exp\left(2\frac{\mu_S(L-y)}{\sigma_S^2}\right)\Phi\left(\frac{M-y-\mu_S\widetilde{\tau}-2(L-y)}{\sigma_S\sqrt{\widetilde{\tau}}}\right)\end{aligned}$$

In Kahle et al.'s book [52], it has been demonstrated that the first time when degradation exceeds a critical threshold, follows an inverse-Gaussian distribution for a univariate Wiener-based process. Therefore, based on Kahle et al.'s proof [52] and the provided formulation of the cumulative distribution function of the first hitting time page 18, $p_3(y,\widetilde{\tau})$ *verifies*

$$p_3(y,\widetilde{\tau}) = \mathbb{P}\left(\sup_{s\in[0,\widetilde{\tau}[}\Delta X^S(s)>L-y\right) = \mathbb{P}\left(\inf\{s\ge0|\Delta X^S(s)>L-y\}<\widetilde{\tau}\right)$$

$$=\Phi\left(\frac{\mu_S\widetilde{\tau}-(L-y)}{\sigma_S\sqrt{\widetilde{\tau}}}\right)+\Phi\left(-\frac{\mu_S\widetilde{\tau}+(L-y)}{\sigma_S\sqrt{\widetilde{\tau}}}\right)\exp\left(\frac{2\mu_S(L-y)}{\sigma_S^2}\right)$$

Let us notice that when M is equal to L, it satisfies $p_3(y,\widetilde{\tau}) = 1-p_1(y,\widetilde{\tau})$, meaning that when the system does not undergo preventive replacement, then it is either repaired or correctively replaced after an inspection.
Finally,

$$q_4(y,\widetilde{\tau}) = \mathbb{E}\left[\widetilde{\tau}-t|\ Y(0)=y\right] = \int_0^{\widetilde{\tau}} \big(\widetilde{\tau}-t\big) f_{\inf\{s\geq 0|\Delta X^S(s)>L-y\}}(t)dt$$

where $f_{\inf\{s\geq 0|\Delta X^S(s)>L-y\}}(t)$ represents the PDF of an inverse-Gaussian distribution since it refers to the first passage time of a Wiener process with drift. An expression of this PDF can be found in Kahle et al. [52], p. 16, and then,

$$\begin{aligned}
q_4(y,\widetilde{\tau}) &= \int_0^{\widetilde{\tau}} (\widetilde{\tau}-t)\frac{L-y}{\sqrt{2\pi\sigma_S^2\ t^3}}\exp\big(-\frac{(L-y-\mu_S t)^2}{2\sigma_S^2 t}\big)dt = \widetilde{\tau}I_1 - I_2 \text{ with}\\
I_1 &= \int_0^{\widetilde{\tau}} \frac{L-y}{\sqrt{2\pi\sigma_S^2\ t^3}}\exp\big(-\frac{(L-y-\mu_S t)^2}{2\sigma_S^2 t}\big)dt\\
I_2 &= \int_0^{\widetilde{\tau}} \frac{L-y}{\sqrt{2\pi\sigma_S^2\ t}}\exp\big(-\frac{(L-y-\mu_S t)^2}{2\sigma_S^2 t}\big)dt
\end{aligned}$$

I_1 and I_2 can be computed using the following trick. First, let us notice that $(L-y-\mu_S t)^2 = (L-y+\mu_S t)^2 - 4(L-y)\mu_S t$. Then, I_1 can be expressed as the difference between two other integrals I_a and I_b such that

$$\begin{aligned}
I_a &= \frac{1}{\sqrt{2\pi}}\int_0^{\widetilde{\tau}} \frac{1}{2\sigma_S}\big(\frac{\mu_S}{\sqrt{t}}+\frac{L-y}{\sqrt{t^3}}\big)\exp\big(-\frac{(L-y-\mu_S t)^2}{2\sigma_S^2 t}\big)dt\\
I_b &= \frac{1}{\sqrt{2\pi}}\int_0^{\widetilde{\tau}} \frac{1}{2\sigma_S}\big(\frac{\mu_S}{\sqrt{t}}-\frac{L-y}{\sqrt{t^3}}\big)\exp\big(\frac{2(L-y)\mu_S}{\sigma_S^2}\big)\exp\big(-\frac{(L-y+\mu_S t)^2}{2\sigma_S^2 t}\big)dt
\end{aligned}$$

Afterwards, the following changes of variable $u = \frac{\mu_S t-(L-y)}{\sigma_S\sqrt{t}}$ and $v = \frac{\mu_S t+(L-y)}{\sigma_S\sqrt{t}}$ can respectively be applied to I_a and I_b, such that $du = \frac{1}{2\sigma_S}\big(\frac{\mu_S}{\sqrt{t}}+\frac{L-y}{\sqrt{t^3}}\big)dt$, $dv = \frac{1}{2\sigma_S}\big(\frac{\mu_S}{\sqrt{t}}-\frac{L-y}{\sqrt{t^3}}\big)dt$, and since $L-y\geq 0$,

$$
\begin{aligned}
I_a &= \int_{-\infty}^{\frac{\mu_S\widetilde{\tau}-(L-y)}{\sigma_S\sqrt{\widetilde{\tau}}}} \frac{1}{\sqrt{2\pi}} \exp\left(-\frac{u^2}{2}\right) du = \Phi\left(\frac{\mu_S\widetilde{\tau}-(L-y)}{\sigma_S\sqrt{\widetilde{\tau}}}\right) \\
I_b &= \exp\left(\frac{2(L-y)\mu_S}{\sigma_S^2}\right) \int_{+\infty}^{\frac{\mu_S\widetilde{\tau}+(L-y)}{\sigma_S\sqrt{\widetilde{\tau}}}} \frac{1}{\sqrt{2\pi}} \exp\left(-\frac{u^2}{2}\right) dv \\
&= \exp\left(\frac{2(L-y)\mu_S}{\sigma_S^2}\right) \Phi\left(-\frac{\mu_S\widetilde{\tau}+(L-y)}{\sigma_S\sqrt{\widetilde{\tau}}}\right)
\end{aligned}
$$

Finally, since $I_2 = \frac{L-y}{\mu_S}(I_a + I_b)$,

$$
q_4 = \left(\widetilde{\tau} - \frac{L-y}{\mu_S}\right)\Phi\left(\frac{\mu_S\widetilde{\tau}-(L-y)}{\sigma_S\sqrt{\widetilde{\tau}}}\right) + \left(\widetilde{\tau} + \frac{L-y}{\mu_S}\right)\Phi\left(-\frac{\mu_S\widetilde{\tau}+L-y}{\sigma_S\sqrt{\widetilde{\tau}}}\right) \exp\left(\frac{2\mu_S(L-y)}{\sigma_S^2}\right)
$$

■

Stationary distribution of the embedded Markov process

To analytically compute the long run average maintenance cost of Equation (4.3), only the expression of the stationary distribution π_∞ of the Markov chain $\{Y_j\}_{j\geq 0}$ is now missing. Let $\pi(.|.)$ denotes the transition probability associated with the distribution of Y_{j+1} given Y_j, which does not depend on j thanks to the homogeneous Markov property. This distribution is globally continuous and can be characterized by a PDF, but it also includes a Dirac mass in 0 which refers to the probability for the next inspection to lead to a replacement. Let $f_{Y_1 \mid R_1=0,\, Y(0)=y}(x)$ be the conditional PDF of degradation levels after maintenance, given that the maintenance action is a repair, and $\delta_0(x)$ the Dirac mass in 0. Then,

$$
\begin{aligned}
\pi(x|y) =& f_{Y_{j+1}|Y_j}(x) = f_{Y_1|Y(0)=y}(x) \qquad (4.5)\\
=& \mathbb{P}\Big(Y(\widetilde{\tau}^-) < M,\ \sup_{s\in[0,\widetilde{\tau}[} Y(s) \leq L \mid Y(0)=y\Big)\ f_{Y_1 \mid R_1=0,\, Y(0)=y}(x) \\
&+ \left[\mathbb{P}\Big(M \leq Y(\widetilde{\tau}^-) \leq L,\ \sup_{s\in[0,\widetilde{\tau}[} Y(s) \leq L \mid Y(0)=y\Big) + \mathbb{P}\Big(\sup_{s\in[0,\widetilde{\tau}[} Y(s) > L \mid Y(0)=y\Big)\right] \delta_0(x) \\
=& p_1(y,\widetilde{\tau})\ f_{Y_1 \mid R_1=0, Y(0)=y}(x)\ +\ (p_2(y,\widetilde{\tau}) + p_3(y,\widetilde{\tau}))\ \delta_0(x) \qquad (4.6)
\end{aligned}
$$

Obtaining the analytic expression of the stationary distribution requires to solve the stationary equation,

$$\pi_\infty(x) = \int_{\mathbb{R}} \pi(x|y)\ \pi_\infty(y)dy \tag{4.7}$$

Let us notice that this integral is defined over $\mathbb{R}$, because, as mentioned at the end of Section 4.2.2, degradation level right after repair can actually be greater than the degradation level right before repair (Figure 4.2). In that case, the degradation level after repair can potentially exceed L, such that $Y(\tau_j^-) < M \leq L < Y(\tau_j^+)$.
Solving the stationary equation presents a significant challenge. Volterra methods, as suggested in previous works [7, 111, 47], offer a numerical approach to obtain it. However, expressing the transition probability density function analytically is a complex task. In addition, solving the stationary equation is not sufficient for computing the conditional expectation of the cost over a stationary semi-regenerative cycle. In fact, the integral presented in Equation (4.3) also needs to be computed. Hence, our approach suggests estimating the cost and the stationary distribution through stochastic simulations of the degradation between inspections, following a Monte Carlo approach.

Estimation of the maintenance cost rate based on simulations of the degradation over inspection intervals

Let us keep in mind that the quantity $\mathbb{E}[c(\widetilde{\tau})|Y(0) = y_i] \equiv g(y_i)$, developed in Equation (4.4), is analytically expressed in Proposition 4.2.1. Afterwards, we suggest to estimate $\mathbb{E}_\pi[c(\widetilde{\tau})]$, the expected cost, over a stationary semi-regenerative cycle using simulations of the degradation.
Let $(Y_j)_{j\geq 0}$ represent the sample of the first degradation levels right after repair or replacement, collecting from simulated degradation on one trajectory. In general, to obtain a nearly i.i.d. sample following the distribution π_∞, one typically considers the values $\{Y_{jN}\}_{j\geq 1}$ where N is chosen big enough to ensure independence. However, this approach significantly increases the number of required simulations and is time-consuming. Therefore, to simplify the procedure, we set $N = 1$ and $j \in \{1, ..., 5000\}$. Considering $j_{max} = 5000$ post-repair degradation levels effectively reduce the impact of their successive inter-dependence, and ensure convergence towards the stationary distribution: As depicted in Figure A.1, the empirical stationary distributions do not visually evolve when considering more degradation levels. Then, as depicted in Figure A.2, adjusting N to 1 does not impact the estimations

of the cost. Let us also note that the minimal number of considered degradation levels to ensure convergence towards the stationary distribution, depends on the model parameters, on the chosen inter-inspection period and on the values of the degradation thresholds. However, considering 5000 degradation values appears to be widely enough to ensure convergence for any model parameters and decision variables (M and $\widetilde{\tau}$). Thus, $\mathbb{E}[c(\widetilde{\tau})]$ is estimated by $\frac{1}{5000}\sum_{j=1}^{5000} g(Y_j)$.

In order to illustrate the behavior of the stationary distribution π_∞, each histogram presented in Figure 4.3 represent the 5000 first observations of $\{Y_j\}_{1\leq j\leq 5000}$ for different values of M and $\widetilde{\tau}$. Figure 4.3 shows histograms of the empirical stationary distribution, each coming from one simulated degradation trajectory for different values of the decision variables M and $\widetilde{\tau}$. From now and for the following numerical experiments, the corrective replacement threshold L is set at 1000. Within each histogram, 5000 values corresponding to degradation levels after maintenance or replacements are displayed. For instance, the Figure 4.4 illustrates an example of a simulated degradation trajectory over eight life cycles. The black dots represent the degradation levels defining the empirical stationary distribution. In these examples the corrective replacement L threshold is set at 1000. These histograms are intentionally depicted in counts rather than in frequencies, allowing a direct observation of the number of replacements and repairs in the distribution. For either $\widetilde{\tau} = 10$ or $\widetilde{\tau} = 30$, when M increases and gets closer to L, the weight of the Dirac mass at zero decreases, which corresponds to a decrease in the number of replacements. As the value of M rises, there is an increase in the number of repairs and a decrease in the number of replacements when $\tilde{\tau} = 10$ within the interval $[0, 50000]$, or when $\widetilde{\tau} = 30$ within the interval $[0, 150000]$. In addition, with an increase in M , the potential value of Y_j also rises, as preventive replacements occur only when $Y(\tau_j^-) \geq M$. Alternatively, the life cycles of systems lengthen since it requires more time for degradation to exceed M. This phenomenon corresponds to an increase in the number of repairs and then to a larger dispersion in the empirical stationary distribution.

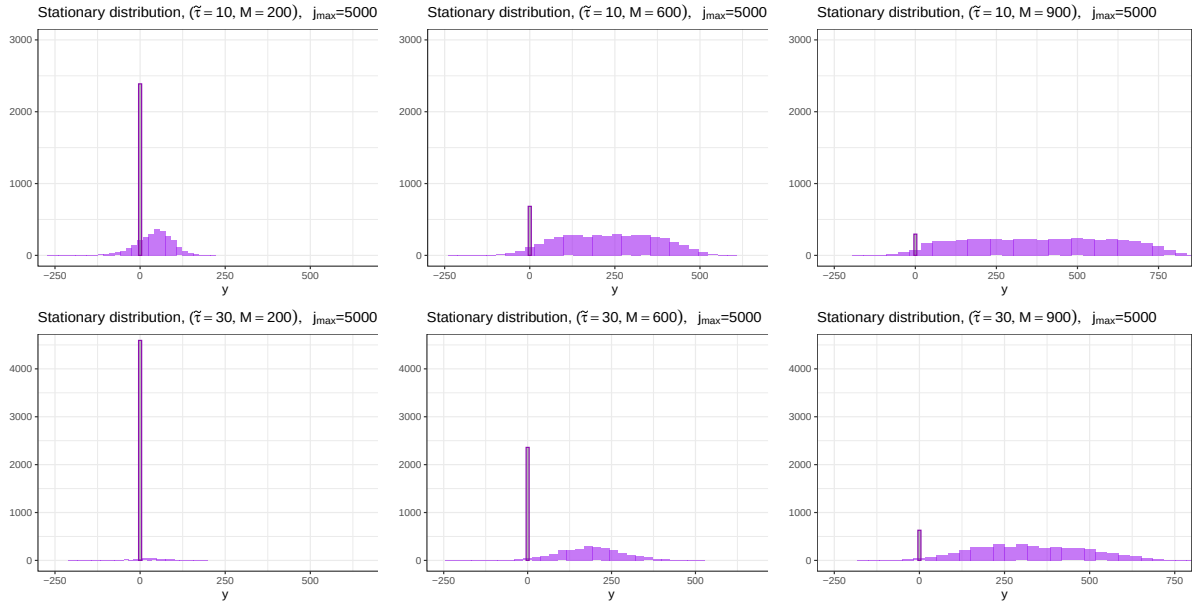

Figure 4.3: Examples of simulated stationary distributions π_∞, constructed with simulated post-repair degradation levels $(Y_j)_{j\geq 1}$ and according to various values of $\widetilde{\tau}$ and M, based on the next parameters: $\mu_U = 7$, $\mu_M = 10$, $\sigma_U^2 = 400$, $\sigma_M^2 = 600$, $r_{UM} = 0.7$, $\rho = 1, L = 1000$

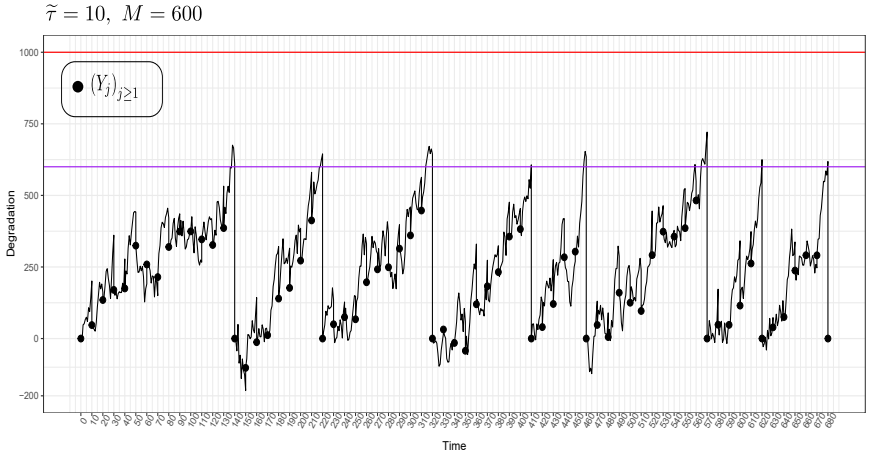

Figure 4.4: Example of a simulated degradation trajectory over eight life cycles, when $\widetilde{\tau} = 10$ and $M = 600$

Figure 4.5: Flowchart illustrating the different possible methods employed in assessing or computing the long run average maintenance cost.

4.2.5 Comparison of the two methods

Figure 4.5 outlines the distinction between the two simulation methods employed for assessing the analytic cost. The purely simulation-based method is described only by numerical simulations of the renewal cycles, whereas the hybrid method uses both the analytic expressions presented in the conditional expectation under the stationary measure in Equation (4.4) and simulation of the stationary distribution. A third method is suggested, based on analytic expressions of both the stationary distribution and the quantities mentioned in Equation (4.4). Yet, as previously mentioned, due to the apparent complexity in obtaining the analytic expression of the stationary distribution, this last method has not been taken into account in the cost assessment presented in this chapter.

In Figure 4.8, the maintenance cost rate is assessed using both the purely simulation-based method and the hybrid method. The solid lines depict the purely simulation-based method, while the dashed lines represent the hybrid method. Each line illustrates the long run average maintenance cost for different values of the preventive threshold. The cost rates obtained with the purely simulation-based method are estimated using simulated degradation trajectories over 5000 system life cycles based on the following parameters: $\mu_U = 7$, $\mu_M = 10$, $\sigma_U^2 = 400$, $\sigma_M^2 = 600$, $r_{UM} = 0.7$, $\rho = 1$, $c_{IR} = 12$, $c_{IP} = 50$, $c_{IC} = 100$, $c_D = 50$. As illustrated in Figure A.3, 5000 cycles seem largely sufficient to guarantee the convergence of the assessed cost rate for different values of $\widetilde{\tau}$ and M and for a specific set of model parameters. Let us keep in mind that different sets of model parameters may alter the convergence results. Yet, the deliberate choice if 5000 life cycles is intended to ensure convergence for all sets of model parameters studied in the following numerical experiments. For each method, and considering the chosen theoretical values of the parameters, the degradation trajectories are simulated using different time steps : 0.01, 0.1 and 1.

At a time step of 0.01, the purely simulation-based method aligns with the hybrid method, as the estimated cost values are highly similar. When the time step equals 1, the estimations of the cost loose precision for both methods. Specifically, the hybrid method shows less precision when the preventive threshold approaches the corrective threshold (when $M > 900$), and the maintenance cost rate values are further from the cost values with a time step at 0.01. Alternatively, with an increase in the preventive threshold M, the purely simulation-based method tends to underestimate cost values. Let us note that, for this method, when the step is set at 1, a few failures occur precisely at the maintenance

time. For example, using the same degradation trajectory with a time step of 1 depicted in this figure, when $M = L$, 237 failures out of 5000 occur exactly at the maintenance time. Although in theory and as well as in practice, this situation has no chance to happen, it can occur when using simulations based on a large time step. As mentioned earlier, in this specific case, preventive replacements are carried out.

Furthermore, as the time step rises, there is reduced information about the degradation, leading to fewer chances to detect a failure (Figure 4.6) or detect it later (Figure 4.7). For these reasons, compared to a smaller time step method, preventive replacements or repairs are favored over corrective ones and the potential unavailability time is shortened. Since the cost coefficients for preventive replacement are lower than those for corrective ones, these remarks explain why the purely simulation-based method with a time step of 1 results in underestimated cost values. Nevertheless, when time steps are set at 0.1 and 0.01, all the failures occur between maintenance times.

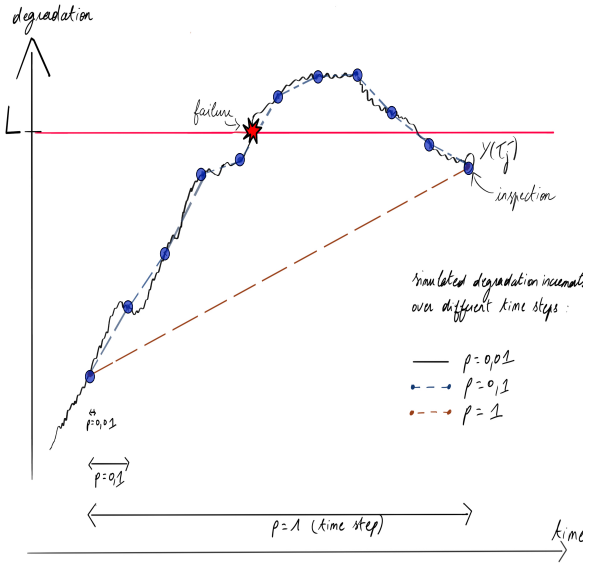

Figure 4.6: Example of degradation increments simulated over different time steps, resp. $p = \{0.01, 0.1, 1\}$. In this scenario, when $p = 1$, failure is not even detected, in contrast to the smaller considered time steps.

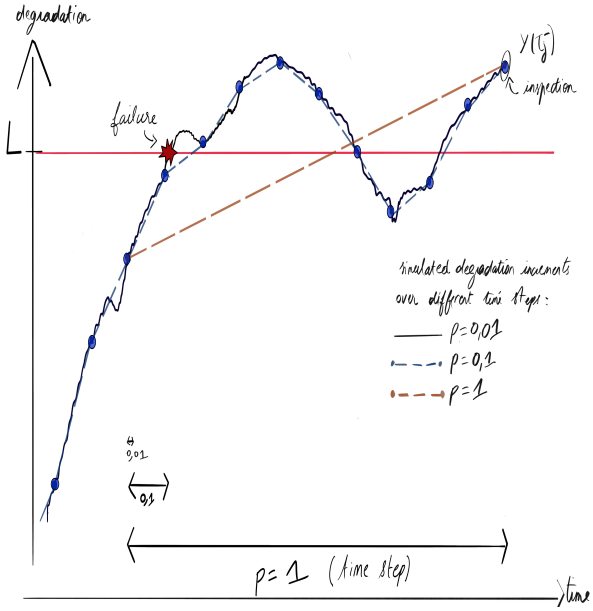

Figure 4.7: Example of degradation increments simulated over different time steps, resp. $p = \{0.01, 0.1, 1\}$. In this scenario, when $p = 1$, failure is identified at the exact maintenance time, i.e. later compared to the smaller considered time steps.

On the other hand, for a reasonable value of the preventive replacement threshold ($M \leq 900$), the hybrid method keeps precision regardless of the chosen time step, in contrast to the purely simulation-based method with time steps set at 0.1 and 1. Indeed, for the hybrid method, the resulting estimated cost values are closer from those obtained with a smaller time step. Additionally, the same comparative analyses, using the same model parameters and cost coefficients, have been conducted employing different values for the inspection period $\widetilde{\tau}$, as presented in Figure A.4 and Figure A.5. In these figures, due to simulation time constraints, two time steps instead of three are depicted, 0.1 and 1. Once again, when $\widetilde{\tau} = 10$ and $\widetilde{\tau} = 40$ and for a reasonable value of M, the hybrid methods are aligning and maintain precision no matter the time step. Moreover, using the hybrid method over bigger time steps is less time-consuming than the purely simulation-based method with very small time steps. Therefore, it appears more accurate to use the hybrid method for the following cost assessments.

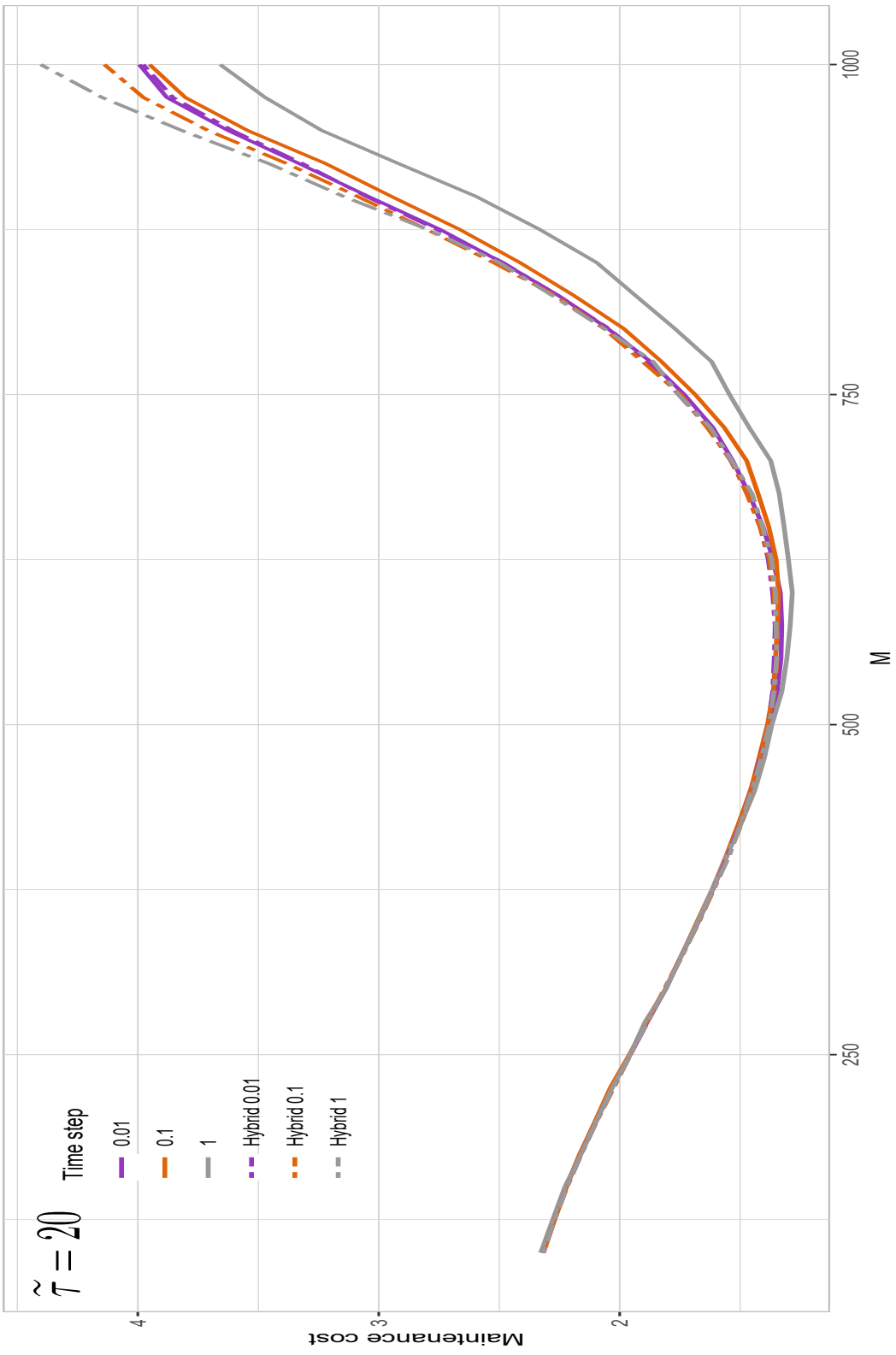

Figure 4.8: The long run average maintenance cost as a function of the preventive replacement threshold M for $\widetilde{\tau} = 20$. Two different methods are employed: one involves a purely simulation-based method (solid lines), considering a regenerative process over one life cycle, while the other is the hybrid method that combines analytic expressions and simulations, considering a semi-regenerative process between two inspections (dashed lines)

4.3 Numerical experiments

For the following numerical experiments, the maintenance cost rate is assessed using the hybrid method. The number of degradation levels used to simulate the empirical stationary distribution is always greater than or equal to the number of replacements (or the number of life cycles). As previously mentioned, 5000 post-repair degradation levels seem to be a reasonable number to ensure convergence of the cost rate using different values of $\widetilde{\tau}$ and M, Figure A.2. Then, to obtain the long run average maintenance cost considering different values of $\widetilde{\tau}$ and M, all the degradation trajectories, as the one presented in Figure 4.1, are simulated over $N_{cyc} = 5000$ life cycles (corresponding to 5000 replacements).

As shown in Figure 4.8, the hybrid method enables the simulation of degradation increments over larger time steps, especially for values of M distant enough from the corrective threshold. Indeed, in this situation, the evaluation of cost rates is not impacted by the time step, and the computational time is largely reduced. Hence, in this section, the hybrid method is employed and each degradation increment is simulated over a time interval set at 1 time unit. To obtain the asymptotic cost per time unit, a degradation trajectory, as the one presented in Figure 4.1, is simulated over $N_{cyc} = 5000$ life cycles, corresponding to 5000 replacements. As previously mentioned, 5000 life cycles seem to be a reasonable number to ensure convergence of the cost rate using different values of $\widetilde{\tau}$ and M, Figure A.3. Furthermore, this approach is also used with different values of $\widetilde{\tau}$ and M in order to evaluate the optimal maintenance policy $(\widetilde{\tau}^*, M^*)$ by minimizing the cost rate. For the computation of the cost rates, $\widetilde{\tau} \in [2.5\ ;\ 50]$ and its values are discretized every 2.5 time unit. $M \in [100\ ;\ 900]$ and its values are discretized every 25 degradation unit. Let us note that optimizing the maintenance policy for the given decision variables is very time-consuming. Naturally, a finer discretization and more considered cost rates and coefficients will provide more accurate results. For the following experiments, it is reasonably assumed that $0 \leq c_I \leq c_R \leq c_P \leq c_C + c_D$. From now on, to simplify notations, as inspections are necessarily followed by either a repair or a replacement, we note $c_{IR} = c_I + c_R$, $c_{IP} = c_I + c_P$ and $c_{IC} = c_I + c_C$.

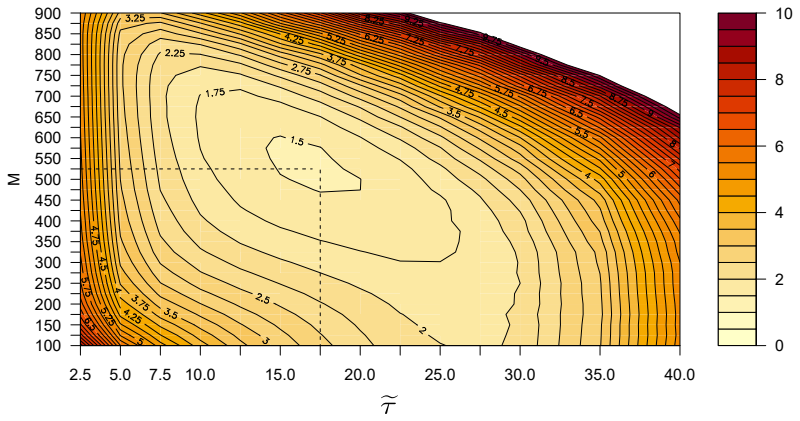

Figure 4.9: Surface long run average maintenance cost rates as a function of the inter-inspection time $\widetilde{\tau}$ and the preventive threshold M, computed with a corrective threshold equal to 1000 and the following cost coefficients: $c_{IR} = 12$, $c_{IP} = 50$, $c_{IC} = 100$, $c_D = 200$ and the set of parameters presented in Situation 1, Table 4.1.

In Figure 4.9, 5000 cycles are simulated for each value of $\widetilde{\tau}$ and M and the maintenance cost rates are computed with the hybrid method. For the given cost coefficients and model parameters, the optimal policy, i.e. for which the maintenance cost rate is minimal, is $(\widetilde{\tau}^*, M^*) = (17.5, 525)$.

4.3.1 Cost assessment and optimization

In this section, the long run average maintenance cost is computed using the hybrid method according to the decision variables $\widetilde{\tau}$ the inspection period, and M the preventive replacement threshold. τ^* and M^*, the optimal values of $\widetilde{\tau}$ and M which minimized the long run average maintenance cost presented in Equation (4.3), are analyzed taking into account different specific cost coefficients and model parameters. Let us also keep in mind than the chosen value for the corrective replacement threshold remains $L = 1000$ for all the following numerical experiments. Consequently, all optimal maintenance policies should be evaluated with respect to this corrective threshold.

Table 4.1: Parameters employed in simulating degradation trajectories

Situation \ parameters	μ_U	μ_M	σ_U^2	σ_M^2	r_{UM}	ρ
1	7	10	400	600	0.7	1
2	7	10	400	600	0.1	1
3	7	30	400	600	0.7	1
4	7	10	400	600	0.7	0.1

Different situations are considered in Table 4.1 in order to assess the possible influence of the model parameters on the optimal maintenance policy. Thus, in each situation, simulated degradation trajectories are based on a specific set of model parameters. On the one hand, the following section analyze the effect of the predefined cost coefficients c_{IP} and cost rate c_D on the optimal policy. On the other hand, this section also studies the impact of the drift of the maintained process μ^M, the correlation coefficient r_{UM} between the two underlying Wiener processes X^M and X^U, and the repair efficiency parameter ρ on the optimal maintenance policy.

4.3.2 Influence of the preventive replacement cost coefficient and the unavailability cost rate

To assess the potential influence of the given costs coefficients, multiple values of both preventive cost coefficients and unavailability cost rates are examined. The long run average maintenance cost is computed as a function of these cost coefficients.

Influence of the preventive replacement cost

To evaluate the impact of the preventive replacement cost, the maintenance cost rate is calculated using the hybrid method and for the following preventive cost coefficients: $c_{IP} = \{12, 25, 50, 100, 150\}$. In order to respect the previously mentioned assumption $0 \leq c_I \leq c_R \leq c_P \leq c_C + c_D$, the other cost coefficients are set at $c_{IR} = 12$, $c_{IC} = 100$ and $c_D = 50$,

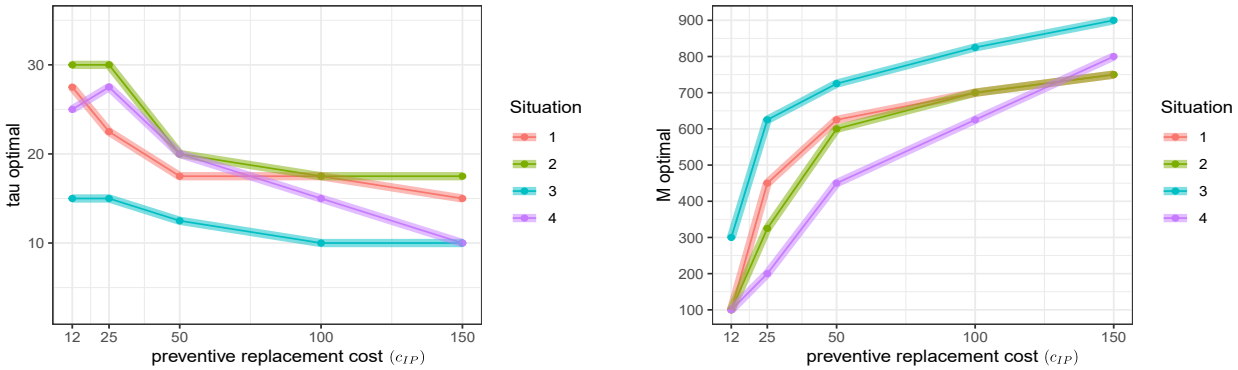

Figure 4.10: Optimal values of $\widetilde{\tau}$ and M considering different preventive cost coefficients (c_{IP})

For reasonable values of $\widetilde{\tau}$ and M, over the system life cycle, trade-offs exist between the number of repairs, the preventive threshold M and the length of the inter-inspection time $\widetilde{\tau}$ (Equation (4.3)). As the preventive threshold M approaches the corrective threshold L, the number of failures tends to increase. This phenomenon also contributes to an increase in the number of repairs and an extension of the life cycle. Moreover, for a given preventive threshold M, a decrease in the value of $\widetilde{\tau}$ rises the number of repairs, lengthens the life cycle and preventive replacements are more likely to be performed than corrective ones. Furthermore, a too small value of $\widetilde{\tau}^*$ would result in an excessive number of repairs, potentially leading to a high maintenance cost. Similarly, too long inter-inspection periods tend to favor failures, shorten system life cycles and elevate the cost (Equation (4.2)).

In Figure 4.10, for each situation, the following observations and possible explanations arise:

- As preventive cost coefficients rise, an increase in the optimal preventive threshold results in a decrease in the optimal inter-inspection time.

  In general, an increase in the preventive cost coefficients tends to slightly favor corrective replacements over preventive replacements. Here, as c_{IP} rises, a higher value of the preventive threshold and a lower value of the inter-inspection time, minimize the maintenance cost rate. In this situation, more repairs over a system life cycle, as well as more corrective replacements (over the 5000 initially simulated) are observed on the degradation trajectories.

- When $c_{IP} \geq 50$, the optimal inter-inspection time stabilize for the first three situations and a more moderate increase is observed in the optimal values of M. Specifically, in situations 2 and 3, when $c_{IP} \geq 100$, the values of $\widetilde{\tau}$ no longer decrease, while values of M^* slightly increase.

  Based on the observation of the degradation trajectories, this case results in more repairs over a life cycle and extended durations of life cycles.

  This trend can explain the convergence of optimal values for M towards the corrective threshold L in all situations. Opting for a higher risk of failure is favored in order to manage the maintenance cost rate. There also can be economic benefits in accepting a higher risk of failure rather than performing unnecessary or prematurely scheduled preventive replacements.

- When the preventive replacement cost coefficient is equal to the failure cost coefficient $c_{IP} = c_{IC} + c_D = 150$, $\widetilde{\tau}^* \in [10, 20]$ and $M^* \geq 700$ for all situations. Let us remark that, in that case, the type of replacement no longer affects the maintenance cost rate, allowing more failures and corrective replacements. Only the number of repairs and the length of $\widetilde{\tau}$ influence the cost. This can also explain why the values of M approaches the corrective threshold L when $c_{IP} = 150$ (examples of these degradation cycles are presented in Appendix Figures A.8 and A.9).

- When the preventive cost coefficient is equal to the repair cost coefficient ($c_{IR} = c_{IP} = 12$), the optimal preventive threshold is minimal. Based on the observation of the simulated degradation trajectories, these preventive replacements are always prioritized over corrective ones and the number of repairs strongly decreases even though life cycles are shortened, Appendix Figures A.6 and A.7.

Influence of the unavailability cost rate after failure

The impact of the unavailability cost rate c_D is also studied with values set at $\{12, 20, 50, 100, 150, 200\}$. For each of these values, to respect the assumption regarding the order of the maintenance cost coefficients, the other cost coefficients are set at $c_{IR} = 12$, $c_{IP} = 50$ and $c_{IC} = 100$.

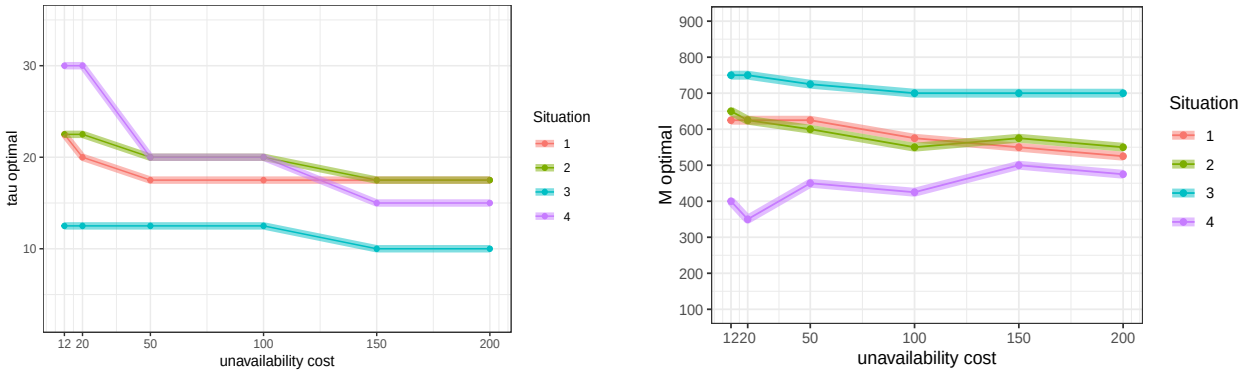

Figure 4.11: Optimal values of $\widetilde{\tau}$ and M considering different unavailability cost rates (c_D)

- In Figure 4.11, in contrast to Figure 4.10, the optimal values of M show less variability for all the situations. In the first three situations, as the unavailability cost rate rises, both $\widetilde{\tau}^*$ and M^* remain approximately at the same moderate level.

  Therefore, for these model parameters and for the other considered cost coefficients, the unavailability cost rate does not seem to impact the optimal policy $(\widetilde{\tau}^*, M^*)$ that much.

  It is worth noticing that, given the chosen cost coefficients ($c_{IR} = 12$, $c_{IP} = 50$ and $c_{IC} = 100$), a corrective replacements will always be more expensive than a preventive one, regardless of the unavailability cost coefficient. This explains the limited variability in the resulting optimal policies.

- In the initial three situations, in contrast to Figure 4.10, a slight reduction in $\widetilde{\tau}*$ corresponds to a marginal reduction in $M*$.

- For all situations,when $c_D > 150$, the optimal values of $\widetilde{\tau}$ and M stabilize.

  Sufficiently low values of both $\widetilde{\tau}^*$ and M^* tend to avoid failures. Prioritizing preventive replacements appears more suitable to minimize the risk of costly failures, Appendix Figure A.11.

- In the first three situations, when the unavailability cost rate is sufficiently low, M^* and τ^* are slightly higher.

In that situation, a failure is less costly. Then, for these optimal policies, failures are slightly more susceptible to occur, Appendix Figure A.10.

- Similar to Figure 4.10, in situation 4, the lower the $\widetilde{\tau}^*$, the higher M^*. As unavailability cost rate rises, the optimal inter-inspection significantly decreases, while the optimal preventive threshold sees only a slight increase, leading to favor preventive replacement.

  Situation 4 refers to a low repair efficiency parameter leading to an acceleration of the degradation. Thus, as the unavailability cost rises, a strong reduction in the inter-inspection period is more inclined to efficiently control the degradation and avoid too costly failures. Meanwhile, a slight increase in the optimal preventive threshold can lengthen the duration of life cycles, reducing maintenance cost rates.

4.3.3 Influence of the model parameters

To identify potential effects of model parameters on the optimal maintenance policy, one can observe how the curves behave relative to each other in both Figure 4.10 and Figure 4.11.

Influence of the correlation parameter, r_{UM}

Situations 1 and 2 show similar behaviors of the curves. For the optimal M, these curves are generally located between situation 3 and 4. Indeed in these first two situations, between two repairs, degradation increases less than in situation 3 but equally to situation 4 and maintenance effects are less pronounced than in situation 3 but more effective than in situation 4.

Since the first two situations lead to a similar behavior of the curves, the coefficient correlation r_{UM} between the two underlying processes X^U and X^M in the model, appears to have minimal impact on the maintenance cost rate.

Influence of the drift of the maintained process, μ_M

In situation 3, compared to the other situations, more extreme maintenance policies arise. Optimal inter-inspection periods $\widetilde{\tau}^*$ are always lower, and optimal preventive replacement thresholds M^* are always greater.

As only process X^M is affected by repairs, a higher value of the second process drift (μ_M) results in a more pronounced maintenance effect. Let us note that in the first three

situations, as $\rho = 1$, degradation level after repair remains $X^U(\tau_j)$. However, over the inter-inspection interval $\widetilde{\tau}$, degradation accelerates when the drift value is higher. Consequently, in this situation, there are higher risks of failures and shorter life cycles.

As degradation accelerated over the inter-inspection period, a lower value of $\widetilde{\tau}^*$ seems necessary to avoid too costly failures. Meanwhile, a greater value of M^* is more likely to favor multiple repairs and lengthen life cycles.

Influence of the repair efficiency parameter, ρ

Compared to the other situations, situation 4 shows greater variability in its optimal policies.

Compared to situation 3, when $c_{IP} \leq 100$ and for all the given values of c_D, a higher value of $\widetilde{\tau}^*$ and lower value of M^* are obtained. In this situation, repairs are almost ineffective, leading to an acceleration of the degradation. Then, for a moderate value of the preventive cost coefficient, performing multiple repairs over a cycle is not economically interesting as increasing their frequency has no significant impact on degradation but does increase the cost. It appears more interesting to reduce their frequency until a replacement is scheduled.

Yet, as the preventive cost coefficient becomes excessively high, $\widetilde{\tau}^*$ clearly decreases while M^* strongly increases. Even though maintenances are not very effective in this situation, their impact on the degradation over a life cycle seems to become significant when performed a sufficient amount of time. It appears necessary to significantly increase the number of repairs to avoid premature preventive replacements.

Let us also notice that optimal value of $\widetilde{\tau}$ is a non-monotonically function of the preventive cost coefficient. Indeed, the maximal value of $\widetilde{\tau}^*$ is obtained for $c_{IP} = 25$. When c_{IP} is sufficiently low ($c_{IP} < 25$), $\widetilde{\tau}^*$ tends to slightly decrease and M^* is minimal favoring preventive replacements over corrective ones.

4.4 Overview of a post-repair inspection/replacement policy

From now on, different inspection assumptions are considered. Degradation levels are assumed to be inspected right after repairs and replacements. Compared to the previous inspection policy, inspecting right after repairs, a policy already considered in practice, can offer further insights into the repair effect. For instance, in Chapter 2, observing degradation levels after repairs provides effective parameter assessments, even with a limited

number of observations. In addition, in the case of an optimal repair ($\rho = 1$), post-repairs inspections provide information about the degradation level of the unmaintained component, since $Y(\tau_j^+) = X^U(\tau_j)$, at the repair time. On the other hand, for this new inspection policy, the degradation level might exceed M before a repair and drop below this preventive threshold right after performing the repair. Then, considering this new inspection policy might significantly impact the optimal maintenance policy (τ^*, M^*).

Nevertheless, under this inspection policy, the analytic writing of the long run average maintenance cost appears to be much more complicated to obtain, even partially. Then, this section introduces the new considered maintenance assumptions and proceeds directly to numerical experiments using the purely simulation-based method.

4.4.1 Maintenance assumptions

As previously, the system undergoes inspections, repairs, preventive and corrective replacements. Repairs are performed periodically and degradation levels are only observed right after every repair. $\forall\ j \geq 1$, over $[\tau_{j-1}, \tau_j[$, the following rules apply:

- If there exists a time $t\ \in [\tau_{j-1}, \tau_j[$ such that $Y(t) > L$, then a failure occurs when degradation first exceeds the threshold L over the interval $[\tau_{j-1},\ \tau_j[$, leading to temporary unavailability which incurs a cost. The whole system undergoes a corrective replacement at the next maintenance time τ_j, such that $Y(\tau_j^+) = 0$. No inspection is carried out in this situation. If degradation does not exceed the threshold L over $[\tau_{j-1},\ \tau_j[$, then either a repair alone or a repair followed by a preventive replacement is performed at time τ_j according to the following rules.

- If $Y(\tau_j^+) < M$ after the repair, the system do not necessitate any further interventions and is left unchanged.

- If $M \leq Y(\tau_j^+) \leq L$, a preventive replacement is performed right after the repair, such that $Y(\tau_j^+) = 0$. Let us notice that, if a failure occurs at the scheduled maintenance time (which is a zero probability event), no unavailability time is considered, and a preventive maintenance is performed.

For this policy, maintenance assumptions are slightly different: when the observed degradation level right after repair is between M and L, then a preventive as-good-as-new replacement is instantaneously performed on the entire system. In that specific situation, two

maintenance actions are simultaneously performed on the system. Therefore, every preventive replacement necessarily involves one inspection and one repair at the same maintenance time. In addition, compared to the previous inspection policy, failures are self-declared and corrective replacements do not involve any inspections. Figure 4.12.

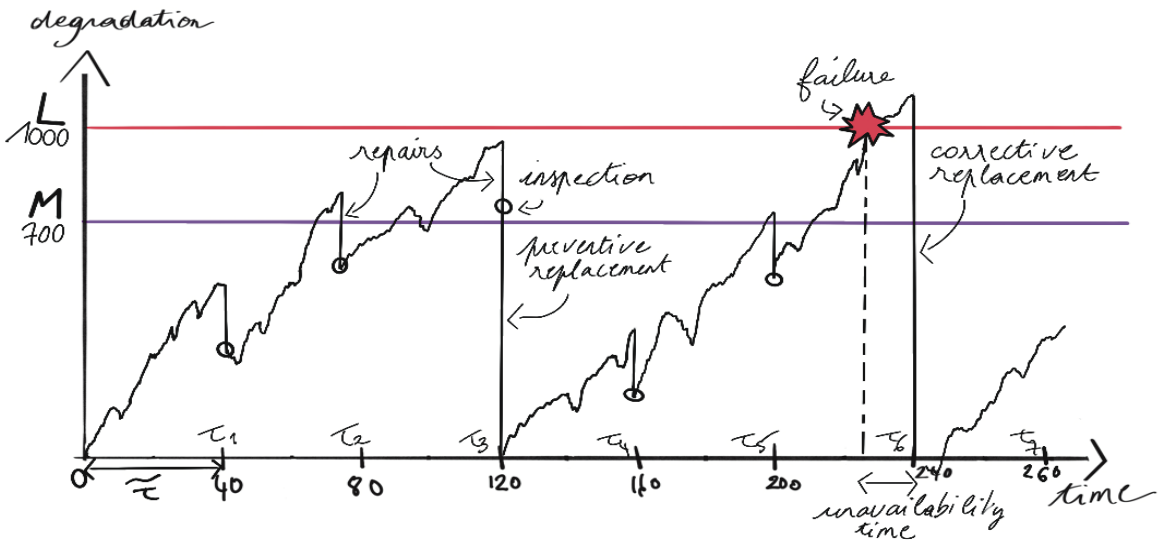

Figure 4.12: Degradation trajectory $Y(t)$ as a function of time

4.4.2 Cost optimization and numerical experiments

Previously, as presented in Equation (4.3), a semi-regenerative Markov process is considered to evaluate the long run average maintenance cost under the stationary measure, with the aim of writing a fully or partially analytic cost expression. However, the introduction of this new inspection scheme has increased the complexity of the analytic cost assessment $\frac{\mathbb{E}_\pi[c(\widetilde{\tau})]}{\widetilde{\tau}}$ between two inspections. As previously, the cost involves calculating various quantities, including $\mathbb{P}\left(Y(\tau_j^+) < M,\ \sup_{s\in[0,\widetilde{\tau}[} Y(s) \leq L \mid Y_{j-1}^+ = y\right)$, $\mathbb{P}\left(M \leq Y(\tau_j^+,\ \sup_{s\in[0,\widetilde{\tau}[} Y(s) \leq L \mid Y_{j-1}^+ = y\right)$, $\mathbb{P}\big(\sup_{s\in[0,\widetilde{\tau}[} Y(s) > L | Y_{j-1}^+ = y\big)$ and the conditional expectation of the unavailability time. In these probabilities, $Y(\tau_j^+)$, defined as $Y(\tau_j^+) = X^U(\tau_j)$ (when repairs are assumed to be

optimal, i.e. $\rho = 1$), represents the degradation level immediately after repairs and before any potential preventive replacements. Between two repairs, degradation evolves according to the process X^S, such that $Y(s) = X^S(s)$. Consequently, the assessment of the cost involves two dependent processes, X^U and X^S, significantly complicating its evaluation.
Thus, in this section, the long run average maintenance cost presented in Equation (4.2), is only numerically assessed, using the purely stochastic simulation-based method over regenerative periods. As outlined in the previous pre-inspection policy, degradation trajectories are simulated based on successive degradation increments over small time steps (increments are simulated every 0.1 time unit). All the degradation trajectories are simulated over N_{cyc} life cycles. Optimal policies are determined by minimizing the long run average maintenance cost according to the same discretized values of $\widetilde{\tau}$ and M presented previously.
As mentioned earlier, compared to the previous inspection policy, for a given inter-inspection time and preventive threshold, an inspected degradation level can exceed M before a repair and drop below M right after the repair. This scenario tends to increase the number of repairs over one life cycle. In general, for moderate values of $\widetilde{\tau}$ and M, it also leads to a higher risk of failure. This is why, in the following numerical experiments, the optimal preventive threshold is lower than the one obtained in the previous inspection policy, avoiding either too many repairs or too many failures.

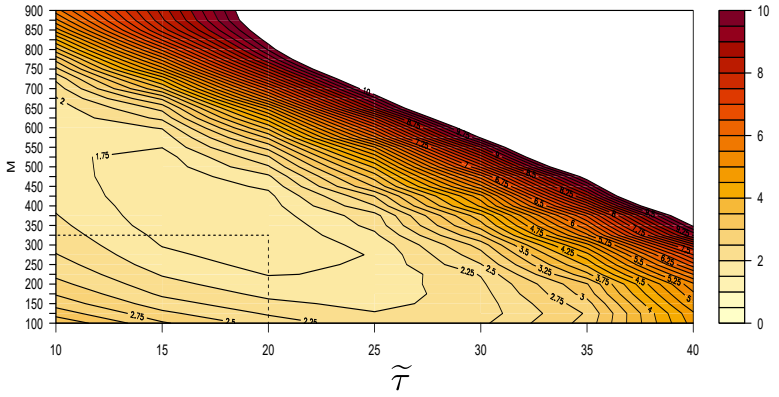

Figure 4.13: Surface long run average maintenance cost rates as a function of the inter-inspection time $\widetilde{\tau}$ and the preventive threshold M, considering post-repair inspections. Cost coefficients include $c_I + c_R = 12$, $c_I + c_P = 50$, $c_C = 100$, $c_D = 200$, with model parameters specified in Situation 1, Table 4.1

Figure 4.13 gives an example of an optimal policy given the same specific cost coefficients and model parameters as Figure 4.9 previously. In Figure 4.13, the optimal decision variables, $\widetilde{\tau}^* = 20$ and $M^* = 325$, are optimized using Monte Carlo simulations composed of successive small degradation increments, each one generated over 0.1 time unit. The whole degradation trajectory is simulated over $N_{cyc} = 5000$ cycles. Compared to Figure 4.9 where $\widetilde{\tau}^* = 17.5$ and $M^* = 525$, the optimal $\widetilde{\tau}$ does not really change, whereas M^* significantly decreases. In this scenario, preventive replacements are favored, avoiding expensive failures and corrective replacements.

Influence of the preventive replacement cost

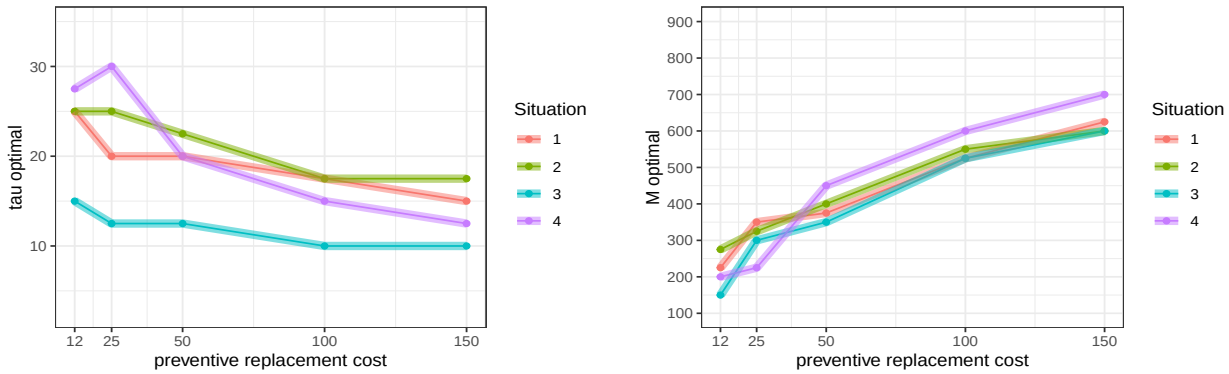

Figure 4.14: Optimal values of $\widetilde{\tau}$ and M considering different preventive cost coefficients

In Figure 4.14, for all situations, the optimal inter-inspection time decreases as the preventive replacement cost coefficient rises. When the cost coefficient exceeds 100, the optimal inter-inspection time tends to stabilize at a certain optimal value. Meanwhile, M^* increases as the cost coefficient rises.

Compared to the previous optimal policies outlined in Figure 4.10, the curves for $\widetilde{\tau}$ show similar trends, while M^* are generally lower for all situations. As expected, when $c_{IP} \geq 25$, the optimal values of M are notably lower compared to the values of M^* in the inspection assumptions previously considered, potentially avoiding an excessive number of repairs and failures. On the other hand, when $c_{IP} = c_{IR} = 12$, the optimal values of M are slightly higher. In this case, prioritizing both repairs and preventive replacements over corrective replacements becomes economically interesting. However, setting the preventive threshold

too low may result in an excessive frequency of preventive replacements, thereby shortening life cycles and elevating the maintenance cost rate. Let us also note that, compared to the pre-inspection policy, the optimal policies show less sensitivity to changes in the preventive cost coefficient, as there is reduced variability in the obtained optimal policies.

Influence of the unavailability cost rate

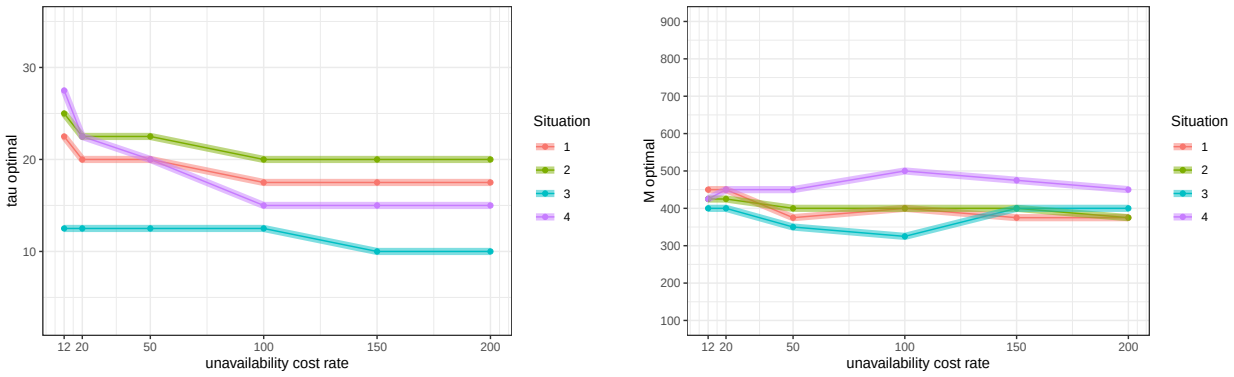

Figure 4.15: Optimal values of $\widetilde{\tau}$ and M considering different preventive cost coefficients

In Figure 4.15, there is minimal variability among the optimal values of the decision variables. Specifically, the optimal values of M^* show marginal variation.

Just as in Figure 4.14, compared to the pre-repair inspection policy, the optimal values of $\widetilde{\tau}$ are very similar, whereas the optimal values of M are strongly reduced. However, the optimal values of $\widetilde{\tau}$ tend to stabilize earlier than in the previous inspection policy (here the same $\widetilde{\tau}^*$ is observed when $c_D \geq 100$ for the first three situations). As mentioned in the previous section, here again, failures involve two cost rates: the corrective and the unavailability cost rate. The chosen cost coefficients are set such that $c_{IC} = 100, c_{IP} = 50, c_I = 12$. Thus, regardless the chosen cost rate coefficient associated with the unavailability of the system, failures will always incur higher costs than preventive replacements. Therefore, given the chosen cost coefficients, the unavailability cost rate does not have a significant impact on the optimal policy $(\widetilde{\tau}^*, M^*)$.

4.4.3 Influence of the parameters

Similarly to the previous inspection policy, the impact of the model parameters can be studied by comparing the resulting optimal policies with each other.

- In both Figure 4.14 and Figure 4.15, for a given value of the preventive cost coefficient and unavailability cost rate, the optimal values of M are highly similar between the first three situations. Consequently, the considered model parameters (μ_M, r_{UM}) do not show a notable influence on the optimal values of the preventive replacement threshold.

- Just as in the pre-repair inspection policy, the optimal policies in situations 1 and 2 are very similar, indicating that the coefficient correlation between the two underlying Wiener processes X^U and X^M, does not significantly impact the optimal policy.

- In situations 1 and 3, values of M^* are highly similar and values of $\widetilde{\tau}^*$ follow the same trend in both Figure 4.14 and Figure 4.15. Let us remark that the first three situations where $\rho = 1$, the inspected degradation level after repair corresponds to $Y(\tau_j^+) = X_U(\tau_j)$. Then, as μ_M is not considered in the post-repair inspected degradation, the inspected degradation levels are equivalent in situations 1 and 3. The only distinction in the optimal policy between these two situations comes from the evolution of the degradation between the inspections. Between two inspections, degradation is higher in situation 3. Then, for the considered values of $\widetilde{\tau}$ and M, more failures are likely to occur in this situation, leading to a slightly different maintenance policy. Indeed, different values of $\widetilde{\tau}^*$ are observed between these two situations.

- In situation 3, the observed values of M^* are much lower compared to the pre-repair inspection policy (Figure 4.10, Figure 4.11). This difference comes from the fact that in the pre-repair inspection policy, the inspected degradation levels are much higher, $Y(\tau_j^-) = X^U(\tau_j) + X^M(\tau_j)$, whereas, in the post-repair inspection policy, inspected degradation levels are given by $Y(\tau_j^+) = X^U(\tau_j)$. Necessarily, these different inspection values significantly alters the optimal policy.

- In situation 4, optimal values of $\widetilde{\tau}$ and M are quite similar, whether degradation levels are inspected before or after repairs. In this situation, with $\rho = 0.1$ and maintenance being nearly ineffective, degradation levels inspected right before repairs are very close from those inspected right after. As expected, when the repair efficiency parameter is

close to zero, the inspection assumptions, whether inspections are conducted before or after repairs, show marginal impact on the optimal policy.

4.5 Conclusion on the inspection/replacement policy

In this chapter, a maintenance policy is established using the Wiener-based degradation model with partial maintenance effects. The long run average maintenance cost is assessed using both the regenerative and semi-regenerative properties of the maintained degradation process. These two approaches are respectively referred to the purely simulation-based Monte Carlo method that relies on simulated degradation trajectories over one life cycle, and the hybrid method that combines analytic expressions and numerical simulations of the stationary distribution, both involved in the cost rate assessment. This hybrid method appears to be less time-consuming and give efficient results for a preventive threshold reasonably distant from the corrective threshold. Two maintenance policies are considered. On the one hand, degradation levels are inspected before any type of maintenance action. On the other hand, in the second maintenance policy, degradation levels are inspected right after each repair. In both maintenance policies, the inter-inspection time $\widetilde{\tau}$ and the preventive threshold M are the decision variables. Variations of these optimal policies are also analyzed considering different values for model parameters and various cost coefficients: In both inspection policies, the increase in the preventive cost coefficient leads to a reduction in the optimal inter-inspection time and an increase in the optimal preventive threshold. Moreover, in both pre-repair and post-repair inspection policies, the correlation coefficient between the two underlying Wiener processes does not significantly affect the optimal policy. However, besides these similarities, the inspection scheme noticeably impacts the derived optimal policies. When degradation is inspected before repairs, variations in the maintained drift parameter μ_M and the repair efficiency parameter ρ significantly alter the optimal policy $(\widetilde{\tau}^*\ ,\ M^*)$. On the opposite, in the post-repair inspection policy, μ_M does not affect the optimal policy as, when $\rho = 1$, this parameter is not considered in the evaluation of the degradation after repair. As this post-repair inspection policy tends to increase the number of failures for moderate values of $\widetilde{\tau}$ and M^*, the value of the optimal preventive threshold is lowered to ensure cheaper preventive replacements.

Future investigations may consider an exploration of the complete analytic form of the long run average maintenance cost, requiring the assessment of the stationary distribution. In this chapter, as the simulation of degradation trajectories can be very time-consuming, five situations, referring to five different sets of model parameters, have been studied and compared to determine the possible influence of model parameters and cost coefficients on the maintenance cost rates. Yet, additional situations and further studies involving more

various values of model parameters, could be conducted in the future to precisely evaluate the impact of all the model parameters and cost coefficients on the maintenance cost rates, considering both inspection policies.

Conclusion

This manuscript presents two degradation models with maintenance effects: the first model relies on a univariate Wiener process with drift (Chapter 2), while the second novel model is built on a bivariate Wiener process with drift, where only one out of two processes is affected by maintenance effects (Chapter 3). For this last model, and based on inference outcomes, two models emerge: The perturbed ARD_1 model, defined by a usual Wiener-based degradation model perturbed by a white noise, and the partial replacement model, where maintenance effects are optimal on the maintained component.

For each model described in Chapters 1 and 2, and inspired by actual observation schemes used in the industry, multiple observation schemes are taken into account for statistical inference. For both models, the observation scheme influences parameter estimations. Specifically, numerical results using the first degradation model described in Chapter 1 show that when only a limited number of observations is provided, observing degradation levels right after repairs offers better parameter estimations than observing degradation only before repairs. Moreover, for both models, better estimations results are obtained when degradation is observed close to maintenance times. However, for this first presented model, observing degradation both just before and just after repairs leads to deterministic jump values, failing to properly reflect reality. On the opposite, the proposed degradation model with partial maintenance effects proves to be well-suited for practical scenarios and bypass statistical inference issues encountered with the initial Wiener-based model. Nevertheless, to ensure identifiability of this new model, constraints need to be imposed either on the maintenance efficiency parameter ($\rho = 1$) or on drift parameters ($\mu_U = \mu_M$). The realistic partial replacement situation ($\rho = 1$) allows statistical inference in all possible observation schemes.

Afterwards, based on the degradation model with partial maintenance effects, two main-

tenance policies are established, involving inspections either right before maintenance or right after repairs, imperfect repairs, preventive and corrective replacements (Chapter 4). A specific cost coefficient is associated to each of these maintenances. The long run average maintenance cost is assessed using two different approaches. One employs the regenerative properties of the maintained process over a system life cycle, and the other one, called the hybrid method, uses a semi-regenerative Markov process over the inter-inspection time. The first approach is based on fully numerical Monte Carlo simulations while the hybrid method includes analytic expressions in the asymptotic cost assessment. This hybrid method is more time-efficient, providing precise results for a reasonable preventive replacement threshold (not too close to the corrective threshold). Furthermore, maintenance cost rates are assessed with the hybrid method, according to the inter-inspection time $\widetilde{\tau}$ and the preventive threshold M. These two decision variables are optimized by minimizing the long run average maintenance cost, and the resulting optimal policies, considering various values of model parameters, specific cost coefficients, and different inspection schemes, are discussed. For both inspection policies (whether degradaiton is inpsected before or after maintenance), given specific cost coefficients, the optimal policy ($\tilde{\tau}^*$, M^*) appears to be sensitive to changes in the preventive cost coefficient. The rise in the preventive cost coefficient leads to a decrease in the optimal inter-inspection time and simultaneously an increase in the optimal preventive threshold. Some model parameters also impact the optimization results. The correlation coefficient r_{UM} between the two underlying Wiener processes does not significantly influences the optimal policy, whereas the value of the drift parameter of the maintained process μ_M, as well as the value of the maintenance efficiency parameter ρ significantly impact $(\widetilde{\tau}^*, M^*)$. In addition, the inspection scheme influences the optimal policy outcomes. Indeed, the post-repair inspection policy entails new resulting optimal policies, especially when maintenance actions are sufficiently effective. In general, failures are more likely to happen in this inspection policy, resulting in different optimization outcomes. On the one hand, the obtained values of M^* are significantly lower compared to those assessed in the pre-maintenance inspection scheme. On the other hand, these resulting optimal policies show less variability when considering different cost coefficients specific to the type of maintenance.

Based on this work, further analyses can still be explored. In Chapter 2, a multi-modal empirical PDF of the first hitting time arise using the degradation model with partial maintenance effects. Then, the analytic expression of the first passage time distribution and the Remaining Useful Life are worth investigating for this model. In Chapter 4, another ap-

proach to assess the optimal policy could be considered, consisting in the search for the analytic writing of the stationary distribution involved in the stationary equation (Equation (4.3)). This will result in a fully analytic form of the asymptotic cost per time unit, when inspections occur before repairs. This last method will enable the computation of the maintenance cost rate, without concern for computational time. A further analytic analysis regarding the cost rate assessment could also be conducted considering the post-repair inspection policy. Additionally, conducting more numerical studies, such as considering more values of model parameters and cost coefficients, could allow a better understanding of the impact of all cost coefficients and model parameters on the optimal maintenance policy, considering both pre-maintenance and post-repair inspection policies. Furthermore, studying other inspection schemes, such as those outlined in Chapter 1, will also enable us to determinate the precise impact of observation locations on the resulting optimal maintenance policies. Besides, alternative maintenance strategies can also be proposed based on the degradation model with partial maintenance effects.

The degradation model with partial maintenance effects could also be adapted to more general practical situations. For instance, multivariate processes could be considered for this model. Notably, the model could include two co-dependent multivariate processes, instead of being limited to two univariate processes. In such cases, random vectors should be considered for inference. Such a model would be capable of describing the degradation of a multi-component system, where components are more or less correlated to each other. Given the partial maintenance effect, only a few specific components would undergo maintenance. In addition, to specify the degradation phenomena, covariates could also be integrated into this model. In the example illustrated in Figures 7 and 8, degradation is inspected in both hot and cold leg pipes of a steam generator, depicting different values of degradation levels. Therefore, factors such as temperature or humidity could be considered as additional variables influencing the degradation process. Naturally, the selection of these covariates would depend on the specifics of the studied practical scenario. Besides, in practice, degradation of different dependent components are not necessary inspected simultaneously within the same asset. Hence, this new difficuly lies in considering different sets of inspection times for each involved process for statistical inference and decision making.

Bibliography

[1] M. Abdel-Hameed, *A Gamma Wear Process*, IEEE Transactions on Reliability **R-24** (1975), no. 2, 152–153.

[2] R. B. Ash, *Basic probability theory*, Courier Corporation, 2008.

[3] N. Balakrishnan and C. Qin, *First Passage Time of a Lévy Degradation Model with Random Effects*, Methodology and Computing in Applied Probability **21** (2019), no. 1, 315–329.

[4] C.T. Barker and M.J. Newby, *Optimal non-periodic inspection for a multivariate degradation model*, Maintenance Modeling and Application **94** (2009), no. 1, 33–43.

[5] R. E. Barlow, A. Madansky, F. Proschan, and E. M. Scheuer, *Statistical Estimation Procedures for the "Burn-In" Process*, Technometrics **10** (1968), no. 1, 51–62, Publisher: Taylor & Francis.

[6] L. Bautista, I. T. Castro, C. Bérenguer, O. Gaudoin, and L. Doyen, *First hitting time distribution and cost assessment in a two-unit system with dependent degradation processes subject to imperfect maintenance*, Proceedings of the Institution of Mechanical Engineers, Part O: Journal of Risk and Reliability (2023), 1748006X231211378, Publisher: SAGE Publications.

[7] S.A. Belbas and Yuriy Bulka, *Numerical solution of multiple nonlinear Volterra integral equations*, Applied Mathematics and Computation **217** (2011), no. 9, 4791–4804.

[8] W. R. Blischke and DN P. Murthy, *Reliability: modeling, prediction, and optimization*, John Wiley & Sons, 2011.

[9] L. Bordes, C. Paroissin, and A. Salami, *Parametric inference in a perturbed gamma degradation process*, Communications in Statistics - Theory and Methods **45** (2016), no. 9, 2730–2747, Publisher: Taylor & Francis.

[10] C. Bérenguer, A. Grall, L. Dieulle, and M. Roussignol, *Maintenance policy for a continously monitored deteriorating system*, Probability in the Engineering and Informational Sciences **17** (2003), no. 2, 235–250, Edition: 2003/02/27 Publisher: Cambridge University Press.

[11] S. Bressi, J. Santos, and M. Losa, *Optimization of maintenance strategies for railway track-bed considering probabilistic degradation models and different reliability levels*, Reliability Engineering & System Safety **207** (2021), 107359.

[12] C. G. Broyden, *The Convergence of a Class of Double-rank Minimization Algorithms 1. General Considerations*, IMA Journal of Applied Mathematics **6** (1970), no. 1, 76–90.

[13] G. M. Calvi, M. Moratti, G. J. O'Reilly, N. Scattarreggia, Ricardo Monteiro, D. Malomo, P. M. Calvi, and R. Pinho, *Once upon a Time in Italy: The Tale of the Morandi Bridge*, Structural Engineering International **29** (2019), no. 2, 198–217, Publisher: Taylor & Francis.

[14] B. Castanier, C. Bérenguer, and A. Grall, *A sequential condition-based repair/replacement policy with non-periodic inspections for a system subject to continuous wear*, Applied Stochastic Models in Business and Industry **19** (2003), no. 4, 327–347 (en).

[15] I. T. Castro and L. Landesa, *A dependent complex degrading system with non-periodic inspection times*, Computers & Industrial Engineering **133** (2019), 241–252.

[16] H. Che, S. Zeng, and J. Guo, *Reliability assessment of man-machine systems subject to mutually dependent machine degradation and human errors*, Reliability Engineering & System Safety **190** (2019), 106504.

[17] G. Chen, A. Yamaguchi, and K. Miya, *A novel signal processing technique for eddy-current testing of steam generator tubes*, IEEE Transactions on Magnetics **34** (1998), no. 3, 642–648.

[18] C. Chuang, L. Ningyun, J. Bin, and X. Yin, *Condition-based maintenance optimization for continuously monitored degrading systems under imperfect maintenance actions*, Journal of Systems Engineering and Electronics **31** (2020), no. 4, 841–851.

[19] E. Cinlar, *Markov renewal theory*, Advances in Applied Probability **1** (1969), no. 2, 123–187, ISBN: 0001-8678 Publisher: Cambridge University Press.

[20] C. Cocozza-Thivent, *Convergence de fonctionnelles de processus semirégénératifs*, Prépublications de l'Université de Marne la Vallée **2** (2000).

[21] F. Corset, M. Fouladirad, and C. Paroissin, *Imperfect condition-based maintenance for a gamma degradation process in presence of unknown parameters*, Proceedings of the Institution of Mechanical Engineers, Part O: Journal of Risk and Reliability (2022), 1748006X221134132.

[22] J. N. Darroch and D. Ratcliff, *A Characterization of the Dirichlet Distribution*, Journal of the American Statistical Association **66** (1971), no. 335, 641–643, Publisher: Taylor & Francis.

[23] G. De Matteis, M. Zizi, and A. Prete, *Structural features of typical Italian bridges built in the '50s: Four case studies in the province of Caserta*, April 2019.

[24] A. P. Dempster, N. M. Laird, and D. B. Rubin, *The expectation-maximization algorithm*, Journal of the Royal Statistical Society, Series B (Methodological) **39** (1977), no. 1, 1–38.

[25] K. A. Doksum and S. L. T. Normand, *Gaussian models for degradation processes-Part I: Methods for the analysis of biomarker data*, Lifetime Data Analysis **1** (1995), no. 2, 131–144.

[26] J. L. Doob, *What is a Stochastic Process?*, The American Mathematical Monthly **49** (1942), no. 10, 648–653, Publisher: Taylor & Francis.

[27] J.L. Doob, *Renewal theory from the point of view of the theory of probability*, Transactions of the American Mathematical Society **63** (1948), no. 3, 422–438, ISBN: 0002-9947.

[28] L. Doyen and O. Gaudoin, *Classes of imperfect repair models based on reduction of failure intensity or virtual age*, Reliability Engineering & System Safety **84** (2004), no. 1, 45–56.

[29] X. Duan, H. Su, and D. Wang, *State Maintenance Strategy of Wind Turbine Based on Stochastic Degradation Model*, 2020 Chinese Control And Decision Conference (CCDC), August 2020, pp. 4537–4543.

[30] S. O. Duffuaa and M. A. Ben Daya, *Turnaround maintenance in petrochemical industry: practices and suggested improvements*, Journal of Quality in maintenance Engineering **10** (2004), no. 3, 184–190, ISBN: 1355-2511 Publisher: Emerald Group Publishing Limited.

[31] E. B. Dynkin, *Markov processes*, Springer, 1965.

[32] V. Esslinger, R. Kieselbach, R. Koller, and B. Weisse, *The railway accident of Eschede – technical background*, Engineering Failure Analysis **11** (2004), no. 4, 515–535.

[33] W. Feller, *On the integral equation of renewal theory*, The Annals of Mathematical Statistics **12** (1941), no. 3, 243–267, ISBN: 0003-4851 Publisher: JSTOR.

[34] P. E. Gill and W. Murray, *Newton-type methods for unconstrained and linearly constrained optimization*, Mathematical Programming **7** (1974), 311–350, ISBN: 0025-5610 Publisher: Springer.

[35] M. Giorgio and G. Pulcini, *A new state-dependent degradation process and related model misidentification problems*, European Journal of Operational Research **267** (2018), no. 3, 1027–1038.

[36] A. Grall, C. Bérenguer, and L. Dieulle, *A condition-based maintenance policy for stochastically deteriorating systems*, Reliability Engineering & System Safety **76** (2002), no. 2, 167–180.

[37] A. Grall, L. Dieulle, C. Berenguer, and M. Roussignol, *Continuous-time predictive-maintenance scheduling for a deteriorating system*, IEEE Transactions on Reliability **51** (2002), no. 2, 141–150.

[38] M. Guida, F. Postiglione, and G. Pulcini, *A time-discrete extended gamma process for time-dependent degradation phenomena*, ESREL 2010 **105** (2012), 73–79.

[39] M. Guida and G. Pulcini, *The Inverse Gamma process: A family of continuous stochastic models for describing state-dependent deterioration phenomena*, Reliability Engineering & System Safety **120** (2013), 72–79.

[40] C. Guo, W. Wang, B. Guo, and X. Si, *A maintenance optimization model for mission-oriented systems based on Wiener degradation*, Reliability Engineering & System Safety **111** (2013), 183–194.

[41] A. Hameed, F. Khan, and S. Ahmed, *A risk-based methodology to estimate shutdown interval considering system availability*, Process Safety Progress **34** (2015), no. 3, 267–279, Publisher: John Wiley & Sons, Ltd.

[42] H. Hanachi, J. Liu, A. Banerjee, Y. Chen, and A. Koul, *A Physics-Based Modeling Approach for Performance Monitoring in Gas Turbine Engines*, IEEE Transactions on Reliability **64** (2015), no. 1, 197–205.

[43] B.P. Harlamov, *On statistics of Inverse Gamma process as a model of wear*, Probability, Statistics and Modelling in Public Health (Boston, MA) (M. Nikulin, D. Commenges, and C. Huber, eds.), Springer US, 2006, pp. 187–201.

[44] R. A. Howard, *System Analysis of Semi-Markov Processes*, IEEE Transactions on Military Electronics **8** (1964), no. 2, 114–124.

[45] M. H. Hsieh and S. L. Jeng, *Accelerated Discrete Degradation Models for Leakage Current of Ultra-Thin Gate Oxides*, IEEE Transactions on Reliability **56** (2007), no. 3, 369–380.

[46] K. T. Huynh, *An adaptive predictive maintenance model for repairable deteriorating systems using inverse Gaussian degradation process*, Reliability Engineering & System Safety **213** (2021), 107695.

[47] K.T. Huynh and A. Grall, *A condition-based maintenance model with past-dependent imperfect preventive repairs for continuously deteriorating systems*, Proceedings of the Institution of Mechanical Engineers, Part O: Journal of Risk and Reliability **234** (2020), no. 2, 333–358, Publisher: SAGE Publications Sage UK: London, England.

[48] V. S. Huzurbazar, *The likelihood equation, consistency and the maxima of the likelihood function*, Annals of Eugenics **14** (1947), no. 1, 185–200, ISBN: 2050-1420 Publisher: Wiley Online Library.

[49] B. Jonge and P. A. Scarf, *A review on maintenance optimization*, European Journal of Operational Research **285** (2020), no. 3, 805–824.

[50] W. Kahle, *Imperfect repair in degradation processes: A Kijima-type approach*, Applied Stochastic Models in Business and Industry **35** (2019), no. 2, 211–220.

[51] W. Kahle and A. Lehmann, *The Wiener Process as a Degradation Model: Modeling and Parameter Estimation*, Advances in Degradation Modeling: Applications to Reliability, Survival Analysis, and Finance (M.S. Nikulin, N. Limnios, N. Balakrishnan, W. Kahle, and C. Huber, eds.), Birkhäuser Boston, Boston, MA, 2010, pp. 127–146.

[52] W. Kahle, S. Mercier, and C. Paroissin, *Degradation processes in reliability*, John Wiley & Sons, 2016.

[53] M. J. Kallen and J. M. Van Noortwijk, *Statistical inference for Markov deterioration models of bridge conditions in the Netherlands*, 2006, pp. 16–19.

[54] H. Kamranfar, M. Fouladirad, and N. Balakrishnan, *Inference for a gradually deteriorating system with imperfect maintenance*, Communications in Statistics - Simulation and Computation (2021), 1–19.

[55] A. Khatab, C. Diallo, E-H. Aghezzaf, and U. Venkatadri, *Condition-based selective maintenance for stochastically degrading multi-component systems under periodic inspection and imperfect maintenance*, Proceedings of the Institution of Mechanical Engineers, Part O: Journal of Risk and Reliability **232** (2018), no. 4, 447–463, Publisher: SAGE Publications.

[56] M. Kijima, *Some results for repairable systems with general repair*, Journal of Applied Probability **26** (1989), no. 1, 89–102.

[57] S. Kotz, N. Balakrishnan, and N.L. Johnson, *Continuous multivariate distributions: Models and application*, vol. 1, New York: John Wiley and Sons, 2000.

[58] R. Laggoune, A. Chateauneuf, and D. Aissani, *Preventive maintenance scheduling for a multi-component system with non-negligible replacement time*, International Journal of Systems Science **41** (2010), no. 7, 747–761, Publisher: Taylor & Francis.

[59] J. Lawless and M. Crowder, *Covariates and Random Effects in a Gamma Process Model with Application to Degradation and Failure*, Lifetime Data Analysis **10** (2004), no. 3, 213–227.

[60] M. D Le and Ch. M. Tan, *Optimal maintenance strategy of deteriorating system under imperfect maintenance and inspection using mixed inspectionscheduling*, Reliability Engineering & System Safety **113** (2013), 21–29.

[61] J. Lee, *Teleservice engineering in manufacturing: challenges and opportunities*, International Journal of Machine Tools and Manufacture **38** (1998), no. 8, 901–910.

[62] M. Leroy, C. Bérenguer, L. Doyen, and O. Gaudoin, *Statistical inference for a Wiener-based degradation model with imperfect maintenance actions under different observation schemes*, Applied Stochastic Models in Business and Industry (2023).

[63] X. Li, Y. Ran, F. Wan, H. Yu, G. Zhang, and Y. He, *Condition-based maintenance strategy optimization of meta-action unit considering imperfect preventive maintenance based on Wiener process*, Flexible Services and Manufacturing Journal (2021).

[64] X. Liu, K. N. Al-Khalifa, A. Elsayed, D. W. Coit, and A. Hamouda, *Criticality measures for components with multi-dimensional degradation*, IIE Transactions **46** (2014), no. 10, 987–998, Publisher: Taylor & Francis.

[65] X. Liu, Y. Dijoux, J. Vatn, and H. Toftaker, *Performance of prognosis indicators for superimposed renewal processes*, Probability in the Engineering and Informational Sciences **36** (2022), no. 1, 17–40, Publisher: Cambridge University Press.

[66] X. Liu, K. Yeo, and J. Kalagnanam, *A statistical modeling approach for spatio-temporal degradation data*, Journal of Quality Technology **50** (2018), no. 2, 166–182, Publisher: Taylor & Francis.

[67] P. Lévy, *Calcul des probabilités*, Gauthier-Villars, Paris, 1925.

[68] H. G. Ma, J. P. Wu, X. Y. Li, and R. Kang, *Condition-Based Maintenance Optimization for Multicomponent Systems Under Imperfect Repair—Based on RFAD Model*, IEEE Transactions on Fuzzy Systems **27** (2019), no. 5, 917–927.

[69] J. Ma, L. Cai, G. Liao, H. Yin, X. Si, and P. Zhang, *A multi-phase Wiener process-based degradation model with imperfect maintenance activities*, Reliability Engineering & System Safety **232** (2023), 109075.

[70] D. McDonald, *On semi-Markov and semi-regenerative processes I*, Zeitschrift für Wahrscheinlichkeitstheorie und Verwandte Gebiete **42** (1978), no. 4, 261–277.

[71] C Meier-Hirmer, G Riboulet, F Sourget, and M Roussignol, *Maintenance optimization for a system with a gamma deterioration process and intervention delay: Application to track maintenance*, Proceedings of the Institution of Mechanical Engineers, Part O: Journal of Risk and Reliability **223** (2009), no. 3, 189–198, Publisher: SAGE Publications.

[72] S. Mercier and I. T. Castro, *On the Modelling of Imperfect Repairs for a Continuously Monitored Gamma Wear Process Through Age Reduction*, Journal of Applied Probability **50** (2013), no. 4, 1057–1076.

[73] ———, *Stochastic comparisons of imperfect maintenance models for a Gamma deteriorating system*, European Journal of Operational Research **273** (2019), no. 1, 237–248.

[74] S. Mercier, C. Meier-Hirmer, and M. Roussignol, *Bivariate Gamma wear processes for track geometry modelling, with application to intervention scheduling*, Structure and Infrastructure Engineering **8** (2012), no. 4, 357–366.

[75] N. Metropolis and S. Ulam, *The monte carlo method*, Journal of the American statistical association **44** (1949), no. 247, 335–341, ISBN: 0162-1459 Publisher: Taylor & Francis.

[76] M. Modarres, M. P. Kaminskiy, and V. Krivtsov, *Reliability engineering and risk analysis: a practical guide*, CRC press, 2016.

[77] S. M. Mulani, A. Kumar, H. N. A. Shaikh, A. Saurabh, P. K. Singh, and P. C. Verma, *A review on recent development and challenges in automotive brake pad-disc system*, International Conference on Materials, Machines and Information Technology-2022 **56** (2022), 447–454.

[78] J. A. Nelder and R. Mead, *A Simplex Method for Function Minimization*, The Computer Journal **7** (1965), no. 4, 308–313.

[79] K. T. P. Nguyen, M. Fouladirad, and A. Grall, *New Methodology for Improving the Inspection Policies for Degradation Model Selection According to Prognostic Measures*, IEEE Transactions on Reliability **67** (2018), no. 3, 1269–1280.

[80] S. A. Niknam, R. Acosta-Amado, and J. E. Kobza, *A value-based maintenance strategy for systems under imperfect repair and continuous degradation*, 2017 Annual Reliability and Maintainability Symposium (RAMS), January 2017, Journal Abbreviation: 2017 Annual Reliability and Maintainability Symposium (RAMS), pp. 1–6.

[81] M. Oumouni and F. Schoefs, *A Perturbed Markovian process with state-dependent increments and measurement uncertainty in degradation modeling*, Computer-Aided Civil and Infrastructure Engineering **36** (2021), no. 8, 978–995, Publisher: John Wiley & Sons, Ltd.

[82] C. S. Peirce, *A theory of probable inference*, (1883), Publisher: Little, Brown and Co.

[83] R. D. Richtmyer, *The evaluation of definite integrals, and a quasi-Monte-Carlo method based on the properties of algebraic numbers*, Tech. report, Los Alamos National Lab.(LANL), Los Alamos, NM (United States), 1951.

[84] M. A. Rodríguez, *Corrosion control of nuclear steam generators under normal operation and plant-outage conditions: a review*, **38** (2020), no. 3, 195–230.

[85] M. B. Salem, M. Fouladirad, and E. Deloux, *Variance Gamma process as degradation model for prognosis and imperfect maintenance of centrifugal pumps*, Reliability Engineering & System Safety **223** (2022), 108417.

[86] G. Salles, *On the modelling and statistical analysis of a gamma deteriorating system with imperfect maintenance*, Phd thesis, Université de Pau et des Pays de l'Adour, October 2020.

[87] G. Salles, S. Mercier, and L. Bordes, *Semiparametric estimate of the efficiency of imperfect maintenance actions for a Gamma deteriorating system*, Journal of Statistical Planning and Inference **206** (2020), 278–297.

[88] N. A.F Smith, *The failure of the bouzey dam in 1895*, Dams. (2017).

[89] W. L. Smith, *Regenerative stochastic processes*, Proceedings of the Royal Society of London. Series A. Mathematical and Physical Sciences **232** (1955), no. 1188, 6–31, ISBN: 0080-4630 Publisher: The Royal Society London.

[90] L. J. P. Speijker, J. M. Van Noortwijk, M. Kok, and R. M. Cooke, *Optimal maintenance decisions for dikes*, Probability in the Engineering and Informational Sciences

14 (2000), no. 1, 101–121, Edition: 2000/01/01 Publisher: Cambridge University Press.

[91] A. S. B. Tam, W. M. Chan, and J. W. H. Price, *Optimal maintenance intervals for a multi-component system*, Production Planning & Control **17** (2006), no. 8, 769–779, Publisher: Taylor & Francis.

[92] P. D. Van and C. Bérenguer, *Condition-Based Maintenance with Imperfect Preventive Repairs for a Deteriorating Production System*, Quality and Reliability Engineering International **28** (2012), no. 6, 624–633.

[93] J. M. Van Noortwijk, *A survey of the application of Gamma processes in maintenance*, Reliability Engineering & System Safety **94** (2009), no. 1, 2–21.

[94] J. Wang, G. Bai, Z. Li, and M. J. Zuo, *A general discrete degradation model with fatal shocks and age- and state-dependent nonfatal shocks*, Reliability Engineering & System Safety **193** (2020), 106648.

[95] X. Wang, O. Gaudoin, L. Doyen, C. Bérenguer, and M. Xie, *Modeling multivariate degradation processes with time-variant covariates and imperfect maintenance effects*, Applied Stochastic Models in Business and Industry **37** (2021), 592 – 611.

[96] X. Wang and D. Xu, *An Inverse Gaussian Process Model for Degradation Data*, Technometrics **52** (2010), no. 2, 188–197.

[97] L. Wasserman, *All of statistics: a concise course in statistical inference*, Springer Science & Business Media, 2013.

[98] G. A. Whitmore, *Estimating degradation by a Wiener diffusion process subject to measurement error*, Lifetime Data Analysis **1** (1995), no. 3, 307–319.

[99] F. Wu, Seyed A. Niknam, and John E. Kobza, *A cost effective degradation-based maintenance strategy under imperfect repair*, Reliability Engineering & System Safety **144** (2015), 234–243.

[100] D. Xuping, S. Hongsheng, and W. Dantong, *State Maintenance Strategy of Wind Turbine Based on Stochastic Degradation Model*, 2020 Chinese Control And Decision Conference (CCDC), August 2020, Journal Abbreviation: 2020 Chinese Control And Decision Conference (CCDC), pp. 4537–4543.

[101] Z. S. Ye and N. Chen, *The Inverse Gaussian Process as a Degradation Model*, Technometrics **56** (2014), no. 3, 302–311.

[102] Z.S. Ye, N. Chen, and Y. Shen, *A new class of Wiener process models for degradation analysis*, Reliability Engineering & System Safety **139** (2015), 58–67, Publisher: Elsevier.

[103] Q. Zhai, Z.-S. Ye, J. Yang, and Y. Zhao, *Measurement errors in degradation-based burn-in*, Reliability Engineering & System Safety **150** (2016), 126–135.

[104] M. Zhang, O. Gaudoin, and M. Xie, *Degradation-based maintenance decision using stochastic filtering for systems under imperfect maintenance*, European Journal of Operational Research **245** (2015), no. 2, 531–541.

[105] X. Zhang and H. Gao, *Road maintenance optimization through a discrete-time semi-Markov decision process*, Reliability Engineering & System Safety **103** (2012), 110–119.

[106] Y. Zhang, J. Liu, H. Hanachi, X. Yu, and Y. Yang, *Physics-based Model and Neural Network Model for Monitoring Starter Degradation of APU*, 2018 IEEE International Conference on Prognostics and Health Management (ICPHM), June 2018, Journal Abbreviation: 2018 IEEE International Conference on Prognostics and Health Management (ICPHM), pp. 1–7.

[107] Z. Zhang, X. Si, C. Hu, and Y. Lei, *Degradation data analysis and remaining useful life estimation: A review on Wiener-process-based methods*, European Journal of Operational Research **271** (2018), no. 3, 775–796, Publisher: Elsevier.

[108] X. Zhao, P. Chen, O. Gaudoin, and L. Doyen, *Accelerated degradation tests with inspection effects*, European Journal of Operational Research **292** (2021), no. 3, 1099–1114.

[109] X. Zhao, O. Gaudoin, L. Doyen, and M. Xie, *Optimal inspection and replacement policy based on experimental degradation data with covariates*, IISE Transactions **51** (2019), no. 3, 322–336.

[110] X. Zhao, S. He, and M. Xie, *Utilizing experimental degradation data for warranty cost optimization under imperfect repair*, Reliability Engineering & System Safety **177** (2018), 108–119.

[111] W. Zhu, M. Fouladirad, and C. Bérenguer, *Condition-based maintenance policies for a combined wear and shock deterioration model with covariates*, Computers & Industrial Engineering **85** (2015), 268–283.

Chapter A

Appendices

A.1 Maximum likelihood estimator of μ in the third observation scheme

The maximum likelihood estimator of μ in the third observation scheme is given by Equation (2.23):

$$\hat{\mu} = \frac{1}{t_{k,n_k}} \left[\sum_{j=1}^{k+1} \sum_{i=1}^{n_j} \Delta Y_{j,i} \; + \; \frac{1}{1-\hat{\rho}} \sum_{j=1}^{k} \left(Z_j^3 + \hat{\rho} \sum_{i=1}^{n_j} \Delta Y_{j,i} \right) \right]$$

We have $$\frac{1}{1-\hat{\rho}} \sum_{j=1}^{k} Z_j^3 \; = \; \frac{\hat{\rho}}{1-\hat{\rho}} \sum_{j=1}^{k} Z_j^3 + \sum_{j=1}^{k} Z_j^3$$

Furthermore $$Y(\tau_k^+) = \sum_{j=1}^{k} \sum_{i=1}^{n_j} \Delta Y_{j,i} + \sum_{j=1}^{k} Z_j^3$$

$$Y(t_{k,n_k}) = \sum_{j=1}^{k+1} \sum_{i=1}^{n_j} \Delta Y_{j,i} + \sum_{j=1}^{k} Z_j^3$$

Thus, $$\hat{\mu} = \frac{1}{t_{k,n_k}} \left[Y(t_{k,n_k}) + \frac{\hat{\rho}}{1-\hat{\rho}} Y(\tau_k^+) \right]$$

A.2 Biases of the parameter estimators

Some of the model parameters estimators computed in Section 2.2 are biased. These eventual biases are computed below according to each observation scheme.

Complete observation scheme

The expressions for the estimators in the complete observation scheme are provided in Equation (2.9) and Equation (2.10).

$$\mathbb{E}[\hat{\mu}] = \frac{\sum_{j=1}^{k+1} \sum_{i=1}^{n_j+1} \mathbb{E}\left[\Delta Y_{j,i}\right]}{\tau} = \mu$$

and,

$$\hat{\sigma}^2 = \frac{1}{N+k+1} \left[\sum_{j=1}^{k+1} \sum_{i=1}^{n_j+1} \frac{\Delta Y_{j,i}^2}{\Delta t_{j,i}} + \hat{\mu}^2 \sum_{j=1}^{k+1} \sum_{i=1}^{n_j+1} \Delta t_{j,i} - 2\, \hat{\mu} \sum_{j=1}^{k+1} \sum_{i=1}^{n_j+1} \Delta Y_{j,i} \right]$$

We have $\sum_{j=1}^{k+1} \sum_{i=1}^{n_j+1} \Delta t_{j,i} = \tau$ and $\sum_{j=1}^{k+1} \sum_{i=1}^{n_j+1} \Delta Y_{j,i} = \hat{\mu}\, \tau$. Therefore,

$$\hat{\sigma}^2 = \frac{1}{N+k+1} \left[\sum_{j=1}^{k+1} \sum_{i=1}^{n_j+1} \frac{\Delta Y_{j,i}^2}{\Delta t_{j,i}} - \hat{\mu}^2\, \tau \right]$$

$$\mathbb{E}[\hat{\sigma}^2] = \frac{1}{N+k+1} \left[\sum_{j=1}^{k+1} \sum_{i=1}^{n_j+1} \frac{\mathbb{E}[\Delta Y_{j,i}^2]}{\Delta t_{j,i}} - \mathbb{E}[\hat{\mu}^2]\, \tau \right]$$

We have $\mathbb{E}[\Delta Y_{j,i}^2] = \sigma^2 \Delta t_{j,i} + \mu^2 \Delta t_{j,i}^2$ and $\mathbb{E}[\hat{\mu}^2] = \frac{\sigma^2}{\tau} + \mu^2$, thereby,

$$\mathbb{E}[\hat{\sigma}^2] = \frac{1}{N+k+1} \left[\sigma^2 (N+k+1) - \mu^2 \tau - \sigma^2 + \mu^2 \tau \right] \;=\; \frac{N+k}{N+k+1} \sigma^2$$

Therefore, $\hat{\sigma}^2$ is a biased estimator and $\tilde{\sigma}^2 = \dfrac{N+k+1}{N+k}\, \hat{\sigma}^2$ is an unbiased estimator of σ^2.

Second observation scheme

The maximum likelihood estimator of μ in the second observation scheme is given by Equation (2.16) and Equation (2.18).

$$\hat{\mu} = \frac{1}{\tau}\left[\sum_{j=1}^{k+1}\sum_{i=1+\mathbb{1}_{j>1}}^{n_j+1}\Delta Y_{j,i} + \sum_{j=1}^{k} Y(t_{j,1}) - Y(\tau_j^-) + \hat{\rho}\sum_{j=1}^{k} Y(\tau_j^-) - (1-\hat{\rho})\sum_{j=1}^{k}\sum_{i=0}^{j-1}\hat{\rho}^{j-i}Y(\tau_i^-)\right]$$

We have,

$$\forall i \in \{1+\mathbb{1}_{j>1}, ..., n_j+1\},\ \forall j \in \{1, ..., k+1\},\ \ \mathbb{E}[\Delta Y_{j,i}] = \mu\Delta t_{j,i}$$

and

$$\mathbb{E}[Y(t_{j,1}) - Y(\tau_j^-)|\mathcal{O}^2_{\tau_j^-}] = \mu\Delta t_{j,1} - \hat{\rho}y(\tau_j^-) + (1-\hat{\rho})\sum_{i=1}^{j-1}\hat{\rho}^{j-1}y(\tau_i^-)$$

Then,

$$\mathbb{E}[\hat{\mu}] = \frac{1}{\tau}\left[\mu\sum_{j=1}^{k+1}\sum_{i=1+\mathbb{1}_{j>1}}^{n_j+1}\Delta t_{j,i} + \mu\sum_{j=1}^{k}\Delta t_{j,1}\right] = \mu$$

Thus, $\hat{\mu}$ is an unbiased estimator of μ in the second observation scheme.
The maximum likelihood estimator of σ^2 in the second observation scheme is given by Equation (2.18). Given that degradation increments are independent and that they are also independent of jumps given previous observations, we have:

$$\begin{aligned}\mathbb{V}[\hat{\mu}] &= \frac{1}{\tau^2}\left[\sum_{j=1}^{k+1}\sum_{i=1+\mathbb{1}_{j>1}}^{n_j+1}\mathbb{V}[\Delta Y_{j,i}] + \sum_{j=1}^{k}\mathbb{V}[Y(t_{j,1}) - Y(\tau_j^-) + \hat{\rho}y(\tau_j^-) - (1-\hat{\rho})\sum_{i=1}^{j-1}\hat{\rho}^{j-1}y(\tau_i^-)|\mathcal{O}^2_{\tau_j^-}]\right] \\ &= \frac{1}{\tau^2}\left[\sigma^2\sum_{j=1}^{k+1}\sum_{i=1+\mathbb{1}_{j>1}}^{n_j+1}\Delta t_{j,i} + \sigma^2\sum_{j=1}^{k}\Delta t_{j,1}\right] = \frac{\sigma^2}{\tau}\end{aligned}$$

Let us denote (A) and (B) such that $\hat{\sigma}^2 = (A) + (B)$:

$$
\begin{aligned}
(A) =& \frac{1}{N+k+1} \sum_{j=1}^{k+1} \sum_{i=1+\mathbb{1}_{j>1}}^{n_j+1} \frac{\left(\Delta Y_{j,i} - \hat{\mu}\ \Delta t_{j,i}\right)^2}{\Delta t_{j,i}} \\
=& \frac{1}{N+k+1} \left[\sum_{j=1}^{k+1} \sum_{i=1+\mathbb{1}_{j>1}}^{n_j+1} \frac{\Delta Y_{j,i}^2}{\Delta t_{j,i}} + \hat{\mu}^2 \sum_{j=1}^{k+1} \sum_{i=1+\mathbb{1}_{j>1}}^{n_j+1} \Delta t_{j,i} - 2\hat{\mu} \sum_{j=1}^{k+1} \sum_{i=1+\mathbb{1}_{j>1}}^{n_j+1} \Delta Y_{j,i} \right] \\
(B) =& \frac{1}{N+k+1} \sum_{j=1}^{k} \frac{\left(Y(t_{j+1,1}) - \hat{\mu}\ \Delta t_{j+1,1} - (1-\hat{\rho}) \sum_{i=0}^{j} \hat{\rho}^{j-i} Y(\tau_i^-) \right)^2}{\Delta t_{j+1,1}} \\
=& \frac{1}{N+k+1} \left[\hat{\mu}^2 \sum_{j=1}^{k} \Delta t_{j+1,1} + \sum_{j=1}^{k} \frac{\left(Y(t_{j+1,1}) - Y(\tau_j^-) + \hat{\rho} Y(\tau_j^-) - (1-\hat{\rho}) \sum_{i=0}^{j-1} \hat{\rho}^{j-i} Y(\tau_i^-) \right)^2}{\Delta t_{j+1,1}} \right. \\
& \left. - 2\hat{\mu} \sum_{j=1}^{k} \left(Y(t_{j+1,1}) - Y(\tau_j^-) + \hat{\rho}\ Y(\tau_j^-) - (1-\hat{\rho}) \sum_{i=0}^{j-1} \hat{\rho}^{j-i} Y(\tau_i^-) \right) \right]
\end{aligned}
$$

Then,

$$
\begin{aligned}
\hat{\sigma}^2 =& (A) + (B) \\
=& \frac{1}{N+k+1} \left[\sum_{j=1}^{k+1} \sum_{i=1+\mathbb{1}_{j>1}}^{n_j+1} \frac{\Delta Y_{j,i}^2}{\Delta t_{j,i}} + \sum_{j=1}^{k} \frac{\left(Y(t_{j+1,1}) - Y(\tau_j^-) + \hat{\rho} Y(\tau_j^-) - (1-\hat{\rho}) \sum_{i=0}^{j-1} \hat{\rho}^{j-i} Y(\tau_i^-) \right)^2}{\Delta t_{j+1,1}} \right. \\
& \left. - \hat{\mu}^2 \tau \right]
\end{aligned}
$$

Furthermore, based on the previous writing of $\hat{\sigma}^2$, we have:

$$\mathbb{E}[\Delta Y_{j,i}^2] = \mathbb{V}[\Delta Y_{j,i}] + \mathbb{E}[\Delta Y_{j,i}]^2 = \sigma^2 \Delta t_{j,i} + \mu^2 \Delta t_{j,i}^2$$

$$\text{and } \mathbb{E}[\big(Y(t_{j+1,1}) - Y(\tau_j^-) + \hat{\rho} Y(\tau_j^-) - (1-\hat{\rho}) \sum_{i=0}^{j-1} \hat{\rho}^{j-i} Y(\tau_i^-) | \mathcal{O}_j^2\big)^2]$$

$$= \mathbb{V}[Y(t_{j+1,1}) - Y(\tau_j^-) | \mathcal{O}_j^2] + \mathbb{E}[Y(t_{j+1,1}) - Y(\tau_j^-) + \hat{\rho} Y(\tau_j^-) - (1-\hat{\rho}) \sum_{i=0}^{j-1} \hat{\rho}^{j-i} Y(\tau_i^-) | \mathcal{O}_j^2]^2$$

$$= \sigma^2 \Delta t_{j+1,1} + \mu^2 \Delta t_{j,1}^2$$

$$\mathbb{E}[\hat{\mu}^2] = \mathbb{V}[\hat{\mu}] + \mathbb{E}[\hat{\mu}]^2 = \frac{\sigma^2}{\tau} + \mu^2$$

$$\text{Thus, } \mathbb{E}[\hat{\mu}^2] = \frac{1}{N+k+1} \left[\sigma^2 (1+N) + \mu^2 \sum_{j=1}^{k+1} \sum_{i=1+\mathbb{1}_{j>1}}^{n_j+1} \Delta t_{j,i} + \sigma^2 k + \mu^2 \sum_{j=1}^{k} \Delta t_{j+1,1} - \sigma^2 - \mu^2 \tau \right]$$

$$\mathbb{E}[\hat{\sigma}] = \sigma^2 \frac{k+N}{k+1+N}$$

Thus, $\hat{\sigma}^2$ is biased and an unbiased estimator of σ^2 is $\tilde{\sigma^2} = \frac{k+N+1}{k+N} \hat{\sigma}^2$.

Third observation scheme

The expressions for the estimators in the third observation scheme are provided in Equation (2.23) and Equation (2.24).

$$\mathbb{E}[Y(\tau_j^+) - Y(t_{j,n_j}) | O_{t_{j,n_j}}^3] = \mu(1-\rho) \Delta t_{j,n_j+1} - \hat{\rho} \sum_{i=1}^{n_j} \Delta y_{j,i}$$

$$\text{Then, } \mathbb{E}[\hat{\mu} | \mathcal{O}_{t_{j,n_j}}^3] = \frac{1}{t_{k+1,n_{k+1}}} \left[\mu \sum_{j=1}^{k+1} \sum_{i=1}^{n_j} \Delta Y_{j,i} + \mu \sum_{j=1}^{k} \Delta t_{j,n_j+1} \right] = \mu$$

Therefore, $\hat{\mu}$ is unbiased in the third observation scheme.
Based on Equation (2.24), and given that the degradation increments are independent and that they are also independent of jumps given previous observations, we have:

$$\mathbb{V}[\hat{\mu}] = \frac{1}{t_{k+1,n_k+1}} \left[\sum_{j=1}^{k+1} \sum_{i=1}^{n_j} \mathbb{V}\left[\Delta Y_{j,i}\right] + \frac{1}{(1-\hat{\rho})^2} \sum_{j=1}^{k} \mathbb{V}\left[Y(\tau_j^+) - Y(t_{j,n_j}) + \hat{\rho} \sum_{i=1}^{n_j} \Delta Y_{j,i} | \mathcal{O}^3_{t_{j,n_j}} \right] \right]$$

$$\begin{aligned} \text{Then, } \mathbb{V}[\hat{\sigma}^2] =& \frac{\sigma^2}{t^2_{k+1,n_{k+1}}} \sum_{j=1}^{k+1} \sum_{i=1}^{n_j} \Delta t_{j,i} + \sum_{j=1}^{k} \Delta t_{j,n_j+1} \\ =& \frac{\sigma^2}{t_{k+1,n_{k+1}}} \end{aligned}$$

Let us develop the writing of $\hat{\sigma}^2$ written in Equation (2.24):

$$\begin{aligned} \hat{\sigma}^2 =& \frac{1}{N+k} \left[\sum_{j=1}^{k+1} \sum_{i=1}^{n_j} \frac{\Delta Y^2_{j,i}}{\Delta t_{j,i}} + \hat{\mu}^2 \sum_{j=1}^{k+1} \sum_{i=1}^{n_j} \Delta t_{j,i} - 2\hat{\mu} \sum_{j=1}^{k+1} \sum_{i=1}^{n_j} \Delta Y_{j,i} \right. \\ & + \sum_{j=1}^{k} \frac{\left(Y(\tau_j^+) - Y(t_{j,n_j}) + \hat{\rho} \sum_{i=1}^{n_j} \Delta y_{j,i} \right)^2}{(1-\hat{\rho})^2 \Delta t_{j,n_j+1}} \\ & + \hat{\mu}^2 \sum_{j=1}^{k} \Delta t_{j,n_j+1} \\ & \left. - 2\frac{\hat{\mu}}{1-\hat{\rho}} \sum_{j=1}^{k} \left[Y(\tau_j^+) - Y(t_{j,n_j}) + \hat{\rho} \sum_{i=1}^{n_j} \Delta y_{j,i} \right] \right] \\ =& \frac{1}{N+k} \left[\sum_{j=1}^{k+1} \sum_{i=1}^{n_j} \frac{\Delta Y^2_{j,i}}{\Delta t_{j,i}} + \sum_{j=1}^{k} \frac{\left(Y(\tau_j^+) - Y(t_{j,n_j}) + \hat{\rho} \sum_{i=1}^{n_j} \Delta y_{j,i} \right)^2}{(1-\hat{\rho})^2 \Delta t_{j,n_j+1}} - \hat{\mu}^2 \, t_{k+1,n_{k+1}} \right] \end{aligned}$$

Knowing that,

$$
\begin{aligned}
\mathbb{E}[\Delta Y_{j,i}^2] =& \sigma^2 \Delta t_{j,i} + \mu^2 \Delta t_{j,i}^2 \\
\mathbb{E}\big[\big(\big(Y(\tau_j^+) - Y(t_{j,n_j}) + \hat{\rho} \sum_{i=1}^{n_j} \Delta y_{j,i}\big)^2 | \mathcal{O}^3_{t_{j,n_j}}\big] =& \mathbb{V}[Y(\tau_j^+) - Y(t_{j,n_j})] + \mathbb{E}\big[Y(\tau_j^+) - Y(t_{j,n_j}) + \hat{\rho} \sum_{i=1}^{n_j} \Delta y_{j,i}\big]^2 \\
=& \sigma^2 (1-\hat{\rho})^2 \Delta t_{j,n_j+1} + \mu^2 (1-\hat{\rho})^2 \Delta t_{j,n_j+1}^2 \\
\mathbb{E}[\hat{\mu}^2] =& \frac{\sigma^2}{t_{k+1,n_{k+1}}} + \mu^2
\end{aligned}
$$

One can easily write $\mathbb{E}[\hat{\sigma}^2]$ in the third observation scheme:

$$
\begin{aligned}
\mathbb{E}[\hat{\sigma}^2] =& \frac{1}{k+N} \left[\sigma^2 \ N + \mu^2 \sum_{j=1}^{k+1} \sum_{i=1}^{n_j} \Delta t_{j,i} + \sigma^2 \ k + \mu^2 \sum_{j=1}^{k} \Delta t_{j,n_j+1} - \sigma^2 - \mu^2 t_{k+1,n_{k+1}} \right] \\
=& \frac{k+N-1}{k+N} \sigma^2
\end{aligned}
$$

Hence, $\hat{\sigma}^2$ is biased and an unbiased estimator of σ^2 would be $\tilde{\sigma^2} = \frac{k+N}{k+N-1} \hat{\sigma}^2$.

General observation scheme

The expressions of the estimators in the general observation scheme is given by Equation (2.32) and Equation (2.33). We have,

$\mathbb{E}[\Delta \tilde{Z}^g | \mathcal{O}^g_{\tau_j}] = \mu u - v$ and,

$$
\begin{aligned}
\mathbb{E}[\hat{\mu}] =& \frac{u(\hat{\rho})^t \ \Sigma^{-1}(\hat{\rho}) \ v(\hat{\rho}) + u(\hat{\rho})^t \ \Sigma^{-1} \mathbb{E}[\Delta \tilde{Z}^g | \mathcal{O}^g_{\tau_j}] + \sum_{j=1}^{k+1} \sum_{i=1+\mathbb{1}_{j>1}}^{n_j} \mathbb{E}[\Delta Y_{j,i}]}{u(\hat{\rho})^t \Sigma^{-1}(\hat{\rho}) u(\hat{\rho}) + \sum_{j=1}^{k+1} \sum_{i=1+\mathbb{1}_{j>1}}^{n_j} \Delta t_{j,i}} \\
=& \frac{u(\hat{\rho})^t \ \Sigma^{-1}(\hat{\rho}) \ v(\hat{\rho}) + u(\hat{\rho})^t \ \Sigma^{-1}(\hat{\rho}) (\mu u(\hat{\rho}) - v(\hat{\rho})) + \mu \sum_{j=1}^{k+1} \sum_{i=1+\mathbb{1}_{j>1}}^{n_j} \Delta t_{j,i}}{u(\hat{\rho})^t \Sigma^{-1}(\hat{\rho}) u(\hat{\rho}) + \sum_{j=1}^{k+1} \sum_{i=1+\mathbb{1}_{j>1}}^{n_j} \Delta t_{j,i}} = \mu
\end{aligned}
$$

Then $\hat{\mu}$ is an unbiased estimator of μ.

Furthermore, based on Equation (2.32), we have,

$$\mathbb{V}[\hat{\mu}] = \frac{\mathbb{V}[u(\hat{\rho})^t\ \Sigma^{-1}(\hat{\rho})Z^g] + \sum_{j=1}^{k+1}\sum_{i=1+\mathbb{1}_{j>1}}^{n_j}\mathbb{V}[\Delta Y_{j,i}]}{\left(u(\hat{\rho})^t\ \Sigma^{-1}(\hat{\rho})u(\hat{\rho}) + \sum_{j=1}^{k+1}\sum_{i=1+\mathbb{1}_{j>1}}^{n_j}\Delta t_{j,i}\right)^2}$$

Since degradation increments are independent to each other, and they are independent from the jumps given the previous observations, we have,

$$\mathbb{V}[\hat{\mu}] = \sigma^2\frac{u(\hat{\rho})^t\ \Sigma^{-1}(\hat{\rho})\Sigma\hat{\rho})\Sigma^{-1^t}\hat{\rho}u(\hat{\rho})+)\sum_{j=1}^{k+1}\sum_{i=1+\mathbb{1}_{j>1}}^{n_j}\Delta t_{j,i}}{\left(u(\hat{\rho})^t\ \Sigma^{-1}(\hat{\rho})u(\hat{\rho}) + \sum_{j=1}^{k+1}\sum_{i=1+\mathbb{1}_{j>1}}^{n_j}\Delta t_{j,i}\right)^2}$$

Then, since Σ is symmetric,

$$\mathbb{V}[\hat{\mu}] = \frac{\sigma^2}{u(\hat{\rho})^t\ \Sigma^{-1}(\hat{\rho})u(\hat{\rho}) + \sum_{j=1}^{k+1}\sum_{i=1+\mathbb{1}_{j>1}}^{n_j}\Delta t_{j,i}}$$

The expression of $\hat{\sigma}^2$, described in Equation (2.33), can be developed as follows.

$$\begin{aligned}\hat{\sigma}^2(\rho) = \frac{1}{N}\Big[&Z^{g^t}\Sigma^{-1}(\hat{\rho})Z^g - \hat{\mu}Z^{g^t}\Sigma^{-1}(\hat{\rho})u(\hat{\rho}) + Z^{g^t}\Sigma^{-1}(\hat{\rho})v(\hat{\rho})\\ &- \hat{\mu}u(\hat{\rho})^t\Sigma^{-1}(\hat{\rho})Z^g + \hat{\mu}^2u(\hat{\rho})^t\Sigma^{-1}(\hat{\rho})u(\hat{\rho}) - \hat{\mu}u(\hat{\rho})^t\Sigma^{-1}(\hat{\rho})v(\hat{\rho})\\ &+ v(\hat{\rho})^t\Sigma^{-1}(\hat{\rho})Z^g - \hat{\mu}v(\hat{\rho})^t\Sigma^{-1}(\hat{\rho})u(\hat{\rho}) + v(\hat{\rho})^t\Sigma^{-1}(\hat{\rho})v(\hat{\rho})\\ &+ \sum_{j=1}^{k+1}\sum_{i=1+\mathbb{1}_{j>1}}^{n_j}\frac{\Delta Y_{j,i}^2}{\Delta t_{j,i}} + \hat{\mu}^2\sum_{j=1}^{k+1}\sum_{i=1+\mathbb{1}_{j>1}}^{n_j}\Delta t_{j,i} - 2\hat{\mu}\sum_{j=1}^{k+1}\sum_{i=1+\mathbb{1}_{j>1}}^{n_j}\Delta Y_{j,i}\Big]\end{aligned}$$

Since $\Sigma^{-1}(\hat{\rho})$ is symmetric, $u(\hat{\rho})^t\Sigma^{-1}(\hat{\rho})Z^g = Z^{g^t}\Sigma^{-1}(\hat{\rho})u(\hat{\rho})$. Then, $-\hat{\mu}Z^{g^t}\Sigma^{-1}(\hat{\rho})u(\hat{\rho}) - \hat{\mu}u(\hat{\rho})\Sigma^{-1}(\hat{\rho})Z^g = -2\hat{\mu}u(\hat{\rho})\Sigma^{-1}(\hat{\rho})Z^g$. Furthermore, given Equation (2.32), we have,

$$\sum_{j=1}^{k+1}\sum_{i=1+\mathbb{1}_{j>1}}^{n_j}\Delta Y_{j,i}+u(\hat{\rho})^t\Sigma^{-1}(\hat{\rho})Z^g+u(\hat{\rho})^t\Sigma^{-1}(\hat{\rho})v(\hat{\rho})=\hat{\mu}\left(u(\hat{\rho})^t\Sigma^{-1}u(\hat{\rho})+\sum_{j=1}^{k+1}\sum_{i=1+\mathbb{1}_{j>1}}^{n_j}\Delta t_{j,i}\right)$$

Thus,

$$\begin{aligned}\hat{\sigma}^2(\rho)=&\frac{1}{N}\Big[Z^{g^t}\Sigma^{-1}(\hat{\rho})Z^g+2Z^{g^t}\Sigma^{-1}v(\hat{\rho})+v(\hat{\rho})^t\Sigma^{-1}v(\hat{\rho})\\&+\sum_{j=1}^{k+1}\sum_{i=1+\mathbb{1}_{j>1}}^{n_j}\frac{\Delta Y_{j,i}^2}{\Delta t_{j,i}}-\hat{\mu}^2\left(\sum_{j=1}^{k+1}\sum_{i=1+\mathbb{1}_{j>1}}^{n_j}\Delta t_{j,i}+u(\hat{\rho})^t\Sigma^{-1}u(\hat{\rho})\right)\Big]\end{aligned}$$

Then we compute $\mathbb{E}[\hat{\sigma}^2(\rho)]$ involving the following expectations,

$$\begin{aligned}\mathbb{E}[Z^{g^t}\Sigma^{-1}(\hat{\rho})v(\hat{\rho})]=\mathbb{E}[Z^{g^t}]\Sigma^{-1}v(\hat{\rho})&=(\hat{\mu}u(\hat{\rho})-v(\hat{\rho}))^t\Sigma^{-1}v(\hat{\rho})\\&=\mu u(\hat{\rho})^t\Sigma^{-1}v(\hat{\rho})-v(\hat{\rho})^t\Sigma^{-1}v(\hat{\rho})\\\mathbb{E}[\Delta Y_{j,i}^2]&=\mathbb{V}[\Delta Y_{j,i}]+\mathbb{E}[\Delta Y_{j,i}]^2=\sigma^2\Delta t_{j,i}+\mu^2\Delta t_{j,i}\\\mathbb{E}[\hat{\mu}^2]&=\mathbb{V}[\hat{\mu}]+\mathbb{E}[\mu]^2=\frac{\sigma^2}{u(\hat{\rho})^t\Sigma^{-1}u(\hat{\rho})+\sum_{j=1}^{k+1}\sum_{i=1+\mathbb{1}_{j>1}}^{n_j}\Delta t_{j,i}}+\mu^2\end{aligned}$$

Moreover, one can prove by induction that $\mathbb{E}[Z^{g^t}\Sigma^{-1}(\hat{\rho})Z^g]=Tr(\sigma^2\Sigma\Sigma^{-1})+\mathbb{E}[Z^{g^t}]\Sigma^{-1}(\hat{\rho})\mathbb{E}[Z^g]$, then,

$$\begin{aligned}\mathbb{E}[Z^{g^t}\Sigma^{-1}(\hat{\rho})Z^g]=&Tr(\sigma^2\Sigma\Sigma^{-1})+\mathbb{E}[Z^{g^t}]\Sigma^{-1}(\hat{\rho})\mathbb{E}[Z^g]\\=&\sigma^2Tr(\Sigma(\hat{\rho})\Sigma^{-1}(\hat{\rho}))+(\mu u(\hat{\rho})-v(\hat{\rho}))^t\Sigma^{-1}(\hat{\rho})(\mu u(\hat{\rho})-v(\hat{\rho}))\\=&\sigma^2k+\mu^2u(\hat{\rho})^t\Sigma^{-1}(\hat{\rho})u(\hat{\rho})-\mu u(\hat{\rho})^t\Sigma^{-1}(\hat{\rho})v(\hat{\rho})-\mu v(\hat{\rho})^t\Sigma^{-1}(\hat{\rho})u(\hat{\rho})+v(\hat{\rho})^t\Sigma^{-1}(\hat{\rho})v(\hat{\rho})\\=&\sigma^2k+\mu^2u(\hat{\rho})^t\Sigma^{-1}(\hat{\rho})u(\hat{\rho})-2\mu u(\hat{\rho})^t\Sigma^{-1}(\hat{\rho})v(\hat{\rho})+v(\hat{\rho})^t\Sigma^{-1}(\hat{\rho})v(\hat{\rho})\end{aligned}$$

Therefore,

$$\mathbb{E}[\hat{\sigma}^2] = \frac{1}{\sum_{j=1}^{k+1} n_j} \Bigg[\sigma^2 k + \mu^2 u(\hat{\rho})^t \Sigma^{-1}(\hat{\rho}) u(\hat{\rho}) - 2\mu u(\hat{\rho})^t \Sigma^{-1}(\hat{\rho}) v(\hat{\rho}) + v(\hat{\rho})^t \Sigma^{-1}(\hat{\rho}) v(\hat{\rho})$$
$$+ 2\mu u(\hat{\rho})^t \Sigma^{-1}(\hat{\rho}) v(\hat{\rho}) - 2 v(\hat{\rho})^t \Sigma^{-1}(\hat{\rho}) v(\hat{\rho}) + v(\hat{\rho})^t \Sigma^{-1}(\hat{\rho}) v(\hat{\rho})$$
$$+ \sigma^2 \Big(\sum_{j=1}^{k+1} -k \Big) + \mu^2 \sum_{j=1}^{k+1} \sum_{i=1+\mathbb{1}_{j>1}}^{n_j} \Delta t_{j,i} - \sigma^2 - \mu^2 \big(u(\hat{\rho})^t \Sigma^{-1}(\hat{\rho}) u(\hat{\rho}) + \sum_{j=1}^{k+1} \sum_{i=1+\mathbb{1}_{j>1}}^{n_j} \Delta t_{j,i} \big) \Bigg]$$

Thus, $\mathbb{E}[\hat{\sigma}^2] = \frac{(\sum_{j=1}^{k+1} n_j) - 1}{\sum_{j=1}^{k+1} n_j} \sigma^2$ and $\hat{\sigma}^2$ is biased. An unbiased estimator of σ^2 is $\frac{\sum_{j=1}^{k+1} n_j}{(\sum_{j=1}^{k+1} n_j) - 1} \sigma^2$.

A.3 Parameters initialization for the maximum likelihood estimation algorithm

Model's parameters are estimated by maximizing the log-likelihood with the Nelder-Mead algorithm. In most situations, this method is not really sensitive to its initialization. However, a good initialization provides a more efficient algorithm and avoids potential local minima. In order to provide an efficient initialization, we will use the remark made in Section 3.1.2 saying that (μ_S, σ_S^2) are closely linked to degradation increments while parameters $(\mu_M, \sigma_M^2, \rho)$ are closely linked to degradation jumps, so to maintenance efficiency. For the complete observation scheme with periodic maintenances of periodicity $\Delta\tau$, the initialization of the parameters is made as follows. The initial values of $(\mu_S, \sigma_S^2, \mu_M, \sigma_M^2, r_{SM}, \rho)$ will be denoted $(\mu_S^{(0)}, \sigma_S^{2\,(0)}, \mu_M^{(0)}, \sigma_M^{2\,(0)}, r_{SM}^{(0)}, \rho^{(0)})$.

- **Initialization of μ_S and σ_S^2.** A preliminary estimation of μ_S and σ_S^2 can be done by considering that only the degradation increments $\Delta Y_{j,i}^c$ are observed. These random variables are independent and have respectively the $\mathcal{N}\left(\mu_S \Delta t_{j,i},\ \sigma_S^2 \Delta t_{j,i}\right)$ distributions. So $\mu_S^{(0)}$ and $\sigma_S^{2\,(0)}$ will be the values of μ_S and σ_S^2 which maximize $L(\mu_S, \sigma_S^2) = \prod_j \prod_i f_{\Delta Y_{j,i}^c}(\Delta y_{j,i}^c)$. It is easy to show that:

$$\mu_S^{(0)} = \frac{\sum_{j=1}^{k+1}\sum_{i=1}^{n_j+1} \Delta y_{j,i}^c}{\sum_{j=1}^{k+1}\sum_{i=1}^{n_j+1} \Delta t_{j,i}} = \frac{y(\tau)}{\tau} \text{ and } {\sigma_S^2}^{(0)} = \frac{1}{N+k+1}\sum_{j=1}^{k+1}\sum_{i=1}^{n_j+1} \frac{(\Delta y_{j,i}^c - \mu_S^{(0)}\Delta t_{j,i})^2}{\Delta t_{j,i}},$$

where $N = \sum_{j=1}^{k+1} n_j$.

Note that for the perturbed ARD_1 model ($\mu_S = \mu_M = \mu$), $\mu_S^{(0)}$ is an estimator of μ.

- **Initialization of ρ and μ_M.** The jumps Z_j^c are independent and their respective distributions are $\mathcal{N}\left(-\rho\mu_M\Delta\tau\ ,\ \rho^2\sigma_M^2\Delta\tau\right)$. So $\forall\ j \in \{1,...,k\}$, $\mathbb{E}\left[\frac{Z_j^c}{\mu_M\Delta\tau}\right] = -\rho$. Therefore, for the Perturbed ARD_1 model, one can choose $\mu_M^{(0)} = \mu_S^{(0)}$ and $\rho^{(0)} = -\frac{1}{k\mu_M^{(0)}\Delta\tau}\sum_{j=1}^{k} z_j^c$. For the Partial replacement model, $\rho = 1$ so $\mu_M^{(0)} = -\frac{1}{k\Delta\tau}\sum_{j=1}^{k} z_j^c$.

- **Initialization of σ_M^2.** If only the jumps Z_j^c are observed, the likelihood is $L(\mu_M, \sigma_M^2, \rho) = \prod_{j=1}^{k} f_{Z_j^c}(z_j^c)$. It is easy to show that the parameter values which maximize this function are such that $\sigma_M^2 = \frac{1}{k\rho^2\Delta\tau}\sum_{j=1}^{k}(z_j^c+\rho\mu_M\Delta\tau)^2$. Therefore, for the Perturbed ARD_1 model, ${\sigma_M^2}^{(0)} = \frac{1}{k{\rho^{(0)}}^2\Delta\tau}\sum_{j=1}^{k}(z_j^c+\rho^{(0)}\mu_M^{(0)}\Delta\tau)^2$. And for the Partial replacement model, ${\sigma_M^2}^{(0)} = \frac{1}{k\Delta\tau}\sum_{j=1}^{k}(z_j^c+\mu_M^{(0)}\Delta\tau)^2$.

- **Initialization of r_{SM}.** Since $Z_j^c = -\rho\Delta X_j^M$ and $\Delta Y_j = \Delta X_j^S$, $\mathbb{C}ov\left(\frac{Z_j^c}{-\rho}, \Delta Y_j\right) = \mathbb{C}ov(\Delta X_j^M, \Delta X_j^S) = c_{SM}\Delta\tau$. Therefore, c_{SM} can be estimated by the empirical covariance between the $Z_j^c/(-\rho)$ and the $\Delta Y_j^c/\Delta\tau$:

$$c_{SM}^{(0)} = -\frac{1}{\Delta\tau\rho^{(0)}}\left[\frac{1}{k}\sum_{j=1}^{k} Z_j^c\Delta Y_j - \frac{1}{k^2}\sum_{j=1}^{k} Z_j^c\sum_{i=1}^{k}\Delta Y_i\right], \text{ and } r_{SM}^{(0)} = \frac{c_{SM}^{(0)}}{\sigma_S^{(0)}\sigma_M^{(0)}}.$$

A.4 Empirical stationary distribution based on different considered numbers of degradation levels

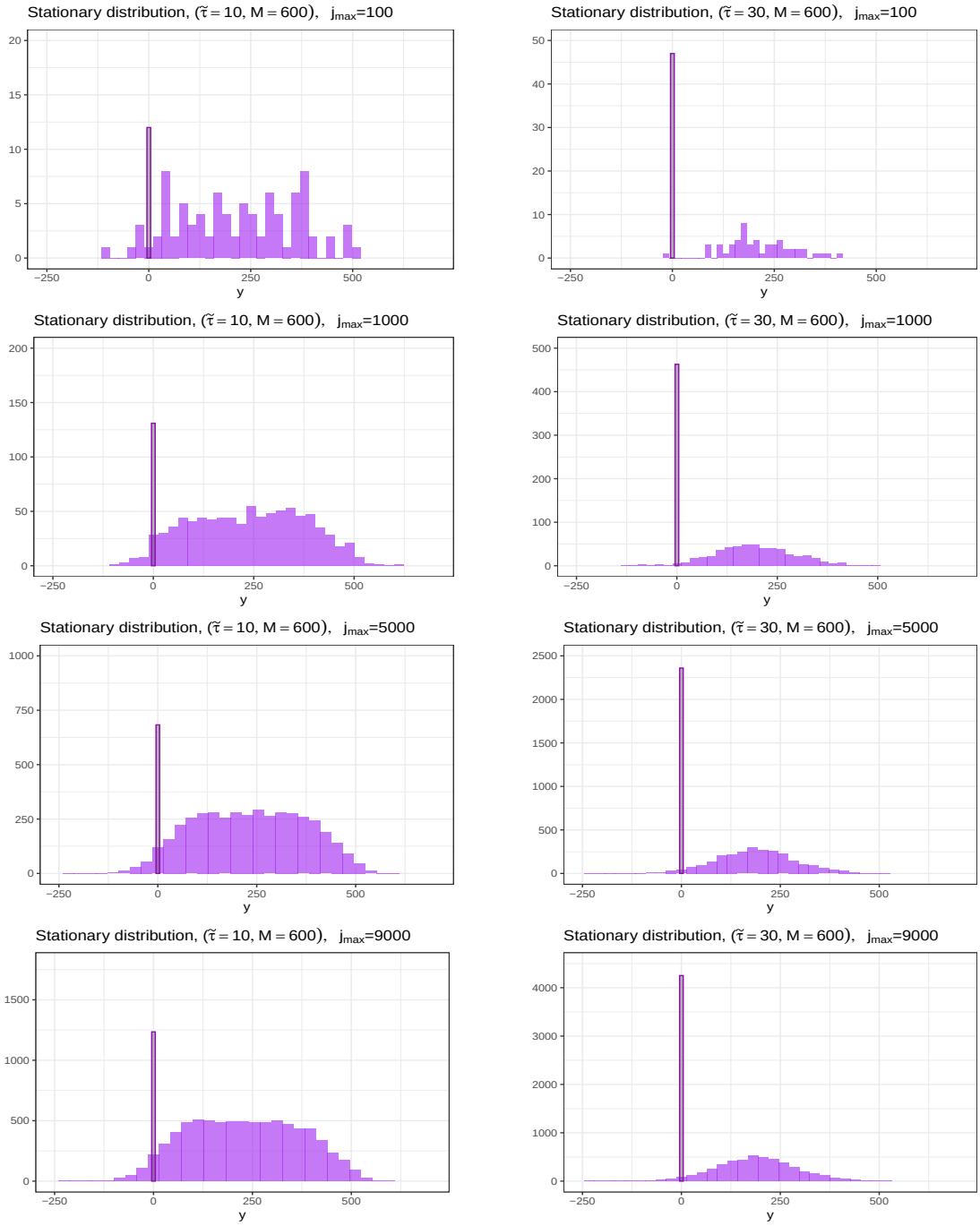

Appendix figure A.1: Histograms of the counts of post-maintenance degradation levels based on various numbers of degradation values and different inter-inspection periods: $\widetilde{\tau} \in \{10, 30\}$, $M = 600$ and $j_{max} = \{100, 1000, 5000, 9000\}$. For each presented stationary distribution, the underlying simulated degradation trajectories are based on the following model parameters: $\mu_U = 7, \mu_M = 10, \sigma_U^2 = 400, \sigma_M^2 = 600, r_{UM} = 0.7, \rho = 1$

A.5 Maintenance cost rates assessment based on different considered numbers of post-maintenance degradation levels

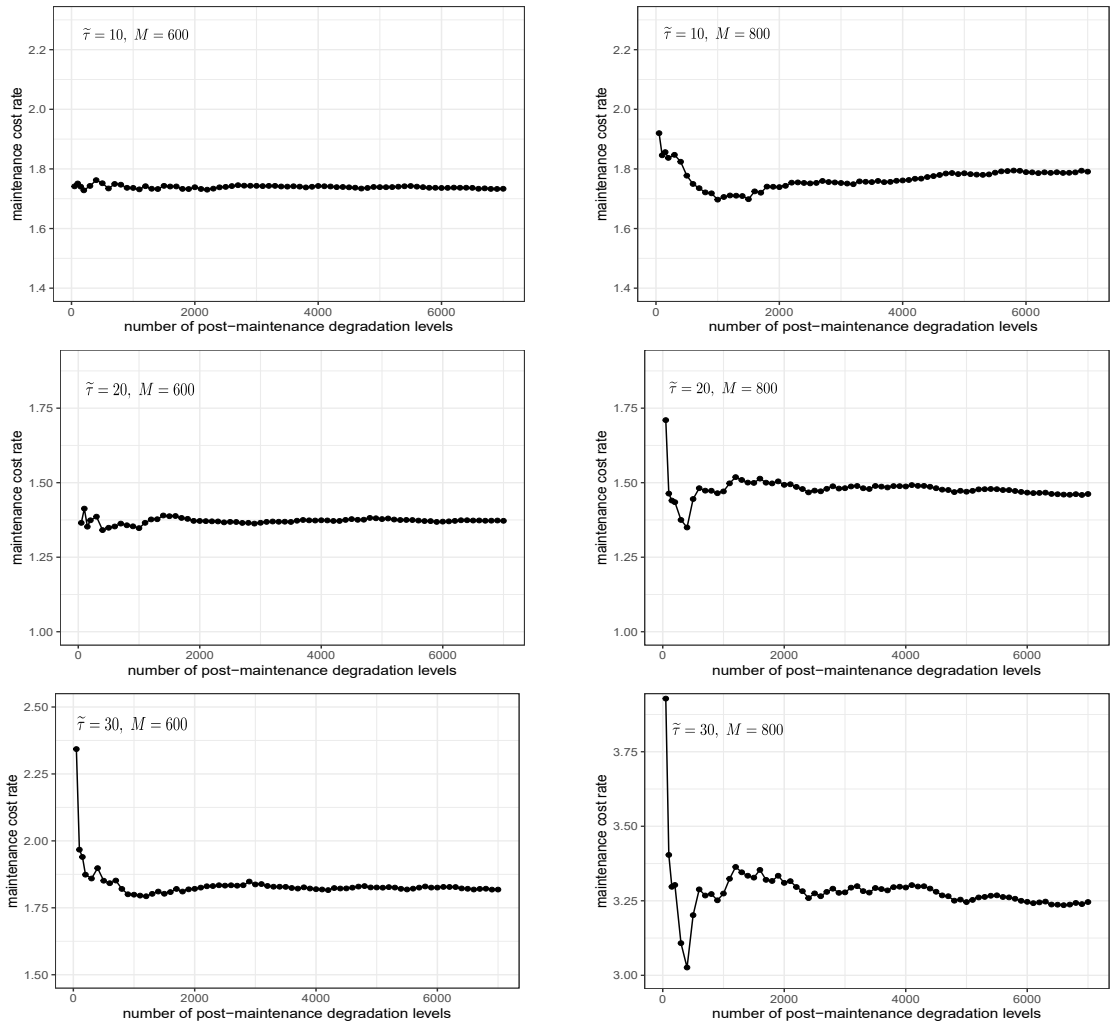

Appendix figure A.2: Various numbers of post-maintenance degradation levels are considered for assessing maintenance cost rates according to different values of $\widetilde{\tau} \in \{10, 20, 30\}$ and $M = \{600, 800\}$. For each cost rate assessment, the simulated degradation trajectories are based on the following set of model parameters: $\mu_U = 7, \mu_M = 10, \sigma_U^2 = 400, \sigma_M^2 = 600, r_{UM} = 0.7, \rho = 1$

A.6 Maintenance cost rates assessment based on different considered numbers of life cycles

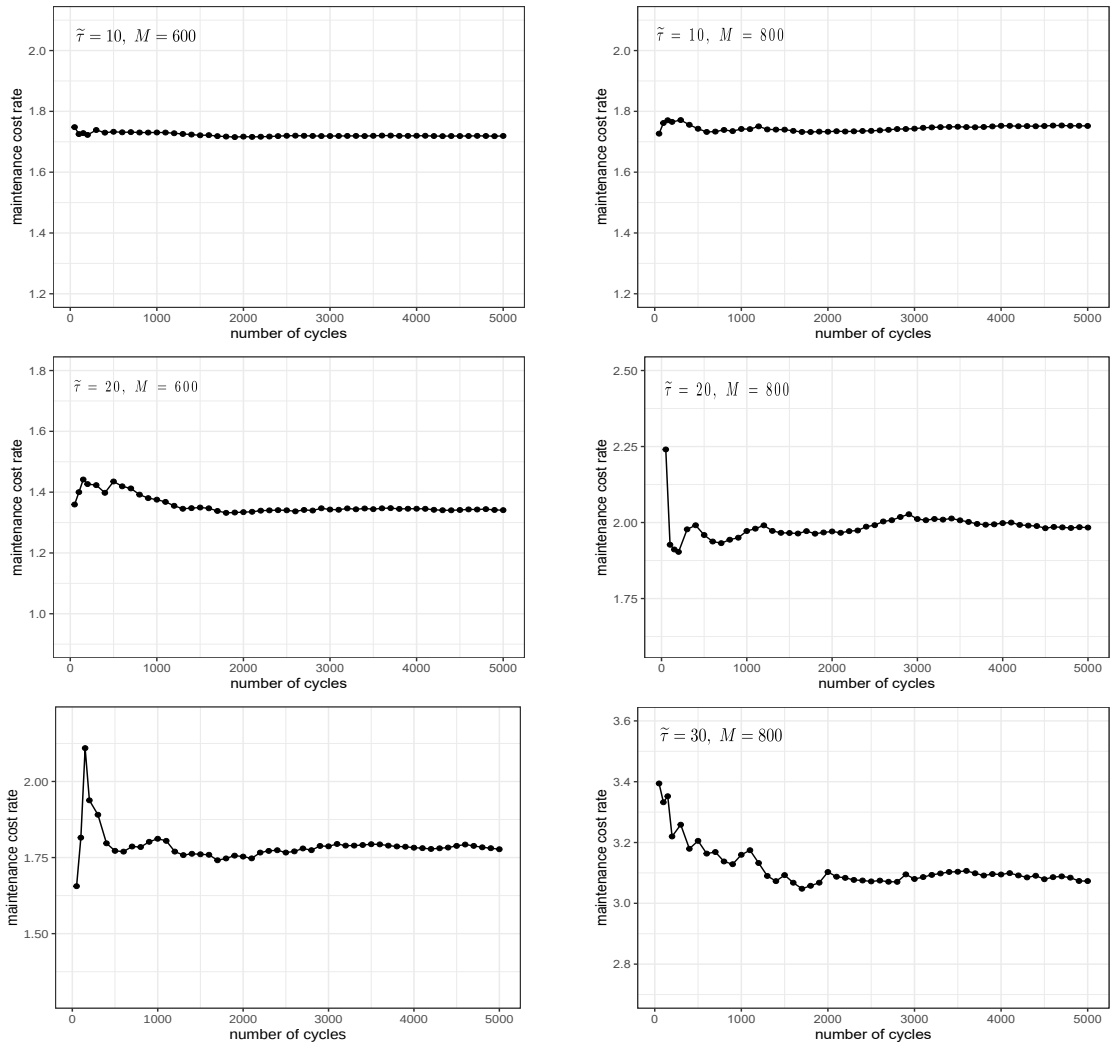

Appendix figure A.3: Various numbers of cycles are considered for assessing maintenance cost rates according to different values of $\widetilde{\tau} \in \{10, 20, 30\}$ and $M = \{600, 800\}$. For each cost rate assessment, the simulated degradation trajectories are based on the following set of model parameters: $\mu_U = 7, \mu_M = 10, \sigma_U^2 = 400, \sigma_M^2 = 600, r_{UM} = 0.7, \rho = 1$

A.7 Comparison between the different methods to assess the maintenance cost

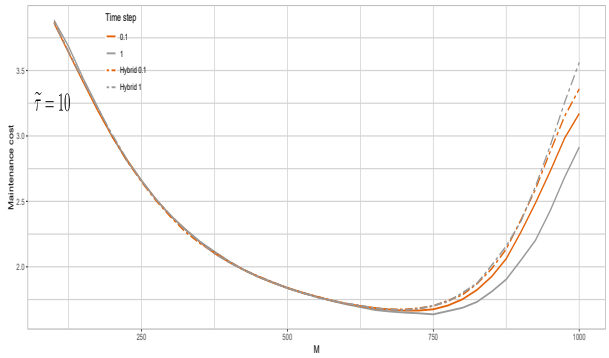

Appendix figure A.4: Long run average maintenance cost as a function of M, for $\widetilde{\tau} = 10$, according to both the purely simulation-based method and the hybrid method. The underlying simulated degradation trajectories are based on various time steps: 0.01 and 1.

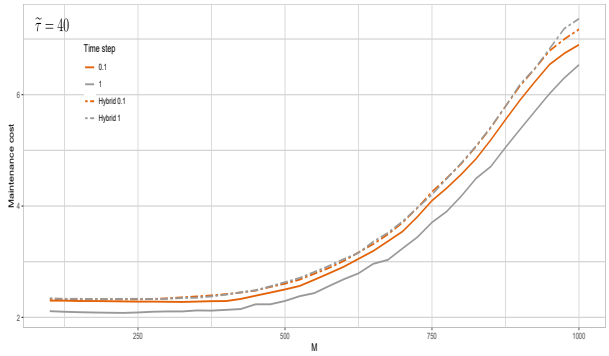

Appendix figure A.5: Long run average maintenance cost as a function of M, for $\widetilde{\tau} = 40$, according to both the purely simulation-based method and the hybrid method. The underlying simulated degradation trajectories are based on various time steps: 0.01 and 1.

A.8 Degradation trajectories

These following figures illustrate the initial ten degradation life cycles based on specific model parameters and a given $(\widetilde{\tau}, M)$ policy when degradation is inspected before repairs.

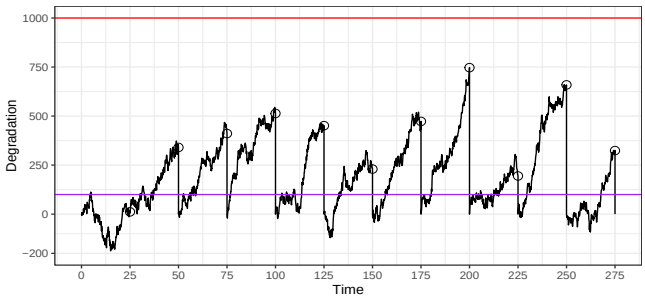

Figure A.6: Situation 4, $\tilde{\tau} = 25$, $M = 100$

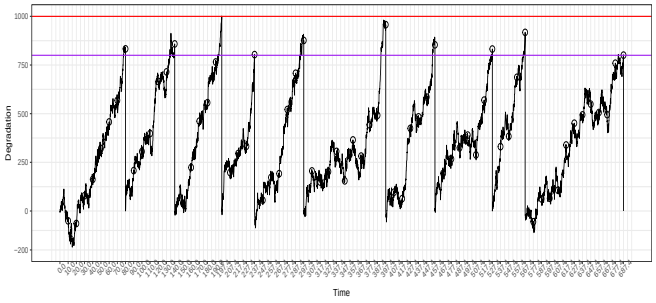

Figure A.9: Situation 4, $\tilde{\tau} = 10$, $M = 800$

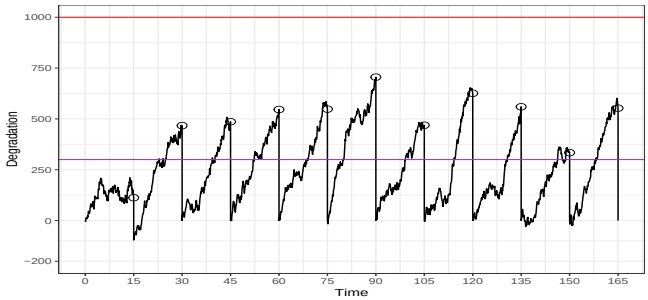

Figure A.7: Situation 3, $\tilde{\tau} = 15$, $M = 300$

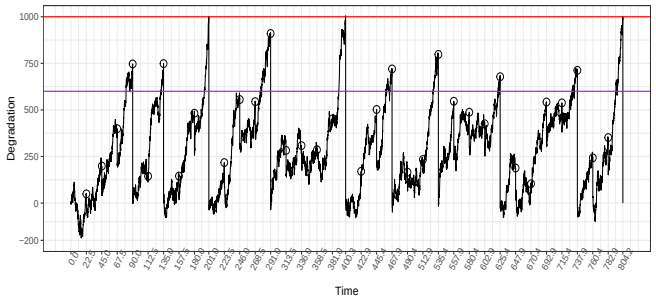

Figure A.10: Situation 1, $\tilde{\tau} = 22.5$, $M = 625$

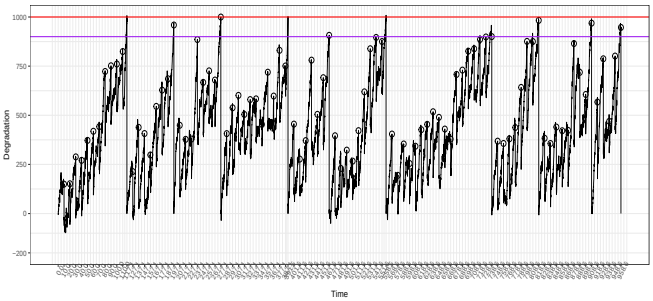

Figure A.8: Situation 3, $\tilde{\tau} = 10$, $M = 900$

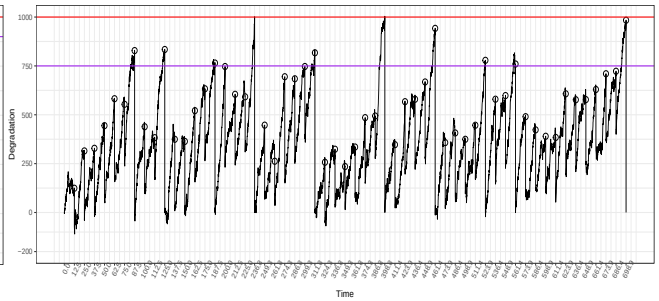

Figure A.11: Situation 3, $\tilde{\tau} = 12.5$, $M = 750$